DISSERTATIONES
BIOLOGICAE
UNIVERSITATIS
TARTUENSIS
422

VLAD-JULIAN PILJUKOV

Biochemical characterization of Irc3 helicase

DISSERTATIONES BIOLOGICAE UNIVERSITATIS TARTUENSIS
422

DISSERTATIONES BIOLOGICAE UNIVERSITATIS TARTUENSIS
422

VLAD-JULIAN PILJUKOV

Biochemical characterization of Irc3 helicase

UNIVERSITY OF TARTU
Press
1632

Institute of Molecular and Cell Biology, University of Tartu, Estonia

This dissertation is accepted for the commencement of the degree of Doctor of Philosophy (in Biochemistry) on August 14th, 2023 by the Council of the Institute of Molecular and Cell Biology, University of Tartu.

Supervisor: Juhan Sedman, PhD, Professor
Department of General and Microbial Biochemistry
Institute of Molecular and Cell Biology
University of Tartu, Tartu, Estonia

Reviewer: Osamu Shimmi, PhD, Professor
Chair of Developmental Biology
Institute of Molecular and Cell Biology
University of Tartu, Tartu, Estonia

Opponent: Jaakko Lauri Olavi Pohjoismäki, PhD, Research Director

Molecular Biology and Genetics Department of Environmental and Biological Sciences, Faculty of Science, Forestry and Technology University of Eastern Finland, Kuopio, Finland

Commencement: Auditorium 105, Riia 23b, Tartu, Estonia on September 19th, 2023, at 14:15.

This work was supported by the University of Tartu ASTRA Project PER ASPERA (European Regional Development Fund). The publication of this dissertation is granted by the Institute of Molecular and Cell Biology at the University of Tartu.

ISSN 1024-6479 (print)
ISBN 978-9916-27-306-7 (print)
ISSN 2806-2140 (pdf)
ISBN 978-9916-27-307-4 (pdf)

University of Tartu Press
www.tyk.ee

TABLE OF CONTENTS

LIST OF ORIGINAL PUBLICATIONS

The following original publications will be referred to in the text by their Roman numerals:

(I) Sedman, T., Garber, N., Gaidutšik, I., Sillamaa, S., Paats, J., Piljukov, V.J. and Sedman, J. (2017), Mitochondrial helicase Irc3 translocates along double-stranded DNA. FEBS Lett, 591: 3831–3841. https://doi.org/10.1002/1873-3468.12903

(II) Piljukov, V., Garber, N., Sedman, T. and Sedman, J. (2020), Irc3 is a monomeric DNA branch point-binding helicase in mitochondria of the yeast *Saccharomyces cerevisiae*. FEBS Lett, 594: 3142–3155. https://doi.org/10.1002/1873-3468.13893

(III) Piljukov VJ, Sillamaa S, Sedman T, Garber N, Rätsep M, Freiberg A, Sedman J. Mitochondrial Irc3 helicase of the thermotolerant yeast *Ogataea polymorpha* displays dual DNA- and RNA-stimulated ATPase activity. Mitochondrion. 2023 Mar; 69:130–139. https://doi.org/10.1016/j.mito.2023.02.004

Journal articles are reprinted with permission from:

(I) John Wiley & Sons

(II) John Wiley & Sons

(III) Elsevier B.V.

My contribution to the articles is as follows:

(I) Performed *in vitro* experiments and edited the manuscript.

(II) Performed *in vitro* experiments, analyzed data, and was involved in the writing of the manuscript.

(III) Designed and performed *in vitro* experiments, analyzed data, and wrote the first version of the manuscript.

ABBREVIATIONS

mtDNA	–	mitochondrial DNA
NTP	–	nucleoside triphosphate
SF	–	superfamily
CTD	–	C-terminal domain
CTE	–	C-terminal extension
RQC	–	RecQ C-terminal
HRDC	–	Helicase RNaseD C-terminal
D-loop	–	displacement loop, where a shorter DNA molecule is inserted between dsDNA duplex
R-loop	–	RNA displacement loop, where a shorter RNA molecule is inserted between dsDNA duplex
OXPHOS	–	oxidative phosphorylation
ROS	–	reactive oxygen species
DSB	–	double-stranded break
BER	–	base excision repair
HR	–	homologous recombination
NHEJ	–	non-homologous end joining
FEN	–	flap endonuclease
MRX	–	Mre11/Rad50/Xrs2 complex
mtEXO	–	mitochondrial degradosome complex
MIOREX	–	mitochondrial organization of gene expression
NA	–	nucleic acid

1. INTRODUCTION

The mitochondrion is a crucial organelle involved in energy production that houses a small genome. While the loss or damage of the mitochondrial genome poses significant challenges for higher eukaryotes, the *Saccharomyces cerevisiae* yeast serves as a valuable model for studying mitochondrial DNA maintenance as it can thrive without oxidative phosphorylation or a functional mitochondrial genome when grown on a fermentable carbon source. Out of approximately 900 proteins in the yeast mitochondrial proteome, around 25% are involved in mitochondrial gene expression and DNA maintenance (Sickmann et al., 2003; Morgenstern et al., 2017). These proteins play a crucial role in synthesizing seven essential respiratory chain subunits encoded by the mitochondrial genome (Foury et al., 1998). Amongst proteins involved in mitochondrial gene expression, *S. cerevisiae* mitochondria contain at least six conserved helicases responsible for mitochondrial nucleic acid metabolism and protein biosynthesis (Lahaye et al., 1991; Sedman et al., 2005; Szczesny et al., 2013).

Helicases are enzymes that utilize the energy of nucleoside triphosphate (NTP) binding and hydrolysis to catalyze structural rearrangements in DNA or RNA. Helicases have a wide range of roles in living cells, from replication, recombination, and repair to transcription, splicing, ribosome biosynthesis, and translation (Singleton et al., 2007). These proteins play vital roles in the stability and proper expression of the mitochondrial genome (Contamine and Picard, 2000). Previous studies have identified three mitochondrial helicases (Mhr4, Mss116, and Suv3) to be involved in mitochondrial RNA metabolism and three (Pif1, Hmi1, and Irc3) to be associated with DNA maintenance (Lahaye et al., 1991; Sedman et al., 2005; Szczesny et al., 2013; Sedman et al., 2014). Recently, the helicase Irc3 has garnered attention for further investigation due to its newly found potential role in mitochondrial translation (Kaur and Datta, 2021).

The definition of the properties of a helicase using only *in vivo* methods is complicated in the *S. cerevisiae* mitochondria due to the functional interconnections of the mitochondrial enzymes. The current thesis focuses on the biochemical characterization of isolated recombinant Irc3 to gain fresh insights into yeast nucleic acid metabolism processes. In the first part of the thesis, I present an overview of helicase structure, function, and common roles in the cell on the example of helicases similar to Irc3. In the second part of my thesis experiment, I conducted a conservation analysis of Irc3 helicases and assessed whether its homolog from a thermotolerant yeast, *O. polymorpha*, could complement the respiratory deficiency phenotype resulting from Irc3 deletion in *S. cerevisiae*. These results are followed by the characterization of nucleic acid ATPase stimulation specificity and evaluation of the helicase translocation mechanism. Finally, the obtained results are discussed in the context of the latest research and proposed potential functions of Irc3 helicase.

2. REVIEW OF LITERATURE

2.1. Helicases, their Structure, and Function

Helicases are a class of enzymes that catalyze the remodeling of nucleic acid (NA) or protein-NA complexes using energy derived from a nucleoside triphosphate (NTP) binding and hydrolysis (Abdel-Monem et al., 1976; Pyle, 2008). Helicase motifs, short sequences of amino acids, form structures responsible for critical functions such as NTP binding and hydrolysis, NA binding, and the transfer of energy from NTP hydrolysis to movement on the NA lattice (Singleton et al., 2007; Fairman-Williams et al., 2010). In practice, nearly all processes involving NA metabolism rely on helicase activity, and defects in helicase function are associated with neurodegenerative symptoms, developmental diseases, and human cancers (Stewart and Chinnery, 2021).

According to the current classification, helicases are divided into six superfamilies (SFs) based on their motif and sequence conservation (Gorbalenya and Koonin, 1993; Singleton et al., 2007). The enzymes of SFs 3 to 6 are typically involved in functions associated with DNA replication and form toroidal multimeric complexes around DNA molecules (Singleton et al., 2007). On the other hand, SF1 and SF2 helicases are monomeric or dimeric in nature. They are involved in a broader range of NA-associated processes such as DNA replication, DNA repair, DNA recombination, RNA splicing, RNA transcription, and translation (Lohman et al., 2008; Bourgeois et al., 2016).

Among helicase superfamilies, SF1 and SF2 have the highest sequence conservation (Gorbalenya and Koonin, 1993; Singleton et al., 2007). The SF1 and SF2 enzymes display a conserved core structure, where the protein is folded to form two cylindrical domains, also known as RecA-like domains (RecA1 and RecA2) (Figure 1) (Singleton et al., 2007; Fairman-Williams et al., 2010). The helicase motifs are located at highly conserved positions on the surface of these domains (Figure 1) (Fairman-Williams et al., 2010). The regions of the helicase core responsible for NTP hydrolysis (motifs Q, I, II, VI) are the most conserved, while the regions responsible for coupling the energy of NTP hydrolysis to movement along the NA lattice (motifs III and Va) are conserved only within a particular SF (Fairman-Williams et al., 2010). For example, the motif III consensus of SF1 helicases is GDxxQL and SF2 helicases – xAT, often used to differentiate the SF1 and SF2 enzymes (Singleton et al., 2007). The regions of the helicase core responsible for binding the NA (formed by motifs Ia, Ib, IV, IVa, V) are the least conserved and differ even within a particular SF, which makes those motifs more helpful in differentiating subfamilies within a SF (Fairman-Williams et al., 2010).

Group of at least three different helicases from a single organism that belong to the same SF (conserved motifs III and Va) and have a high conservation of motif position and sequence is typically called a subfamily (Fairman-Williams et al., 2010). Although the distribution of helicases among different subfamilies

is based solely on amino acid sequence comparison, it has been found that members of a single subfamily share many structural and functional similarities (Singleton et al., 2007; Fairman-Williams et al., 2010). By utilizing the amino acid sequence information, it becomes possible to build hypotheses about the potential activities of the protein and design experimental procedures aimed at characterizing novel helicases.

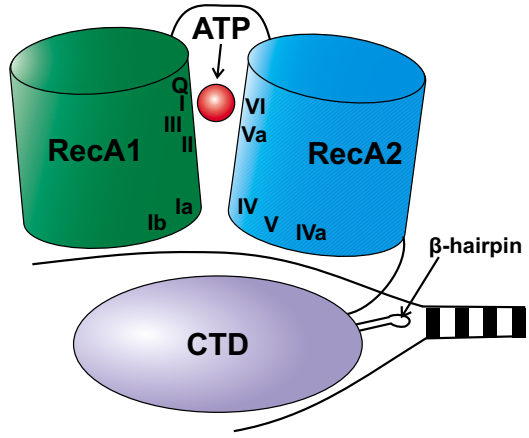

Figure 1. Schematic arrangement of conserved structural domains of an SF2 helicase from RecQ-like subfamily. Conserved helicase core domains are shown in green (RecA1) and blue (RecA2), with a molecule of ATP (red) bound between them. Roman numbers indicate motif positions. The C-terminal domain (CTD) is purple. The β-hairpin structure pushed between pairs of DNA nucleotides is marked with an arrow on the CTD (Pike et al., 2009).

2.2. Characterization of SF2 helicases

Helicases are classified according to motif sequence and location conservation (Gorbalenya and Koonin, 1993; Fairman-Williams et al., 2010). Some helicases also have subfamily-specific domains or structures that help classification (Bernstein and Keck, 2003; He et al., 2010). For example, a β-hairpin required for wedging between the pairs of complementary nucleotides could be located between motifs V and VI of many DEAH/RHA helicases or just after motif VI in RecQ-like helicases (Figures 3 and 4) (He et al., 2010; Kitano et al., 2010). The ratchet domain necessary for stabilizing the unwound ssDNA in Ski2-like helicases is located just after the helicase core of those enzymes (Figure 5) (Johnson and Jackson, 2013). Without a functional β-hairpin or a ratchet domain, the helicase activity in corresponding enzymes is often unlinked from the hydrolysis of NTP (Büttner et al., 2007; Kitano, 2014). Interestingly, not all biochemical activities of a helicase are always conserved within a subfamily. Generally, the polarity of translocation and the ssDNA or dsDNA specificity are better conserved than the specificity for DNA or RNA (Singleton et al., 2007; Fairman-Williams et al., 2010).

In addition to the sequence-based classification, helicases can also be classified based on their enzymatic activity (Singleton et al., 2007). Helicases with fixed translocation polarity are called A (3' to 5' polarity) or B (5' to 3' polarity) type helicases. Single-stranded DNA (ssDNA) specific helicases are called the alpha type, and double-stranded DNA (dsDNA) specific helicases are called the beta type (Table 1) (Singleton et al., 2007). Typically, all helicases use ATP or dATP as the sole energy source, except for DEAH/RHA helicases of viral lineages that can use all types of NTP or dNTP, so the NTP specificity is rarely used for helicase classification (Singleton et al., 2007; Belon and Frick, 2009). However, NA specificity is crucial for understanding the *in vivo* role of a given helicase, as helicases are typically specific to one type of NA: DNA, RNA, or DNA-RNA hybrid molecules (Singleton et al., 2007). The mechanism of nucleic acid unwinding is also essential, as some helicases processively move along the NA lattice while others are distributive (Singleton et al., 2007).

Table 1. List of currently characterized SF2 subfamilies*

SF2 helicase subfamily	Classification	NA specificity
DEAD-box	n.a.**	RNA***
DEAH-box	Aα	DNA/RNA
NS3/NPH-II	Aα	DNA/RNA
Rad3-like	Bα	DNA
RecG-like	Aβ	DNA
T1R/T3R-like	–β	DNA
Rig1-like	Aα/β	DNA/RNA
Swi/Snf-like	–β	DNA
RecQ-like	Aα	DNA
Ski2-like	Aα	DNA/RNA
Suv3-like	Aα	DNA/RNA

(*) Functional classification according to the system proposed by Singleton et al. in 2007. Modified and updated from Fairman-Williams et al., 2010 and Jedrzejczak et al., 2011.
(**) DEAD-box proteins do not translocate along NA molecules and have no defined polarity in this classification system. Still, those proteins can exhibit 3' to 5' or 5' to 3' polarity depending on the type of experiment performed.
(***) Some DEAD-box proteins display DNA-specific activities, but most DEAD-box subfamily representatives are RNA-specific enzymes.

For processive helicases, two main models are proposed that tie together the protein structure with the mechanism of translocation (Patel and Donmez, 2006; Gao and Yang, 2020). One of the best-known models of helicase action is the "inchworm" model (Velankar et al., 1999; Frick, 2006). It proposes that the helicase protein possesses two binding sites for the NA lattice, which undergo conformational changes upon the hydrolysis of NTP. Following that model, the enzyme can function as a monomer where the first helicase domain binds tightly to the

NA. In contrast, the second domain moves forward, followed by the second domain binding tightly to the NA, while the first domain releases NA and moves closer to the second domain (Velankar et al., 1999). This model could also be applied to dimeric helicases, where each subunit functions as a unit capable of binding and releasing the NA, resulting in unidirectional movement (Wong and Lohman, 1992). The "inchworm" model has been demonstrated in the crystal structures of Prp43 with NA (He et al., 2017).

The second best-known model describing the mechanism of helicase translocation is the Brownian motor (Levin et al., 2005; Hwang and Karplus, 2019). Unlike the previously proposed model, the Brownian motor model integrates the statistical Brownian motion at the molecular scale with a directional power stroke, which applies to monomeric and multimeric helicases. The model proposes that the helicase functions through two conformational states, a tight binding state and a weak binding state. The binding of the ATP switches the helicase to a weak binding state, and the helicase can move along DNA randomly in either direction due to Brownian motion. After hydrolyzing ATP, the helicase rebinds to the lattice tightly while making a forward movement or power stroke (Levin et al., 2005; Patel and Donmez, 2006).

In the following paragraphs, I will focus in more detail on the SF2 subfamilies of helicases that are represented in *S. cerevisiae*, have some degree of similarity to the *S. cerevisiae* mitochondrial helicase Irc3 and could help to understand the function of Irc3.

2.2.1. DEAD-box subfamily

The DEAD-box subfamily is the largest group of SF2 helicases, distinguished by containing the conserved motif II Asp-Glu-Ala-Asp (DEAD) (Fairman-Williams et al., 2010). Interestingly, although DEAD-box helicases have different motif II sequence compared to the Irc3 helicase (DEAH), several members of the superfamily display conservation at motif Ia (Daugeron et al., 2001; Kikuma et al., 2004). This motif is typically involved in NA binding and may confer the unique properties of Irc3 NA specificity discussed in the Results section (paragraph 5.4.).

DEAD-box helicases play an essential role in RNA metabolism and participate in various molecular processes, such as transcription, pre-mRNA splicing, ribosome biogenesis, translation, and RNA degradation. At present, at least 37 members of the DEAD-box subfamily have been described in humans and 26 in *S. cerevisiae* (Fairman-Williams et al., 2010; Linder and Jankowsky, 2011). In humans, eIF4A-III is one of the first and best-characterized DEAD-box helicases, eIF4A-III participates in the formation of the exon junction complex (EJC) by remaining bound to mRNA after splicing (Ballut et al., 2005; Nielsen et al., 2009). Mss116 is one of the most researched DEAD-box helicases in *S. cerevisiae* mitochondria, involved in splicing mitochondrial introns (Del Campo and Lambowitz, 2009).

DEAD-box proteins share a highly conserved helicase core that consists of two RecA-like domains tethered by a short, flexible linker (Figure 2) (Mohr et al., 2011). Generally, the core remains loosely packed (as shown in Figure 2) until

RNA and ATP molecules are bound, resulting in a tight protein-ATP-RNA complex. Shortly after the formation of the tightly packed complex, the RNA molecule that has entered a sterically unfavorable state is unwound, ATP hydrolyzed, ADP and inorganic phosphate released, and the protein-RNA complex dissociates (Yang et al., 2007; Theissen et al., 2008). In most DEAD-box proteins, the helicase core is flanked by ancillary N- or C-terminal domains, which are enzyme-specific and contribute to the functional diversity of this protein family. These auxiliary domains direct individual DEAD-box proteins to their functional targets by interacting with specific proteins or RNA sequences or modulating the activity of the helicase core (Cordin et al., 2006; Hilbert et al., 2009). For example, Mss116 and its homologs possess a unique C-terminal extension proposed to force a second kink in the bound RNA strand, potentially increasing its unwinding activity (Figure 2) (Del Campo and Lambowitz, 2009).

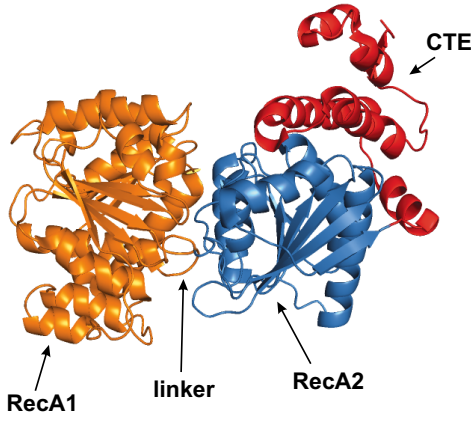

Figure 2. Arrangement of conserved structural domains of Mss116 from *S. cerevisiae* (RCSB ID: 3i5x). Conserved helicase core domains connected by a flexible linker are shown in orange (RecA1) or blue (RecA2). The C-terminal extension domain (CTE) is red (modified using information from Del Campo and Lambowitz, 2009)**.**

Most DEAD-box helicases are non-processive RNA helicases with no defined polarity (Fairman-Williams et al., 2010). However, there are few examples of DEAD-box enzymes capable of unwinding DNA molecules (Kikuma et al., 2004; Talwar et al., 2017). For instance, Dbp9 of *S. cerevisiae* proposed to be involved in the biogenesis of 60S ribosome subunit is capable of unwinding RNA hairpin structures *in vitro* and was also demonstrated to unwind DNA and DNA-RNA hybrid molecules (Daugeron et al., 2001; Kikuma et al., 2004). Moreover, the ATPase activity of Dbp9 is stimulated only by DNA molecules, while RNA molecules showed inhibitory activity (Kikuma et al., 2004). Similarly, the ATPase activity of human DX43 is stimulated by both DNA and RNA, and the enzyme can unwind DNA with a 3' to 5' polarity but displays a 5' to 3' polarity on RNA (Talwar et al., 2017).

2.2.2. DEAH-box subfamily

DEAH-box proteins are a family of SF2 helicases that share many sequence and structural similarities with DEAD-box proteins but have the motif II sequence Asp-Glu-Ala-His (DEAH), which is also the motif II sequence of Irc3 enzyme (Jarmoskaite and Russell, 2014). Interestingly, this single amino acid substitution separates DEAD-box and DEAH-box helicases into subfamilies (Fairman-Williams et al., 2010). Compared to DEAD-box helicases, the DEAH-box helicases have a different tertiary structure of the helicase core and a different mechanism of NA duplex unwinding (Fairman-Williams et al., 2010). Moreover, this subfamily consists of both DNA and RNA-specific enzymes (Pyle, 2008). The best-characterized members of the DEAH-box subfamily from *S. cerevisiae* are the RNA helicase Prp43, which is involved in spliceosome disassembly during mRNA maturation, and the DNA helicase Mph1, which is associated with DNA damage repair by homologous recombination (Tanaka and Schwer, 2006; Bohnsack et al., 2009; Schürer et al., 2004; Tay et al., 2010). DHX15 is one of the most well-studied DEAH-box helicases in humans, with essential functions in RNA metabolism and innate immune sensing of viral RNA (Imamura et al., 1997; Fouraux et al., 2002).

The core of DEAH-box helicases consists of two RecA-like domains, which contain the same set of conserved motifs as DEAD-box proteins (Fairman-Williams et al., 2010; Jarmoskaite and Russell, 2014). Similarly to DEAD-box helicases, the DEAH-box helicases have additional domains or regions flanking their helicase core (Wang and Guthrie, 1998; Ozgur et al., 2015). In the crystal structures of these proteins, the C-terminal domains interact strongly with the helicase core (He et al., 2010; Walbott et al., 2010). The RecA-like domains, along with ancillary C-terminal domains, are densely packed together and surround the NA channel in a ring-shaped structure (Figure 3), which may be a crucial feature of processive translocating helicases (Walbott et al., 2010; Murakami et al., 2017). Another characteristic feature of DEAH-box helicases is the β-hairpin located between motifs V and VI of the RecA2 (Figure 3) (He et al., 2017). The exact function of this long N-terminal β-hairpin is not known, but in Prp43, it is essential for holding the 5’ end of a bound RNA stack inside the binding pocket in the ATP-bound state (He et al., 2017; Hamann et al., 2019). A similar β-hairpin structure has also been observed in DNA helicase Hel308, where it has been proposed to participate in strand separation by disrupting the double-stranded structure of nucleic acids. Hence, it is tempting to speculate that it also may be necessary for strand separation in DEAH-box helicases (Büttner et al., 2007). On the other hand, in a structure of Prp22 in a complex with single-stranded RNA, the location of the β-hairpin is far from the potential RNA duplex, suggesting that the β-hairpin is mainly involved in translocation instead of strand separation (Hamann et al., 2019). The N-terminal region of DEAH-box helicases shows little conservation and is often involved in recruiting the helicase to the correct complex or subcellular location, for example, the mitochondrial transport signal peptide (Wang and Guthrie, 1998). The C-terminal region of DEAH-box

helicases is highly conserved, consisting of three domains: a winged helix (WH), a ratchet-like domain, and an oligosaccharide binding (OB) fold (Figure 3) (Ozgur et al., 2015).

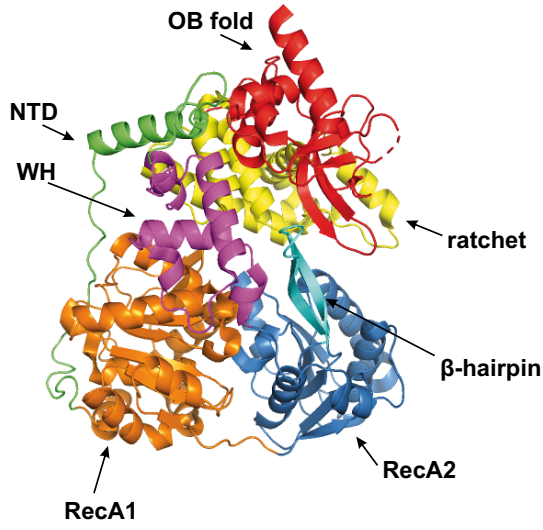

Figure 3. Arrangement of conserved structural domains of Prp43 from *S. cerevisiae* (RCSB ID: 3kx2). Conserved helicase core domains are shown in orange (RecA1) or blue (RecA2). The winged helix (WH) is magenta, the ratchet is yellow, the OB-fold domain is red, and the N-terminal domain (NTD) is green. The β-hairpin structure is cyan (modified using information from Walbott et al., 2010).

DEAH-box helicases predominantly possess 3' to 5' polarity (A type) and single-stranded nucleic acid molecule specificity (α type) (Schwer, 2008; He et al., 2017). Successful loading onto the substrate NA requires a single-stranded 3' overhang (Tanaka and Schwer, 2005; Smaldino et al., 2015). Some DEAH-box proteins lack specificity for ATP and can hydrolyze all four nucleoside triphosphates (Tanaka and Schwer, 2005; Belon and Frick, 2009). The translocation mechanism of DEAH-box helicases is best understood for the Prp43 of *S. cerevisiae* (De Bortoli et al., 2021). The translocation of Prp43 involves the movement of two extended amino acid hairpin structures relative to the RNA strand during the cycles of ATP hydrolysis. These hairpins trap the bases of the bound RNA between them and move in cycles to incorporate a new base on the 5' side and exclude one on the 3' side, resulting in the directional 3' to 5' translocation of the helicase (De Bortoli et al., 2021). Both hairpin structures are highly conserved among DEAH-box helicases and related DExH helicases, with the 3' hairpin being an extension of motif Ib on domain RecA1 and the 5' hairpin being a RecA2 structure that does not correspond to any currently identified motifs (He et al., 2017). One proposed advantage of this translocation model is that the enzyme does not necessarily need to move along the nucleic acid lattice. Instead, it can pull onto one of the strands and remove it from the blocked region (winching model) (Semlow et al., 2016). This type of action was experimentally shown with DEAH-box helicase Prp22 (Semlow et al., 2016).

2.2.3. RecQ-like subfamily

RecQ-like is a subgroup of SF2 helicases, with the prototype representative being RecQ from *E. coli* (Bachrati and Hickson, 2003). Similarly to DEAH-box helicases, RecQ-like helicases have motif II sequence Asp-Glu-Ala-His (DEAH), which is also the motif II sequence of Irc3 (Fairman-Williams et al., 2010). Members of the RecQ-like subfamily consist exclusively of DNA helicases and are widely conserved in bacteria, archaea, yeasts, and higher multicellular organisms (Bachrati and Hickson, 2003). Moreover, representatives of this subfamily have a high similarity of biochemical activities to our protein of interest, Irc3 (paragraph 5.5.2.). Typically, unicellular organisms have one homolog of this helicase, while multicellular organisms have multiple RecQ-like subfamily representatives (Kitano, 2014). Humans have five RecQ-like enzymes: BLM, RECQ1, RECQ4, RECQ5, and WRN (Bachrati and Hickson, 2003). Mutations in the BLM, WRN, and RECQ4 genes are associated with severe autosomal recessive conditions characterized by genomic instability, cancer predisposition, and premature aging (Ellis et al., 1995; Yu et al., 1996; Kitao et al., 1999; Manthei and Keck, 2013). *S. cerevisiae* has only one RecQ-like helicase, Sgs1, involved in double-stranded break repair during homologous recombination in the yeast nucleus (Bennett et al., 1998; De Muyt et al., 2012).

In addition to the conserved helicase core, RecQ-like helicases have other characteristic C-terminal domains: RQC (RecQ C-terminal), which is itself divided into Zn-binding, winged helix (WH), and HRDC (Helicase RNaseD C-terminal) domains (Figure 4) (Kitano et al., 2007, 2010; Kim and Choi, 2010; Kim et al., 2013). Among different representatives of the RecQ-like subfamily, RQC is much more conserved than HRDC (Gupta and Schmidt, 2020).

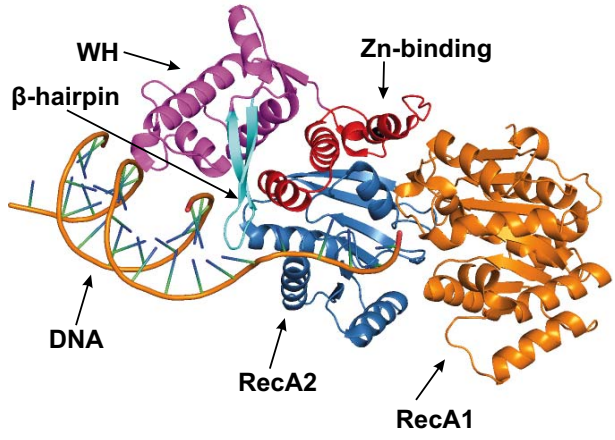

Figure 4. Arrangement of conserved structural domains of the human RECQ1 bound to DNA (RCSB ID: 2wwy). Conserved helicase core domains are shown in orange (RecA1) or blue (RecA2). The winged helix (WH) is magenta, and the Zn-binding domain is red. The β-hairpin structure pushed between pairs of DNA nucleotides is cyan (modified using information from Pike et al., 2009).

For example, human RecQ-like helicase RECQ1 has no HRDC (Figure 4) (Pike et al., 2009; Gupta and Schmidt, 2020). The RQC domain is involved in the specific recognition, binding, and unwinding of branched DNA molecules (Kitano et al., 2010; Kim et al., 2013). HRDC has a less understood function but is thought to facilitate contact with linear DNA molecules or participate in protein-protein interactions (Kim and Choi, 2010).

Unlike other regions, the helicase core sequence inside the RecQ-like subfamily is much better conserved (Bachrati and Hickson, 2003). However, the core cannot unwind NA molecules without a functional RQC domain, with the β-hairpin structure inside RQC being particularly important (Figure 4) (Tadokoro et al., 2012; Swan et al., 2014). This β-hairpin structure is pushed between pairs of NA duplexes, splitting them apart, while the helicase core region is used to push the protein forward (Kitano et al., 2010). RecQ-like enzymes are processive helicases with 3' to 5' polarity (A type) and are stimulated by ssDNA and dsDNA (α type) (Umezu et al., 1990). Additionally, some of the best characterized RecQ helicases, such as BLM and Sgs1, are exceptionally well stimulated by complex DNA structures, such as G-quadruplexes, D-loop, R-loop, replication fork-like, and Holliday junctions (Sun et al., 1998; Karow et al., 2000; van Brabant et al., 2000; Mohaghegh et al., 2001; Huber et al., 2002). Interestingly, all currently characterized RecQ-like helicases except for the founding member RecQ from *E. coli* are inefficient at binding and unwinding blunt-ended dsDNA molecules and need a free single-stranded 3' overhang for efficient substrate loading (Bachrati and Hickson, 2003; Hishida et al., 2004).

2.2.4. Ski2-like subfamily

Ski2-like helicases constitute a subfamily of SF2, with Ski2 from *S. cerevisiae* as the prototype representative (Johnson and Kolodner, 1995). Ski2-like helicases, like DEAH-box and RecQ-like helicases, have a motif II sequence, DExH (Fairman-Williams et al., 2010). In addition, this subfamily encompasses RNA and DNA-stimulated helicases (Richards et al., 2008; Weir et al., 2010). Irc3 protein structure prediction by AlphaFold indicates that the C-terminus of Irc3 protein could resemble the stalk and fist domains of Ski2-like helicases (paragraphs 5.1. and 5.2.). Ski2-like helicases have homologs in yeasts and higher multicellular organisms but are absent in bacteria, except for the archaea, where Hel308 is present (Guy, 2005; Büttner et al., 2007; Weir et al., 2010).

Ski2-like helicases, such as Ski2, Mtr4, Brr2, and Slh1, are stimulated by RNA *in vitro* and play essential roles in RNA metabolism *in vivo*, including transcription, translation, pre-mRNA splicing, and RNA decay (Martegani et al., 1997; Pena et al., 2009; Jackson et al., 2010; Halbach et al., 2012). On the other hand, Hel308 is a processive DNA helicase with 3' to 5' polarity that unwinds branched DNA structures *in vitro*, preferentially unwinding lagging strand replication fork-like structures, and has ssDNA stimulated ATPase activity (Guy, 2005; Li et al., 2008). In addition, Hel308 requires a free 3' or 5' overhang for successful substrate loading and unwinding and is capable of unwinding D-loop and Holliday

junction-like DNA structures (Guy, 2005; Fujikane et al., 2006; Büttner et al., 2007). Furthermore, genetic experiments have associated archaeal Hel308 with stalled replication forks *in vivo*. At the same time, the human homolog of Hel308, HELQ, is involved in DNA double-stranded break repair through homologous recombination and forms complexes with RAD51 and RPA (Marini and Wood, 2002; Muzzini et al., 2008; Woodman et al., 2011; Adelman et al., 2013).

One of the distinctive features of the Ski2-like subfamily is that all helicases in the family have strong conservation of the helicase core while having only structural conservation in the C-terminal part of the protein (Jackson et al., 2010; Halbach et al., 2012). Unlike RecQ-like but similarly to DEAH-box proteins, the β-hairpin is located within the RecA2 domain between motifs V and VI (Figure 5) (Büttner et al., 2007; Bernstein et al., 2008). The C-terminal part of Ski2-like helicases is made up of three main components: a winged helix domain, a fist domain (a β-barrel-like structure composed of multiple antiparallel β-sheets), and a ratchet domain (Figure 5) (Büttner et al., 2007; Jackson et al., 2010; Weir et al., 2010). The ratchet domain is crucial for unwinding nucleic acids and stabilizing unwound single-stranded DNA (Büttner et al., 2007). The winged helix domain links the helicase core with the C-terminal part of the protein, likely serving as a central hub for all necessary motions between the other parts of the protein (Figure 5) (Büttner et al., 2007; Northall et al., 2017). The fist domain (Figure 5), represented by the KOW domain in Mtr4, binds *in vitro* transcribed tRNA but not single-stranded RNA, while in Hel308, it acts as a molecular brake, interacting with ssDNA extruded through the central pore of the helicase, resulting in an autoinhibitory activity (Richards et al., 2008; Weir et al., 2010).

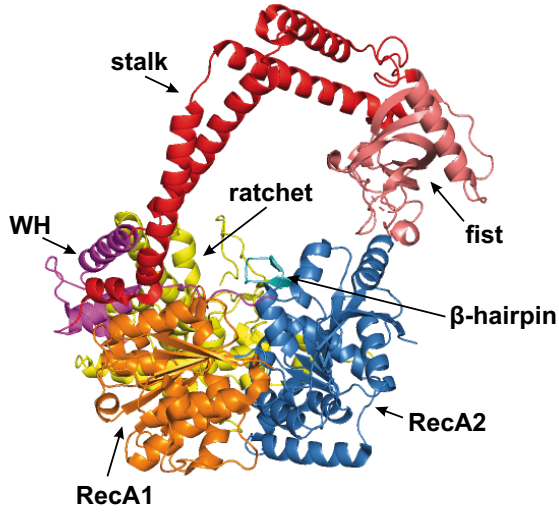

Figure 5. Arrangement of conserved structural domains of Mtr4 from *S. cerevisiae* (RCSB ID: 4u4c). Conserved helicase core domains are shown in orange (RecA1) or blue (RecA2). The winged helix (WH) is magenta, the ratchet domain is yellow, the stalk structure is red, and the fist domain (KOW) is pink. The β-hairpin structure is cyan (modified using information from Weir et al., 2010).

2.3 Mitochondrial DNA metabolism of *S. cerevisiae*

S. Cerevisiae, as a facultative anaerobe with well-characterized genetics, is an excellent model organism for studying mitochondrial NA metabolism (Ephrussi and Slonimski, 1955). Like all eukaryotes, *S. cerevisiae* has a separate autonomous mitochondrial DNA (mtDNA) (Foury et al., 1998). However, a peculiar feature of the mitochondrial function of *S. cerevisiae* is the ability of this yeast to live without a functional mitochondrial genome (Ephrussi and Slonimski, 1955). Cells with functional mitochondrial genome are referred to as rho^{+}, cytoplasmic mutants that have completely absent mitochondrial genome – rho^{0} and cytoplasmic mutants with extensive deletions in mtDNA followed by multiplication of the remaining fragment – rho^{-} (Faye et al., 1973; Dujon, 1981). Most proteins functioning in the mitochondria are of cytoplasmic origin, as the mitochondrial genome encodes only a small subset of genes (Foury et al., 1998; Perocchi et al., 2006). The total mitochondrial nucleic acid metabolism of the yeast consists of multiple processes: DNA replication and reparation, DNA transcription, RNA post-processing, RNA translation, and RNA degradation. These processes probably depend on helicase activity (Contamine and Picard, 2000).

2.3.1. mtDNA replication

Yeast mitochondrial DNA (mtDNA) composition varies among different species, with some having primarily circular double-stranded DNA (dsDNA) and others linear or branched DNA molecules (Maleszka et al., 1991). The mitochondrial DNA is packaged into compact DNA-protein complexes or nucleoids (Chen and Butow, 2005; Kucej and Butow, 2007). Nucleoids are mainly formed by the DNA-binding protein Abf2 and other proteins essential for maintaining mtDNA (Mgm101, Rim1, etc.) (Chen et al., 2005). The 85.8 kb mitochondrial genome of *S. cerevisiae* contains seven to eight *ori*-like elements, three active *ori* regions, and is mainly composed of concatemeric branched or linear DNA molecules that can be double-stranded, single-stranded, or partially single-stranded (Maleszka et al., 1991; Foury et al., 1998). Experimental evidence has shown that *in vitro ori* sequences can be primed by transcription with the mitochondrial RNA polymerase Rpo41, which is essential for the preservation of rho^{+} mtDNA (Baldacci and Bernardi, 1982; Sanchez-Sandoval et al., 2015). However, rho^{-} mtDNA does not require Rpo41 for replication, suggesting other initiation mechanisms *in vivo* (Fangman et al., 1990; Lorimer et al., 1995).

One proposed model for mtDNA replication in yeast is recombination-initiated replication (Maleszka et al., 1991; Ling and Shibata, 2002; Shibata and Ling, 2007; Prasai et al., 2017). Mitochondria contains at least a single double-stranded break (DSB)-generating homing endonuclease – SceI, that could potentially lead to free 3' DNA tail generation required for site-specific homologous recombination (Nakagawa et al., 1991). Sce1 was shown *in vivo* to increase the recombination rate (Pâques and Haber, 1999). Next, the DSB should be processed by one of the 5' – 3' exonucleases present in the mitochondria, for example, the

mtDNA recombination rate was affected by the deletion of the Nuc1 nuclease (Zassenhaus and Denniger, 1994). After generating a free 3' DNA tail, it should be annealed to complementary DNA molecules. For that purpose, at least two proteins were found in the yeast mitochondria, Mhr1 and Mgm101 (Ling et al., 2009; Mbantenkhu et al., 2011). Mhr1 was discovered first, but *MHR1* deletion mutants have only a limited effect on the crossing of unlinked mitochondrial genes, and Mhr1 protein is at least eight times less efficient at binding ssDNA molecules than Mgm101 (Ling et al., 1995; Mbantenkhu et al., 2011). Additionally, independent research has described Mhr1 as an important component of the mitochondrial ribosome, so the observed *in vivo* phenotype could probably be explained by the translation defect of Mhr1 mutants (Amunts et al., 2014). Mgm101 is a Rad52-related protein, and similarly to Rpo41, it is essential for preserving rho^+ mtDNA (Wang and Shadel, 1999; Zuo et al., 2002). It was shown to directly participate in mtDNA recombination events *in vivo* (Mbantenkhu et al., 2011). Recombinant Mgm101 was demonstrated *in vitro* to catalyze the annealing of complementary ssDNA strands, even when ssDNA was bound by the mitochondrial ssDNA binding protein Rim1 (Mbantenkhu et al., 2011). Some rho^- strains also depend on Mgm101 for their mtDNA stability (Zuo et al., 2002). The resulting structures could be a suitable substrate for DNA polymerase Mip1 to begin the synthesis of the leading strand (Foury, 1989). When the whole mtDNA leading strand is synthesized, the polymerase is thought to switch templates onto the first annealed DNA molecule to complete the synthesis of the complementary strand, or the complementary strand is synthesized from a separate round of annealing and synthesis (Chen and Clark-Walker, 2018).

It is poorly understood how most rho^- strains, which lack Mgm101 and Rpo41, can maintain their remaining mtDNA (Zuo et al., 2002). This suggests that there may be a third, undiscovered replication pathway or a successful enzyme-independent formation of recombinational structures (Clark-Walker, 1989; Ling et al., 2007). The fact that multiple linked replication pathways function inseparably makes it particularly challenging to understand mtDNA replication in yeast.

2.3.2. mtDNA repair

The mitochondrion is vital for the oxidative phosphorylation (OXPHOS) pathway. Still, its role also means that it is regularly exposed to various endogenous damaging agents, including reactive oxygen species (ROS) (Kang and Hamasaki, 2005). As a result, repairing newly emerging defects in the mitochondrial DNA is essential for the survival of most higher eukaryotes (Druzhyna et al., 2008).

Current knowledge about the mechanisms involved in *S. cerevisiae* mtDNA repair is fragmented, and all existing models are inferred from protein homology or genetic evidence (Allkanjari and Baldock, 2021). The first layer of defense relies on mitochondrial polymerase Mip1 proof-reading exonuclease activity (Foury et al., 2004). Mutations targeting the exonuclease activity of Mip1 increase mismatch occurrence approximately 500-fold *in vivo* (Foury and Vanderstraeten, 1992).

The next layer of defense depends on multiple intertwined repair pathways (Allkanjari and Baldock, 2021). One of the crucial pathways of mtDNA repair could be associated with HR, which was discussed in the previous paragraph for its potential role in mtDNA replication (Chen and Clark-Walker, 2018). It has been proposed that nuclear Mre11/Rad50/Xrs2 complex (MRX) is transported to the yeast mitochondria, but so far, only the Rad50 protein has been located in the mitochondria (Kalifa et al., 2012; Schulte et al., 2023). In the yeast nucleus, the MRX complex binds the blunt ends of DSB, followed by Mre11 5' – 3' exonuclease activity (Ghodke and Muniyappa, 2013). Rad50 regulates the activity of Mre11 by either repositioning or unwinding DNA ends and directing them toward the active site of Mre11 (Hopfner et al., 2001; Trujillo and Sung, 2001). In addition, Xrs2 participates in DNA binding and is also proposed to regulate Mre11 exonuclease activity (Trujillo et al., 2003). After the exonuclease treatment by MRX, the free 3' tail could be annealed to the complementary DNA strand either by Mgm101 or Mhr1, and new DNA is synthesized by Mip1 (Chen and Clark-Walker, 2018).

Another mtDNA repair pathway was proposed when the Msh1 protein was found to function in the yeast mitochondria (Mookerjee and Sia, 2006). Msh1 is a bacterial MutS protein homolog that presumably participates in the DNA mismatch repair pathway (MMR) (Mookerjee and Sia, 2006). Heterozygous deletion of Msh1 in diploid yeast cells causes at least a seven-fold increase in point mutation accumulation in yeast mtDNA when grown on erythromycin-containing media (Chi and Kolodner, 1994a). Additionally, *in vivo* overexpression of Msh1 was shown to suppress mtDNA hypermutation phenotypes caused by the defective ogg1 gene (Dzierzbicki et al., 2004). *In vitro*, recombinant Msh1 protein efficiently binds dsDNA fragments, and the binding affinity is increased by nucleotide mismatches (Chi and Kolodner, 1994a, 1994b). Other components of the yeast MMR pathway have yet to be described, but they should minimally include a daughter strand-specific endonuclease, helicase, and exonuclease (Foury et al., 2004).

One of the best-characterized mtDNA repair pathways in the yeast mitochondria is base excision repair (BER) (Foury et al., 2004). At least four BER pathway enzymes are currently found to localize to mitochondria, N-glycosylases Ntg1, Ogg1, Ung1, and abasic position (AP) endonuclease Apn1 (Percival et al., 1989; van der Kemp et al., 1996; You et al., 1999; Vongsamphanh et al., 2001). The existence of the BER pathway in mitochondria was further supported by the localization of Rad27 flap endonuclease (FEN) in yeast mitochondria (Kalifa et al., 2009). FEN is essential for the long patch BER pathway, where after damaged base excision by the glycosylase and strand cutting by AP endonuclease, the 5' strand is partially displaced by synthesis of a new DNA strand with Mip1 DNA polymerase (Foury, 1989; Boiteux and Guillet, 2004). When the DNA strand is partially displaced, the formed DNA flap structure could be cut, removing the damaged DNA strand, and the newly synthesized DNA strand ligated to create a unified DNA duplex (Boiteux and Guillet, 2004).

The last mtDNA repair pathway currently discussed in S. cerevisiae mitochondria is nonhomologous end-joining (NHEJ), but currently, the components of that complex have not been definitively proven to localize to mitochondria (Kalifa et al., 2012; Schulte et al., 2023). The yeast nucleus contains the Yku70/80 protein complex, which competes for binding and protection of DSB with Mre11/Rad50/Xrs2 complex and, after binding Yku70/80, religates the dsDNA back together, restoring the original sequence or causes a deletion in between joined mtDNA ends (Clerici et al., 2008; Shim et al., 2010).

2.4. Mitochondrial genome expression of *S. cerevisiae*

S. cerevisiae genome encodes seven proteins that are essential for the functioning of three respiratory chain complexes involved in energy production: apocytochrome b (complex III), subunits I–III of the cytochrome c oxidase (complex IV), and subunits 6, 8, 9 of the F0 component of the mitochondrial ATP synthase (complex V). In addition to these proteins, the genome also encodes 24 tRNAs, two rRNAs, and a component of the small subunit of the mitochondrial ribosome (Foury et al., 1998). According to current understanding, the mitochondrial genome expression is mainly controlled by transcriptional and post-transcriptional means (Costanzo and Fox, 1990; Steele et al., 1996). Protein expression in the yeast mitochondria is primarily based on the balance between transcription, transcript maturation, and RNA degradation (Grivell, 1989). Defective phenotypes of strains deficient in mitochondrial RNA degradation, which ultimately results in a loss of respiratory function, can be partially restored by partial loss-of-function mutations in RNA polymerase Rpo41 or transcription factor Mtf1, effectively reducing the transcription rate (Rogowska et al., 2006).

2.4.1. RNA Synthesis and Maturation

The first step of gene expression in the yeast mitochondria is managed by exclusive RNA polymerase Rpo41 (Greenleaf et al., 1986). Rpo41 in complex with the transcription factor Mtf1 binds 9-nucleotide promoter sequences with a different affinity that determines the transcription rate (Osinga et al., 1982; Jang and Jaehning, 1991). Here it was proposed that transcription initiation is straightforwardly linked to the ATP levels within the organelle, as all newly synthesized transcripts begin with adenine (Amiott and Jaehning, 2006). In addition to this mechanism, binding multiple sequence-specific proteins to the 5' UTR of mitochondrial mRNA transcripts stabilized RNA, increasing molecule longevity *in vivo* (Steele et al., 1996). For example, 5' UTR binding Cbp1 protein is needed for the maturation and stability of the mitochondrial cytochrome b transcripts, and similarly, Aep1 is required for the stability of *ATP9* mRNA (Ziaja et al., 1993; Krause et al., 2004).

The mitochondrial genome of *S. cerevisiae* can contain up to 13 introns in three of its genes, which can vary in number among different yeast strains (Foury

et al., 1998). Specifically, the COX1 gene can have up to seven introns, COB can have up to five, and 21S rRNA can have one (Séraphin et al., 1987). These introns can encode proteins that assist in splicing or DNA repair, endonucleases, and reverse transcriptases that enable intron mobility (Séraphin et al., 1987). Intron splicing in the yeast mitochondria is a multi-step process that involves multiple factors, beginning with sequence-specific intron-binding proteins like Mss18 or Cbp2 and ending with the nuclear-encoded RNA helicase Mss116 (Séraphin et al., 1988; Huang et al., 2005). Mss116 is essential for resolving misfolded RNA structures and guiding other splicing-related proteins to their target sites (Huang et al., 2005; Bifano and Caprara, 2008). For example, *in vitro* studies have shown that Mss116 promotes exon ligation after cutting the cytochrome oxidase 1 (COX1) gene intron aI5β with sequence-specific enzyme Mrs1 (Bifano and Caprara, 2008).

2.4.2. RNA degradation

In *S. cerevisiae* mitochondria, two distinct RNA degradation pathways play a crucial role in the yeast mitochondrial gene expression system (Wiesenberger and Fox, 1997; Dziembowski et al., 2003).

The first pathway is mediated by the 5' to 3' exoribonuclease Pet127, which processes RNA in a non-specific manner (Fekete et al., 2008). However, the activity of this pathway can be regulated by the binding of sequence-specific proteins to the 5' UTR of mRNA molecules. For example, the Cbp1 protein can protect the 5' UTR of the COB gene from complete digestion (Fekete et al., 2008).

The second RNA degradation pathway in *S. cerevisiae* mitochondria is dependent on the mitochondrial degradosome complex (mtEXO), which consists of the RNA helicase Suv3 and an RNase Dss1 (Dziembowski et al., 2003; Malecki et al., 2007). Loss-of-function mutations in either of these components result in the overaccumulation of excised intronic sequences, depletion of mature mRNA transcripts, gradual loss of translational activity, and ultimately, the loss of rho^+ DNA (Stepien et al., 1992; Golik et al., 1995; Dziembowski et al., 2003; Rogowska et al., 2006).

2.4.3. Translation

In yeast mitochondria, transcription is immediately followed by translation using specialized membrane-bound ribosomes (mitoribosomes) (Naithani et al., 2003; Rodeheffer and Shadel, 2003). Simultaneous transcription and translation could increase mRNA stability, making RNA less accessible to nucleases (Naithani et al., 2003). The mitochondrial genome encodes 15S, 21S rRNA, and a component of the small subunit Var1 while the rest of the ribosomal proteins are encoded in the nucleus (Mason et al., 1996).

A recent model proposes that mitoribosomes interact with many transiently bound proteins involved in RNA processing, translation, and even mtDNA

maintenance (Kehrein et al., 2015; Schulte et al., 2023). According to this model, mitoribosomes with their associated proteins could be collectively called mitochondrial organization of gene expression (MIOREX) complexes. For example, purified ribosomes from *S. cerevisiae* mitochondria contain RNA post-processing factors such as Sls1 or Cbp1, as well as RNA helicases Mss116, Mrh4, Suv3, and proteins involved in mtDNA maintenance such as Mgm101, Rim1, Abf2, and Cce1 (Kehrein et al., 2015). Interestingly, this model aligns well with previous finds of ribosome components in the yeast mitochondrial nucleoid preparations (Sato and Miyakawa, 2004; Miyakawa, 2017).

According to this model, the specific interactions between ribosomes and elements involved in mRNA processing suggest that mRNA maturation and translation occur regulated through the MIOREX complexes (Kehrein et al., 2015). In addition to previously discovered RNA processing factors Cbp1 and Sls1, RNA helicases were also found to be associated with the mitoribosome (Rodeheffer and Shadel, 2003; Krause et al., 2004; Kehrein et al., 2015; Schulte et al., 2023). Additionally, ribosomes were found to be linked to RNA processing, maturation, and degradation not only in RNA granules located near the nucleoid but also through the peripheral MIOREX complexes, which could potentially form an expressosome-like assembly (Kehrein et al., 2015). Recent *S. cerevisiae* mitochondrial proteomic studies partially support the MIOREX model, as many RNA post-processing factors such as Sls1, Cbp1, and RNA helicases indeed co-localize with 37S ribosome subunit components like Nam9 and Rt35 (Schulte et al., 2023).

2.4.4. The fragility of *S. cerevisiae* mitochondrial genome

The lack of robustness in the yeast mitochondrial genetic system has been a topic of discussion for a long time (Tzagoloff and Dieckmann, 1990). When grown in glucose media under normal environmental conditions, wild-type S. cerevisiae strains exhibit background mtDNA instability, and this phenotype is always considered when studying mutants deficient in mitochondrial gene expression (Contamine and Picard, 2000).

Given the proposed tight integration of DNA and RNA metabolisms in *S. cerevisiae* mitochondria, it is unsurprising that many factors responsible for RNA post-processing or translation lead to the loss of mitochondrial DNA (Kehrein et al., 2015). For example, the deletion of Mrh4, a DEAD-box RNA helicase that has been shown to participate in the late stages of mitoribosome assembly, results in no mitochondrial protein synthesis, an inability to generate ATP through oxidative phosphorylation, and a transition to rho^{-} or rho^{0} *petites* (Schmidt et al., 2002). Deletion of Suv3 helicase participating in RNA degradation pathways results in a total conversion to rho^{-} or rho^{0} *petites* in strains containing the complete set of mitochondrial introns (Rogowska et al., 2006). Numerous findings where dysregulated gene expression leads to defective mtDNA maintenance have led scientists to question whether there is a specialized feedback pathway involved, as misregulated protein synthesis could potentially

lead to erroneous oxidative phosphorylation and possibly fatal consequences (Duvezin-Caubet et al., 2006). Alternatively, this phenomenon could be just a consequence and limitation of the design of the *S. cerevisiae* mitochondrial gene expression system.

2.5. Yeast mitochondrial helicases

Currently, there are six helicases described to be localized in the mitochondria of *S. cerevisiae*, three of them are RNA helicases (Mss116, Mrh4, Suv3), two are DNA helicases (Pif1, Hmi1, Irc3), and one has ATPase activities with both DNA and RNA cofactors (Irc3) (Séraphin et al., 1989; Lahaye et al., 1991; Stepien et al., 1992; Sedman et al., 2000; Schmidt et al., 2002; Sedman et al., 2014; Piljukov et al., 2023). DNA helicases are thought to take part in some form of mtDNA repair or directly in one of the pathways of mtDNA replication (Lahaye et al., 1991; Sedman et al., 2000). RNA helicases participate in pre-mRNA maturation, ribosome biogenesis, and RNA degradation (Séraphin et al., 1989; Stepien et al., 1992). The data on the yeast mitochondrial helicases is still incomplete, leaving many topics for future clarification and discovery.

2.5.1. Pif1

Pif1 is a conserved helicase in eukaryotes classified as a member of the Pif1-like subfamily of helicases, belonging to the SF1 helicase superfamily (Malone et al., 2022). The PIF1 gene was first discovered in yeasts through genetic screening to detect mtDNA recombination (Lahaye et al., 1991). Pif1 has two isoforms in budding yeast, the longer isoform containing a mitochondrial targeting sequence (MTS) is transported to mitochondria, while the shorter isoform remains in the nucleus, regulating telomerase activity and preventing de novo telomere formation on double-strand break (DSB) sites (Schulz and Zakian, 1994; Zhou et al., 2000; Makovets and Blackburn, 2009). In yeast, the biochemical characterization of Pif1 shows that the mitochondrial Pif1 isoform is a 5’ to 3’ directional (B) distributive DNA helicase and an ssDNA-stimulated ATPase capable of duplex DNA unwinding (Bochman et al., 2011; Ononye et al., 2020).

Even though mutant strains deficient in the mitochondrial form of Pif1 can grow on non-fermentable carbon sources like glycerol, they display higher levels of mtDNA instability resulting in higher levels of point mutations, deletions (rho^{-}), or loss (rho^{0}) of mtDNA (O’Rourke et al., 2002). Pif1 is involved in repairing or preventing dsDNA breaks in mtDNA and is proposed to interact with various factors to promote DNA repair via recombination or participate in controlling unwanted recombination events (Cheng et al., 2007). Additionally, Pif1 has an *in vitro* preference for RNA-DNA hybrids as its favored substrate, mainly when using forked substrates, and can unwind G-quadruplexes, which are most likely frequent in mtDNA (Ribeyre et al., 2009; Zhou et al., 2014; Ononye et al., 2020).

2.5.2. Hmi1

Hmi1 is an 80 kDa mitochondrially targeted protein encoded by S. cerevisiae nuclear genome, which does not have homologs in higher eukaryotes. Curiously, Hmi1 uses a C-terminal mitochondrial targeting signal when other known nuclear-encoded mitochondrial proteins have an N-terminal signal (Lee et al., 1999). Furthermore, Hmi1 is a distributive mitochondrial DNA helicase and ATPase, which according to motif homology, belongs to SF1 (Sedman et al., 2000).

HMI1 gene deletion causes complete or partial loss of mtDNA in rho^+ strains. *HMI1* gene products with mutations that cause loss of ATPase or helicase activity are capable of partially supporting rho^+ mtDNA stability which could indicate that Hmi1 has another important role in mitochondria besides being a helicase (Sedman et al., 2005). In rho^- strains with defective mtDNA, the presence of Hmi1 is not required to preserve the remaining mtDNA fragment (Sedman et al., 2005). Additionally, *HMI1* is not needed for the transcription of mtDNA genes, so the effect of *HMI1* deletion is most likely not caused by deficient transcription of some other mitochondrial genome-encoded gene (Sedman et al., 2000). Biochemical studies have revealed that Hmi1 has a 3' – 5' translocase activity and helicase activity, which requires a 3' single-stranded overhang, and that it needs the presence of Mg^{2+}, ATP and a single-stranded DNA cofactor to perform ATP hydrolysis (Kuusk et al., 2005).

Hmi1 is most likely not the main replicative helicase in the yeast mitochondria as it is not required to stabilize rho^- genomes. At the same time, it still could be involved in the mtDNA replication as *HMI1* deletion causes loss of rho^+ phenotype (Sedman et al., 2000, 2005).

2.5.3. Mss116

Mss116 is an SF2 helicase belonging to the DEAD-box subfamily. In *S. cerevisiae* Mss116 was identified in a genetic screen for nuclear-encoded factors involved in the splicing of the intron-containing transcripts of mitochondrial genes (Séraphin et al., 1989). Its deletion only affected strains containing introns in mitochondrial genes, resulting in a respiratory-deficient phenotype (Séraphin et al., 1989). Mss116 was shown to be required for efficient splicing of all mitochondrial group I and II introns, including those that do not require the assistance of an intron-encoded maturase (Huang et al., 2005). Mss116 was also shown to be involved in translation, with this function being independent of its role in splicing and primarily affecting the translation of *COX1* mRNA (De Silva et al., 2017).

In splicing of a group I intron – ai5β, Mss116 functions by binding the Mrs1 protein bound intron RNA and facilitates the exon ligation (Bifano and Caprara, 2008). Similarly, in the maturase-dependent splicing of the ai2 group II intron, Mss116 acts after the binding of the maturase protein to the intron RNA and helps in forming the catalytically active ribozyme (Bifano and Caprara, 2008). Moreover, Mss116 alone can induce self-splicing of the group II ai5γ intron that does not encode a maturase *in vitro* (Solem et al., 2006).

Purified recombinant Mss116 exhibits RNA-dependent ATPase activity *in vitro* and can separate short RNA duplexes without the requirement of 5' or 3' overhangs (Halls et al., 2007).

2.5.4. Mrh4

Mrh4 is an SF2 helicase belonging to the DEAD-box subfamily, which functions within the yeast mitochondria. The *MRH4* gene was isolated in a genetic screen as a suppressor of a splicing defect of the self-splicing group II ai5γ intron (Schmidt et al., 2002). After *MRH4* gene deletion, yeast cells experience a complete and irreversible loss of respiratory competence and convert to the rho^{-}/rho^{0} phenotype, regardless of the presence or absence of introns in mtDNA. This severe phenotype is inconsistent with a primary function involving splicing, hinting that Mrh4 has other roles in the cell (Schmidt et al., 2002).

Recent studies indicate that Mrh4 is likely associated with the ribosomal fraction in the yeast mitochondria and is involved in the late stages of mitoribosome assembly, where it is required for efficient binding of at least two ribosomal proteins, Mrpl16 and Mrpl39 (De Silva et al., 2013). The association of Mrh4 with mitoribosome biogenesis is further supported by the fact that mutants deficient in mitochondrial protein synthesis exhibit similar phenotypes to those observed in *MRH4*-deleted cells (Contamine and Picard, 2000).

Overall, the Mrh4 helicase appears to have dual roles in the splicing and mitoribosome biogenesis in the mitochondria of *S. cerevisiae* (Schmidt et al., 2002; De Silva et al., 2013).

2.5.5. Suv3

Suv3 is an SF2 helicase localized to the yeast and human mitochondria and a member of the Suv3-like subfamily, bearing a unique DEIQ tetrapeptide in the motif II (Jedrzejczak et al., 2011). Suv3 helicase is essential for RNA metabolism, and its absence also results in a total conversion to rho^{-} or rho^{0} *petites* in strains containing the complete set of mitochondrial introns (Stepien et al., 1992). However, in intronless strains or strains containing only a few mtDNA introns, some rho^{+} mtDNA can be maintained (Golik et al., 1995; Rogowska et al., 2006). Suv3 forms a 1:1 complex with Dss1 that is also known as mtEXO (yeast mitochondrial degradosome), responsible for 3' – 5' exoribonucleolytic processing of RNA in the yeast mitochondria (Dziembowski et al., 2003). The mtEXO complex is the primary pathway for maintaining the balance between RNA synthesis and degradation as the degradation deficient phenotype of the suv3Δ could be partially rescued by point mutations in *RPO41* which decrease the catalytic efficiency of the only mitochondrial RNA polymerase (Rogowska et al., 2006).

In vitro analysis of the mtEXO revealed that Suv3 in complex with Dss1 displays an ATP-dependent directional 3' to 5' RNA duplex unwinding activity and needs a free 3' ssRNA overhang for efficient loading (Malecki et al., 2007, 2008).

Moreover, Suv3 can unwind RNA/DNA and dsDNA duplexes *in vitro*, although with lower efficiency than dsRNA (Malecki et al., 2007). The presence of Suv3 in the mtEXO complex increases the exoribonuclease activity of the Dss1, while point mutations in the Suv3 protein that affect ATP hydrolysis result in a loss of the RNase activity of the degradosome (Malecki et al., 2007). These results suggest that the Suv3 helicase most likely acts as an RNA chaperone that prepares RNA for degradation by Dss1 (Malecki et al., 2007).

2.5.6. Irc3

According to the signature motif sequence, Irc3 belongs to the SF2 of helicases of a currently unclear subfamily bearing DEAH amino acids in the motif II position (De La Cruz et al., 1999; Sedman et al., 2014). Irc3 is highly conserved in different yeast and fungi species with no homologs in other organisms (Piljukov et al., 2023). *IRC3* (increased recombination centers 3) was discovered in a whole genome screen for genes involved in the recombination-driven repair of nuclear DNA in *S. cerevisiae* (Alvaro et al., 2007). Our previous studies have shown that the protein localizes to mitochondria. Moreover, mutants with a defective *IRC3* gene displayed a rapid decline in respiratory activity and loss of the functional mitochondrial genome in *S. cerevisiae* when grown on glucose-containing media (Sedman et al., 2014).

Analysis of rho$^-$ Δirc3 cells using 2D-gel electrophoresis demonstrated the appearance of specific dsDNA breaks and the loss of branched DNA structures. Interestingly, deleting mitochondrial RNA polymerase Rpo41 in Δirc3 restored the branched DNA structures on 2D-gels (Sedman et al., 2014). Those findings indicate that Irc3 is directly involved in mitochondrial NA metabolism, with a possible role in recombination pathways and control over aberrant Rpo41 associated structure formation in mtDNA (Sedman et al., 2014). Moreover, one of the recent studies found that Irc3 cofractionates with the mitochondrial small ribosomal subunits, and deletion of the *IRC3* gene, first of all, leads to decreased mitochondrial translation, which consequently results in the loss of mtDNA as the expression is needed for mtDNA stability (Kaur and Datta, 2021).

Irc3 ATPase and helicase are stimulated by dsDNA and branched DNA molecules, with four-way DNA structures mimicking a Holliday junction and DNA structures mimicking stalled replication forks being efficiently unwound *in vitro* (Gaidutšik et al., 2016). Additionally, Irc3 helicase functions as a monomeric enzyme and can translocate on dsDNA molecules (Sedman et al., 2017; Piljukov et al., 2020).

One of the main problems limiting the research of Irc3 helicase of *S. cerevisiae* ($Irc3_{sc}$) is the rapid inactivation of this enzyme at temperatures exceeding 30 °C. Consequently, a homolog of Irc3 from a thermotolerant yeast species *Ogataea polymorpha* (termed $Irc3_{op}$) has been identified and characterized (Piljukov et al., 2023). $Irc3_{op}$ helicase remains fully active above 40°C and has similar enzymatic properties to Irc3. However, contrary to $Irc3_{sc,}$ $Irc3_{op}$ ATPase is also stimulated by structured RNA molecules and ssDNA (Piljukov et al., 2023).

Overall, right now, it is evident that Irc3 helicases are important players in the yeast mitochondrial NA metabolism with possible ties to the mitochondrial gene expression and translation, but the exact function of Irc3 in the cell is not clear (Sedman et al., 2014; Kaur and Datta, 2021).

3. AIMS OF THE STUDY

Our research primarily aimed to comprehend the role of Irc3 proteins within yeast mitochondria. Despite extensive investigations conducted over decades of research, knowledge regarding yeast mitochondrial DNA and RNA metabolism still needs to be improved. Therefore, we employed various in vivo and in vitro biochemical methodologies to elucidate the biological function of the Irc3 helicase with the objective of gaining fresh insights into the processes of yeast nucleic acid metabolism.

The experimental part of this work concentrated on the following topics:

1. Conservation analysis of Irc3 helicase homologs *in silico*.
2. Evaluation of thermal stability and functional complementarity of $Irc3_{op}$ from *O. polymorpha* as an alternative to $Irc3_{sc}$ from *S. cerevisiae*.
3. Analysis of the oligomerization status of Irc3 proteins through *in vivo* experiments and *in vitro* hydrodynamic measurements and sedimentation studies.
4. Exploration of Irc3 binding preferences with DNA and RNA. Determination of Irc3 specificity, affinity, and translocation mechanism.

4. MATERIALS AND METHODS

The thesis is based on three publications that employed traditional techniques of biochemistry and molecular biology. For each publication, I have included a paragraph that briefly summarizes the methods used. More details about the experiment can be found in the original publications and corresponding supplemental materials. The list of used materials can be found in the supplemental materials of the corresponding articles.

4.1. Reference I

In this publication, two main assays were used, triple helix displacement and ATP hydrolysis assay. In the triple helix displacement assay, a mixture of triple helix substrate and Irc3 was prepared in a buffer solution. The mixture was incubated at 30 °C for a specified duration, after which a reaction-stopping solution was added. The resulting products were then analyzed using polyacrylamide gels with electrophoresis. The gels were subsequently dried, exposed to phosphoimager screens, and analyzed using ImageQuant TL software (GE Healthcare).

For the ATP hydrolysis assays, two different methods were employed. The first method involved monitoring ATP hydrolysis (ATPase) through charcoal binding. The second method utilized an NADH oxidation-coupled spectrophotometric assay. Following ATP conversion to ADP by the enzyme, a multi-step reaction of ATP regeneration occurs. First, pyruvate kinase catalyzes the conversion of phosphoenolpyruvate and ADP to pyruvate and ATP. Second, lactate dehydrogenase catalyzes the conversion of pyruvate and NADH to lactate, and NAD^+ and the equimolar conversion of NADH to NAD^+ is monitored spectrophotometrically at 340 nm using $\varepsilon = 6220$ m–1 cm–1. Finally, the rate of ATP hydrolysis is calculated, considering the equimolar relation of NADH conversion to ATP hydrolysis. The steady-state reaction rate was determined by linear fitting of the linear portion of the reaction curve. The cofactors were tested in triplicate, covering at least a 400-fold range of DNA concentrations. The kinetic parameters v_{max} and K_{DNA} were determined using nonlinear curve fitting in GraphPad Prism v5.

4.2. Reference II

The research conducted in this publication involved four main methods: DNase I Footprinting, Sedimentation Analysis, Size-Exclusion Chromatography, and ATP Hydrolysis Assay.

For DNase I Footprinting, varying amounts of Irc3 protein were blended with radiolabeled DNA cofactors in a buffer solution. These mixtures were then incubated on ice and treated with DNase I enzyme. After being separated on a

denaturing gel, the intensity of the bands was measured to differentiate between the Irc3-DNA complex protected and naked DNA.

The Irc3 protein and Irc3-DNA complex were analyzed through Sedimentation Analysis, which employed running samples on glycerol gradients in an ultracentrifuge. The protein content in the gradient fractions was evaluated using protein ATP Hydrolysis Assay and SDS/PAGE, while the Irc3-DNA complex was detected using electrophoresis in a non-denaturing gel.

In Size-Exclusion Chromatography, a gel filtration column was utilized to determine the Stokes radius of Irc3. A protein sample was run through a 24 mL Superdex-75 gel filtration column, while the column was calibrated using protein standard. Chromatography fractions were analyzed for protein content and ATP hydrolysis activity.

Finally, the NADH oxidation-coupled assay was used to measure Irc3 ATP hydrolysis activity, similar to the method described in paragraph 4.1.

4.3. Reference III

This publication utilized three primary methods for analysis: Circular Dichroism Analysis, Analysis of Irc3op-DNA Complex Formation by Fluorescence Anisotropy, and ATP Hydrolysis Assay.

In order to analyze the Irc3op protein, Circular Dichroism Analysis was conducted. This involved performing Full CD spectra and secondary structure melting experiments within a wavelength range of 180–280 nm using a CD spectrometer. The recorded signals were corrected for protein concentration and presented as molar ellipticity. For the secondary structure melting experiments, CD signals were recorded at 208 nm while gradually increasing the temperature, and the resulting change in molar ellipticity values was plotted as a function of temperature.

In addition, to analyze the Irc3op-DNA Complex Formation, Fluorescence Anisotropy was used. This involved using fluorescein-labeled DNA cofactors and varying the concentration of the Irc3op protein while maintaining a constant DNA concentration. Fluorescence anisotropy measurements were then taken at a specific temperature, and the anisotropy value was calculated based on the parallel and perpendicular emitted fluorescence signals. The resulting data were fitted to a hyperbolic function to determine the apparent dissociation constant (Kd).

Finally, the NADH oxidation-coupled assay was used to measure Irc3 ATP hydrolysis activity, similar to the method described in paragraph 4.1.

5. RESULTS AND DISCUSSION

5.1. Irc3 is a mitochondrial helicase in yeasts

With the growing availability of full genome sequences and protein annotations, we decided to investigate the conservation of the Saccharomyces cerevisiae Irc3 ($Irc3_{sc}$) protein across different organisms. Through *in silico* analysis using the BLAST algorithm, we identified homologs of the Irc3 helicase in both ascomycete and basidiomycete yeasts but not in organisms outside of the fungus kingdom (Fig. 1A, B in III). Of particular note is the presence of a putative mitochondrial matrix targeting signal and conserved set of helicase motifs in all homologs of Irc3. Moreover, these homologs lack additional N-terminal domains, while their C-terminal domains display weak sequence conservation (Fig. 1A, B in III).

When we compared $Irc3_{sc}$ with other *S. cerevisiae* helicases reviewed in this study, we found no homology for regions besides the helicase core. Therefore, we decided to align the helicase core sequences of $Irc3_{sc}$ with helicases of *S. cerevisiae* belonging to the subfamilies reviewed in this study: Mss116, Prp43, Sgs1, and Mtr4 (Figure 6). Interestingly, according to UniProt, Mss116 protein, belonging to the DEAD-box helicase subfamily, showed the highest sequence identity of 26.2% with Irc3sc (The UniProt Consortium, 2023). Similarly, the Prp43 protein from the DEAH-box helicase subfamily exhibited a sequence identity of 20.1% (The UniProt Consortium, 2023). Concurrently, both proteins demonstrated significant conservation in motif sequences and positions compared to $Irc3_{sc}$ (Figure 6).

Notably, DEAD-box helicases are significantly different from DEAH-box helicases biochemically, being distributive enzymes with a more loosely packed helicase core. In contrast, DEAH-box enzymes are tightly packed around the NA channel (Singleton et al., 2007). The intriguing aspect lies in the similarity observed between Irc3 and the DEAD-box helicase subfamily, as $Irc3_{sc}$ was initially annotated as a part of the DEAD-box subfamily, despite featuring a DEAH motif in the motif II position (De La Cruz et al., 1999). This classification was based on the remarkable resemblance of other motifs to enzymes within the DEAD-box-like subfamily (De La Cruz et al., 1999).

The high similarity of the helicase core region of $Irc3_{sc}$ to Mss116 and generally helicases of the DEAD-box subfamily is particularly intriguing concerning domains Ia and V, which are likely responsible for NA specificity and could hint to unique properties of Irc3 enzymes in relation to NA utilization (Figure 6).

	Motif I			Motif Ia			Motif II			Motif III		
Q06683_Irc3	0	TGGGKT	7	30	LILVHRRELA	41	97	DEAH	102	129	SAT	133
P15424_Mss116	0	TGTGKT	7	30	VIVAPTRDLA	41	113	DEAD	118	151	SAT	155
P53131_Prp43	0	TGSGKT	7	26	ACTQPRRVAA	37	97	DEAH	102	129	SAT	133
P35187_Sgs1	0	TGGGKS	7	24	IVISPLISLM	35	106	DEAH	111	141	TAT	145
P47047_Mtr4	0	TSAGKT	7	23	IYTSPIKALS	34	89	DEVH	94	120	SAT	124

	Motif IV			Motif V			Motif Va			Motif VI		
Q06683_Irc3	221	LLFGVD	228	270	VLMNC	276	278	TEGTD	284	303	QMIGRGLR	312
P15424_Mss116	223	IIFAPT	230	275	ILVCT	281	283	ARGMD	289	308	HRIGRTAR	317
P53131_Prp43	225	PLYGSL	232	272	YVVDP	278	280	KQKVY	286	305	QRAGRAGR	314
P35187_Sgs1	203	IIYCHS	210	251	VICAT	257	259	GMGID	265	284	QETGRAGR	293
P47047_Mtr4	237	IVFSFS	244	325	VLFAT	331	333	SIGLN	339	366	QMSGRAGR	375

Figure 6. Alignment of helicase motifs of *S. cerevisiae* helicases. Numbers define the position of previous or subsequent amino acids relative to the helicase motif I position of marked helicases. Motifs sharing 0–50% similarity to $Irc3_{sc}$ are colored orange. Motifs sharing 50–80% similarity – yellow and 80–100% – green. Similarity is defined as identical amino acids or amino acids sharing similar chemical properties in the same position (The UniProt Consortium, 2023).

Our study was followed by modeling the $Irc3_{sc}$ structure using AlphaFold, an artificial intelligence-based system trained on a database of known protein structures and capable of predicting the structure of proteins from their sequences (Jumper et al., 2021). The predicted structure of $Irc3_{sc}$ (Figure 7) has an expected configuration of RecA1 and RecA2 domains at the protein N-terminus and a C-terminal structure resembling the fist domain of the Ski2-like subfamily of helicases at the protein C-terminus (as compared in Figure 7 and Figure 5). This observation aligns with the previous knowledge that the C-terminuses of Ski2-like helicases have a low sequence conservation despite folding into similar structures (Jackson et al., 2010; Halbach et al., 2012). Additionally, Hel308, a well-studied Ski2-like helicase, exhibits biochemical properties similar to those of $Irc3_{op}$, such as preferential binding to single-stranded DNA over double-stranded DNA (with Kd values of 140 nM and 5300 nM, respectively) (Richards et al., 2008), unwinds all types of replication fork-like cofactors with the best specificity for lagging strand replication fork (Guy, 2005), and the ATPase activity of Hel308 could be inhibited by ssDNA (Richards et al., 2008). Moreover, $Irc3_{op}$ ATPase activity is stimulated by structured RNA, such as tRNA and rRNA, which is a characteristic trait of another Ski2-like subfamily helicase – Mtr4 (Weir et al., 2010).

However, it should be noted that the conservation of the Irc3 helicase core sequence and motif position is lower with Ski2-like helicases than with other helicase subfamilies discussed in this work (as demonstrated in Figure 6). Additionally, none of the Ski2-like representatives are measurably stimulated by double-stranded DNA, one of the better nucleic acid stimulants of the ATPase activity of Irc3 (Gaidutšik et al., 2016).

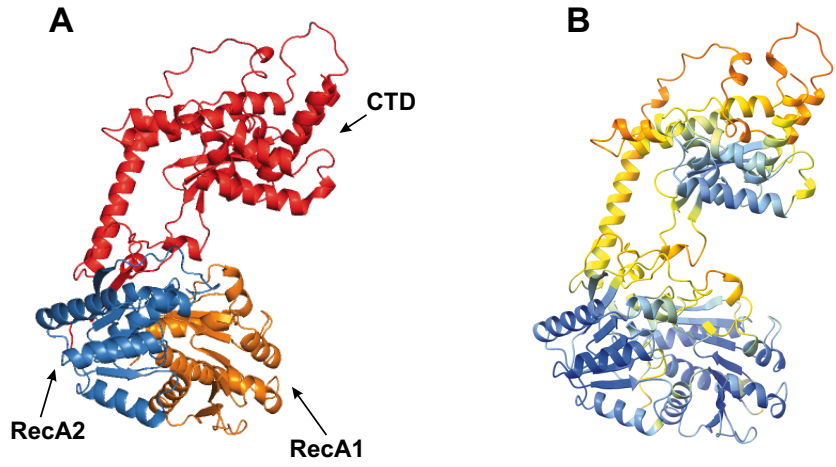

Figure 7. Predicted structure of Irc3 from *S. cerevisiae*. The structure of $Irc3_{sc}$ predicted the protein sequence using AlphaFold (Jumper et al., 2021). Conserved helicase core domains are shown in orange (RecA1) or blue (RecA2). The C-terminal domain (CTD) is red. (B) Predicted structure colored according to AlphaFold per-residue confidence metric (pLDDT), darker blue is > 90% confident, lighter blue is 70–90% confident, yellow is 50–70% confident, and orange is < 50% confident.

5.2. Irc3 of Ogataea polymorpha

Previously recombinant Irc3 of *Saccharomyces cerevisiae* has been used in all of our biochemical experiments. Unfortunately, this has always constrained our assays due to technical difficulties associated with the protein thermal stability (I and II). Particularly, the low thermal stability of $Irc3_{sc}$ limited the duration of our kinetic measurements and hindered purification in concentrations required by protein-NA complex formation studies, which has presented challenges for enzyme characterization (I and II). Given the widespread conservation of Irc3 homologs across different yeast species, we have decided to switch to a homologous Irc3 helicase from a thermotolerant yeast for further purification and experimentation (III). Specifically, we purified $Irc3_{op}$, a 68.5 kDa homolog of $Irc3_{sc,}$ from the thermotolerant yeast *Ogataea polymorpha* (Fig. 2A in III). $Irc3_{op}$ has 82% helicase core sequence similarity to $Irc3_{sc}$ and a comparatively much shorter C-terminal region of 29.9 kDa, compared to 36 kDa in $Irc3_{sc}$ (Fig. 1A, B in III). Our study highlighted the importance of the C-terminal part of $Irc3_{sc}$ in its capacity to bind branched DNA molecules (I). The observed variability in size and sequence of the Irc3 C-terminal region raises the question of whether this domain is structurally and functionally similar between these two homologs of Irc3. Consequently, we performed a comparative analysis of AlphaFold-generated predictions of $Irc3_{sc}$ and $Irc3_{op}$ structures (Figures 7 and 8) and observed that the most C-terminal region of both enzymes is structurally similar and bears resemblance to the fist domain of the Ski2-like subfamily (Figure 5).

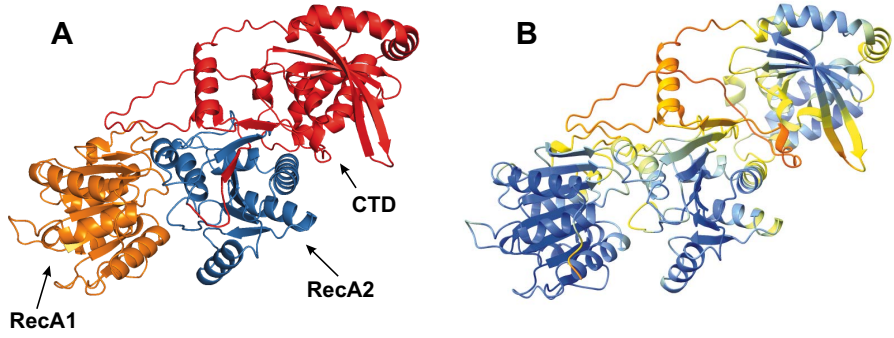

Figure 8. Predicted structure of Irc3 from *O. polymorpha*. The structure of $Irc3_{op}$ was predicted from the protein sequence using AlphaFold (Jumper et al., 2021). (A) Conserved helicase core domains are shown in orange (RecA1) or blue (RecA2). The C-terminal domain (CTD) is red. (B) Predicted structure colored according to AlphaFold per-residue confidence metric (pLDDT), darker blue is > 90% confident, lighter blue is 70–90% confident, yellow is 50–70% confident, and orange is < 50% confident.

Although the high degree of sequence similarity exhibited between $Irc3_{sc}$ and $Irc3_{op}$, we aimed to demonstrate the possibility of *in vivo* complementation of the respiratory deficiency phenotype resulting from the deletion of $Irc3_{sc}$ with $Irc3_{op}$ (Fig. 1C in III), as well as prove the superior stability of $Irc3_{op}$ (Fig. 2B, D in III). For assessment of $IRC3_{op}$ complementation of $IRC3_{sc}$ deletion *in vivo*, the S. cerevisiae $irc3_{sc}\Delta$ strain was transformed with a centromeric plasmid containing $IRC3_{op}$ cloned between the $IRC3_{sc}$ regulatory elements, 400 nucleotides upstream and 400 nucleotides downstream of the naturally occurring $IRC3_{sc}$ gene (III). Next, we assessed the dynamics of loss of respiratory proficiency amongst the cells grown in glucose-containing media with four different strains: previously constructed $IRC3_{op}$ construct, similar $IRC3_{sc}$ construct as a positive control, empty plasmid vector as a negative control, and bacterial RecG helicase that was shown previously to have partial $IRC3_{sc}$ complementation in a similar assay (Fig. 1C in III and Gaidutšik et al., 2016). The assay consisted of three steps: pregrowth of transformed cells in selective glycerol-containing media, the release of cells into liquid synthetic complete medium – Leu containing 2% glucose, and taking samples at 24 h, 72 h, 168 h followed by plating them onto media containing 0.15% glucose and 3% glycerol. Respiration-proficient cells successfully utilize both carbon sources and give rise to distinctly larger colonies on this type of media, while the colonies of respiration-deficient cells remain small. Our experiments showed that $IRC3_{op}$ could partially rescue the $irc3_{sc}\Delta$ phenotype as approximately 60% of the $irc3_{sc}\Delta$ cells expressing $IRC3_{op}$ gave rise to large colonies even after 168 h of growth in a glucose-containing media (Fig. 1C in III). At the same time, $irc3_{sc}\Delta$ cells gave rise to about only 5%, and the positive control strain with wt $IRC3_{sc}$ returned on a plasmid with 100% large colonies on a plate. The complementation of $irc3_{sc}\Delta$ by bacterial RECG resulted in around 20% of the cells giving rise to large colonies, similar to our previous results of 12% (Fig. 1C in III and Gaidutšik et al., 2016).

Next, we aimed to understand whether $Irc3_{op}$ protein has greater thermal stability than $Irc3_{sc}$. For that purpose, we used two distinct methods: measurement of DNA-stimulated ATP hydrolysis by $Irc3_{op}$ at varied temperatures (Fig. 2B in III) and the melting of the secondary structure of the $Irc3_{op}$ protein as a measure of circular dichroism (CD) signal decrease at 208 nm (Fig. 2D in III). First of all, we expressed a recombinant $Irc3_{op}$ protein without mitochondrial import signal from *E. coli* BL21 RIL (DE3) strain as a His10-SUMO-(Δ19)$Irc3_{op}$ fusion protein (III). Then, recombinant $Irc3_{op}$ was obtained by a combination of Ni-NTA agarose affinity chromatography, Sumo-tag specific protease cleavage, and heparin agarose chromatography (III). After purification, the catalytic activity of $Irc3_{op}$ DNA-stimulated ATP hydrolysis was measured by detecting the release of γ-phosphate from the radiolabeled γ^{32}P-ATP (III). During the experiment, the temperature of the ATP hydrolysis reaction was increased from 30 °C to 52 °C. As a result, the maximum rate of ATP hydrolysis for $Irc3_{op}$ was measured at 41 °C, with about 80% of enzymatic activity retained up to 45 °C (Fig. 2B in III).

Another approach used to assess the thermal stability of $Irc3_{op}$ was based on circular dichroism (CD) spectroscopy. Circular dichroism (CD) spectroscopy is a valuable technique for analyzing the secondary structure of proteins. It involves measuring the differential absorption of left- and right-circularly polarized light at different wavelengths by a sample, which can provide information about the presence of alpha-helices and beta-sheets. First, we measured the full CD spectrum from 180 to 280 nm to investigate the secondary structure of the $Irc3_{op}$ protein sample (Fig. 2C in III). From the full spectrum (Figure 2C in III), we have chosen a 208 nm wavelength with a high CD signal, most likely corresponding to mainly alpha-helices (Köster et al., 2015). Next, we continuously recorded the CD signal at 208 nm while gradually increasing the temperature of the protein solution (Fig. 2D in III). This allowed us to monitor the changes in the secondary structures inside the protein as it underwent thermal denaturation. The results showed that as the temperature increased, the protein secondary structures began to melt, causing a gradual decrease in the CD signal (Fig. 2D in III). By analyzing the melting curve, we determined the melting temperature to be around 45 °C, corresponding to the temperature at which half of the change in the CD signal occurred.

The secondary structure melting data is consistent with our ATPase experiment and supports the hypothesis that $Irc3_{op}$ exhibits improved thermal stability when compared to $Irc3_{sc}$ (Fig. 2D in III). It is worth noting that the measured melting temperature is not particularly high, even when compared to other helicases of *S. cerevisiae* that were investigated in a large-scale proteomic study. For example, Ded1, a DEAD-box helicase with nuclear localization, had a melting temperature of 43 °C, while RNA helicase eIF4A had a melting temperature of 50 °C (Leuenberger et al., 2017). However, the higher thermal stability of $Irc3_{op}$ in comparison to $Irc3_{sc}$ was enough to reach our goal of increasing the quality of our kinetic measurements while simultaneously increasing the purity and concentration of our recombinant protein preparations.

5.3. Oligomerization of Irc3 proteins

5.3.1. Irc3 of Saccharomyces cerevisiae

Previously conducted studies have demonstrated that Irc3 has a DNA-stimulated ATPase activity (Gaidutšik et al., 2016). In addition, it has been observed that branched DNA molecules like Y-shaped DNA forks or Holliday junctions exhibit greater ATPase stimulation activity, which aligns with the capabilities of Irc3 to facilitate branch migration and reversal of replication forks (Gaidutšik et al., 2016). However, the intricacies of how Irc3 forms complexes with DNA, moves along the DNA molecule, and unwinds the DNA remains largely unexplored.

In this part, we seek to determine whether Irc3 functions as a monomer or multimer. Our prior research revealed that deleting the $IRC3_{sc}$ gene in *S. cerevisiae* results in a swift decline of respiratory-proficient cells without selection (fermentable growth media) (Sedman et al., 2014). Similarly, in our $irc3_{sc}\Delta$ complementation by $IRC3_{op}$ experiment, we demonstrated that the negative control transformed with empty plasmid primarily produced respiratory-deficient yeast cells that formed small colonies on low glucose media (Fig. 1C in III). Building upon these results, we aimed to examine the phenotypes of *S. cerevisiae* strains with extra copies of mutant or wild-type (wt) $IRC3_{sc}$ genes. We constructed four *in vivo* expression plasmids based on pRS315, containing either wt or mutant $IRC3_{sc}$ genes. The plasmids contained copies of $IRC3_{sc}$ genes bearing point mutations in the helicase motifs I, III, and IV derived from the alignment of Irc3 enzymes (Fig. 1B, Sup. Fig. 1 in III). These point mutations alter amino acids in conserved helicase motifs that are potentially critical for the ATPase or helicase activity of $Irc3_{sc}$. According to current knowledge about helicase motif functions, the Irc3-K65A mutation in the motif I should impair ATP hydrolysis activity and was also shown to be inactive in ATPase and DNA unwinding assays in our previous work (Sedman et al., 2014). Irc3-S190A, T192A bearing mutations in the motif III sequence, which is expected to be essential for linking ATP hydrolysis to movement along the NA lattice, and Irc3-L284A mutation in the motif IV, which is expected to play a role in nucleic acid substrate binding (Singleton et al., 2007). Then, we transformed wt yeast strain W303-1A with the constructed plasmids and analyzed the strains for *petite* colony formation frequency for six days, using the same scheme described previously for the $IRC3_{op}$ complementation experiment (see section 5.2.).

The results indicated that moderate overexpression of wt Irc3 did not alter the frequency of *petite* colony formation (Fig. 1B in II). However, yeast strains transformed with the Irc3 mutants (Irc3-65A; Irc3-190A, 192A, or Irc3-284A) had significantly more *petite* colonies Fig. 1B in II). This dominant negative phenotype could suggest that Irc3 could form an oligomer *in vivo,* and adding mutant Irc3 monomers to the oligomeric structure disables the Irc3 helicase. Alternatively, this phenotype could also result from mutant Irc3 proteins competing with wt Irc3 for a limited number of some specific NA targets in the yeast mitochondria. Thus, we decided to further investigate the oligomerization of Irc3 *in vitro*.

5.3.2. Hydrodynamic analysis of Irc3

One way to analyze the oligomerization of a protein is to calculate its apparent molecular weight from hydrodynamic measurements. The sedimentation coefficient (S) of a given protein indicates the velocity at which it migrates through a gradient. The protein mass affects the sedimentation rate, with increased mass resulting in increased sedimentation. However, larger or asymmetric proteins exhibit decreased sedimentation (Erickson, 2009). Stokes radius (R) is a measure of protein mobility through a gel filtration column defined as the radius of an imaginary sphere that would have the appropriate friction coefficient to explain the observed protein mobility (Erickson, 2009). Knowing the sedimentation coefficient (S) and the friction coefficient defined through the experimentally measured Stokes radius (R), the apparent molecular weight of a protein could be calculated using a simplified equation of Siegel and Monte, Mw(app)=4.205(SR) (Erickson, 2009). Here we used hydrodynamics to investigate the oligomerization state of $Irc3_{op}$ and $Irc3_{sc}$, two members of the Irc3 family. Both proteins were expressed as recombinant proteins without the mitochondrial import signal in E. coli BL21 RIL (DE3) strain as a His10-SUMO-(Δ28)$Irc3_{sc}$ or His10-SUMO-(Δ19)$Irc3_{op}$ fusion proteins. The purification protocol was the same as described for $Irc3_{op}$ purification in the previous paragraph (see section 5.2.). Next, Svedberg coefficients (S) were measured for both proteins from the sedimentation analysis on 10–20% glycerol gradients and Stokes radiuses (R) from the mobility analysis on a Superdex-75 size-exclusion column (Fig. 3A, B in II and Sup. Fig. 2A, B in III). The S values were 3.8S and 3.9S for $Irc3_{sc}$ and $Irc3_{op}$, respectively, less than the S value of bovine serum albumin (BSA) (4.7S). The R values were 4.2 nm and 3.85 nm for $Irc3_{sc}$ and $Irc3_{op}$, respectively, higher than the Stokes radius of BSA (3.6 nm). Using the equation Mw(app)=4.205(SR) (Erickson, 2009), we calculated the apparent molecular weight of $Irc3_{sc}$ and $Irc3_{op}$ to be 67 kDa and 63 kDa, which is close to their theoretical molecular weight of 75.4 kDa and 68.5 kDa derived from the amino acid sequence. This data indicates that both recombinant Irc3 proteins are monomeric in solution.

5.3.3. Hydrodynamic analysis of $Irc3_{sc}$ complexes with DNA

Our analysis revealed no evidence of protein oligomerization in samples containing purified recombinant $Irc3_{sc}$ protein (see section 5.3.2.). However, given that the proteins are always present in cells alongside nucleic acids, we decided to examine the sedimentation rates of $Irc3_{sc}$-DNA complexes (II). For this purpose, we utilized a similar method, sedimentation in 10–20% glycerol gradients. Complexes were formed by combining 100 nM $Irc3_{sc}$ with an equal amount of ^{32}P-labeled DNA cofactors that resembled the lagging strand replication fork or the Holliday junction. The lagging strand replication fork cofactor contains a dsDNA region of 25 bp which branches to a 25 nt ssDNA and a 25 bp dsDNA region, resembling a replication fork with a nascently synthesized lagging strand. The Holliday-junction cofactor contained four 25 bp dsDNA regions joined

together, resembling a DNA recombination intermediate. Next, we fixed the resulting Irc3-DNA complexes with 0.5% glutaraldehyde and proceeded with the fractionation on glycerol gradients. The sedimentation velocity of Irc3-DNA complexes was analyzed by resolving gradient fractions on 5% non-denaturing polyacrylamide gels, followed by autoradiography (Fig. 4C in II). Our analysis revealed that the complex formed by $Irc3_{sc}$ with the replication fork-like substrate exhibited a Svedberg coefficient of 6.4S, while the complex with a Holliday-junction model substrate exhibited a coefficient of 7.8S. These values correspond to globular proteins with molecular weights of 125 kDa and 164.5 kDa, respectively, whereas the calculated molecular weights for these complexes were 116.3 kDa and 140.8 kDa (II).

We designed an alternative experiment to confirm that Irc3sc forms a 1:1 stoichiometric complex with DNA. In that experiment, we purified a 10His-Sumo-$Irc3_{sc}$ (Sumo-$Irc3_{sc}$) fusion undigested protein that can form protein-DNA complexes similarly to the full protocol-purified $Irc3_{sc}$ (II). Sumo-$Irc3_{sc}$ complexes with DNA move more slowly in the electrophoresis mobility shift assay (EMSA) on the native polyacrylamide gels due to their higher molecular weight (Fig. 4B in II). We formed complexes with three different ^{32}P-labeled DNA cofactors resembling the lagging strand replication fork, leading strand replication fork, or the Holliday-junction, using Sumo-$Irc3_{sc}$, $Irc3_{sc}$, or a mixture of both protein types. Our results indicated that the fastest moving complexes, where most of the signal resides, corresponded to 1:1 protein to DNA complexes, as no intermediary band appeared with a mixture of both protein types, only bands corresponding to complexes with either of the protein types separately (Fig. 4B in II). Interestingly, new bands formed in the region with slower-moving complexes, suggesting that a small population of complexes with higher than 1:1 protein-to-DNA ratios are still formed, with this effect being more prominent at higher protein concentrations (Fig. 4B in II). Nonetheless, this experiment supports the idea that most $Irc3_{sc}$-DNA complexes are stoichiometric 1:1 complexes.

5.3.4. Oligomerization of $Irc3_{sc}$ during ATP hydrolysis

Data from the previous experiments indicated that both Irc3 proteins are monomeric in solution, and the majority of complexes of $Irc3_{sc}$ with DNA are 1:1 complexes (see sections 5.3.2. and 5.3.3.). However, the overexpression of mutant $Irc3_{sc}$ proteins had a dominant negative phenotype (Fig. 1B in II), which could mean that the functional form of $Irc3_{sc}$ is multimeric *in vivo* in the presence of ATP and a nucleic acid cofactor. Thus, we decided to use steady-state ATP hydrolysis analysis to determine whether the kinetic properties of $Irc3_{sc}$ are affected by oligomerization.

For the measurement of the ATP hydrolysis rate of $Irc3_{sc,}$ we used an assay where ATP hydrolysis is linked to NADH oxidation. Following ATP conversion to ADP by the enzyme studied ($Irc3_{sc}$ in our case), a multi-step reaction of ATP regeneration occurs. First, pyruvate kinase catalyzes the conversion of phosphoenolpyruvate and ADP to pyruvate and ATP. Second, lactate dehydrogenase

catalyzes the conversion of pyruvate and NADH to lactate, and NAD^+ and the equimolar conversion of NADH to NAD^+ is monitored spectrophotometrically at 340 nm using $\varepsilon = 6220\ m^{-1}\ cm^{-1}$. Finally, the rate of ATP hydrolysis is calculated, taking into account the equimolar relation of NADH conversion to ATP hydrolysis (Figure 9).

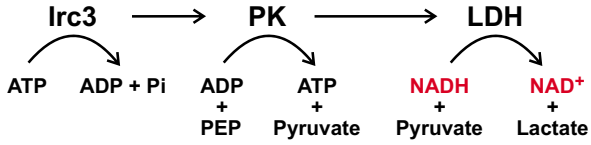

Figure 9. Scheme of the conjugated ATP hydrolysis assay. In the first step, ATP conversion to ADP by Irc3 enzyme is shown, which is followed by ATP regeneration where pyruvate kinase catalyzes the conversion of phosphoenolpyruvate and ADP to pyruvate and ATP and lactate dehydrogenase catalyzes the conversion of pyruvate and NADH to lactate and NAD^+. NADH to NAD^+ (marked red) conversion is monitored spectrophotometrically at 340 nm.

The first set of steady-state ATP hydrolysis experiments was based on the hypothesis that if protein multimerization is necessary for ATPase activity, titration of ATPase inactive mutant $Irc3_{sc}$-K65A to wt $Irc3_{sc}$-containing reactions should generate complexes where one or more monomers are replaced by $Irc3_{sc}$-65A. Therefore, the apparent specific activity should decrease as a response to $Irc3_{sc}$-K65A titration. The ATPase inactive mutant was purified using the same protocol as the wt $Irc3_{sc}$ protein. We found that the ATPase activity of $Irc3_{sc}$ did not change upon adding up to four times higher amounts of $Irc3_{sc}$-K65A to the reaction (Fig. 6A, B in II).

The second set of experiments was based on the assumption that if protein multimerization is required for ATPase activity, increasing the concentration of $Irc3_{sc}$ in the reaction should promote oligomerization, and the measured specific activity at higher enzyme concentrations should be higher than at lower enzyme concentrations (positive cooperativity). However, contrary to our hypothesis, we found that the specific ATPase activity of $Irc3_{sc}$ decreased in response to an increase in enzyme concentration. This indicates that $Irc3_{sc}$ could form multimeric complexes at higher protein concentrations. However, the formed complexes are inactive or less active than the monomeric protein (Fig. 6C, D in II).

5.3.5. $Irc3_{sc}$ enzyme oligomerization during DNA unwinding

After revealing that the specific ATPase activity of $Irc3_{sc}$ is negatively correlated with the enzyme concentration, we asked if this correlation extends to the helicase activity of Irc3, the likely main biochemical activity of the protein in the cell. Similarly to the previous analysis of ATPase activity, we measured the rates of DNA cofactor unwinding in response to an increase of $Irc3_{sc}$ concentration in the helicase assay (II). Here, the activity of Irc3 was followed by the release of

unwound ssDNA. Irc3 was mixed with ATP and an appropriate DNA cofactor labeled with radioactive ^{32}P at one of the strands, followed by taking samples from the reaction mixture at specified time points and analyzing the samples on 10% nondenaturing PAGE (Fig. 7A, B in II). DNA cofactors resembling either the lagging strand replication fork or leading strand replication fork were used, with the nascent DNA strand labeled with ^{32}P at the 5' terminus. The unwinding reaction products were detected by radioactive signal imaging, and the reaction rate was assessed from the relative decrease in the radioactive signal of the substrate band. Similarly to the ATP hydrolysis measurement experiments, the rate of DNA unwinding activity, when normalized to $Irc3_{sc}$ concentration, decreased in response to the increase of enzyme concentration (Fig. 7C, D in II).

The functional studies of Irc3 oligomerization indicated that all components required for the ATPase and helicase activities of $Irc3_{sc}$ are contained in each protein subunit. Therefore, the protein is most likely functioning as a monomer, and the multimeric complexes detected *in vitro* at elevated concentrations of $Irc3_{sc}$ represent inactive or less active forms of the protein.

5.4. Nucleic acid specificity of Irc3 proteins

5.4.1. Stimulation of ATP hydrolysis activity of $Irc3_{op}$ by DNA and RNA cofactors

In this series of experiments, we aimed to investigate whether the NA cofactor specificity of $Irc3_{sc}$ and $Irc3_{op}$ is similar. Our previous research indicated that $Irc3_{sc}$ ATP hydrolysis is stimulated by the mitochondrial DNA of *S. cerevisiae* and synthetic DNA molecules containing dsDNA regions (Sedman et al., 2014; Gaidutšik et al., 2016). To measure the ATPase activity of $Irc3_{op}$, we used a conjugated assay where ATP hydrolysis is linked to NADH oxidation, as previously described in 5.3.4. paragraph. We obtained two parameters for each cofactor: k_{cat}, the rate of ATP hydrolysis normalized to enzyme concentration at the saturating NA concentration, and K_{DNA} (or K_{RNA}), the concentration of a DNA or RNA cofactor when the rate of ATP hydrolysis is half of the maximum obtained with the same NA cofactor. Additionally, we calculated the specificity coefficient k_{cat}/K_{DNA} or k_{cat}/K_{RNA} for each NA cofactor used, which takes into account the maximal rate of ATP hydrolysis for any given NA cofactor and the concentration of a cofactor needed to reach that to gain a more comprehensive understanding of enzyme cofactor specificity.

For these experiments, we prepared a set of synthetic DNA cofactors: replication fork-like cofactor with 25 bp long dsDNA parental duplex and two 25 nt long ssDNA branches, 50 bp long dsDNA cofactor, and 50 nt long ssDNA cofactor. Similar DNA cofactors were used previously with $Irc3_{sc}$ (Gaidutšik et al., 2016). All the DNA cofactors were prepared by annealing commercially purchased oligonucleotides. Equivalent RNA cofactors were assembled similarly to the DNA cofactors, with the only difference being that RNA oligonucleotides

were synthesized by *in vitro* transcription with T7 RNA polymerase. Additionally, we purified structured RNA from *O. polymorpha* mitochondria and separated it into tRNA and rRNA fractions on a Superose-12 column (III).

The specificity factors of $Irc3_{op}$ for all synthetic RNA cofactors fluctuated around 1 s^{-1} μM^{-1} or was immeasurable due to an exceptionally high K_{RNA} value. In contrast, the specificity for corresponding synthetic DNA cofactors was much higher, with values of 39.8 s^{-1} μM^{-1} for ssDNA, 33.2 s^{-1} μM^{-1} for dsDNA, and 376.4 s^{-1} μM^{-1} for replication fork-like DNA cofactors. Measurements with structured RNA revealed specificity factors of 6.3 s^{-1} μM^{-1} for rRNA and 9.8 s^{-1} μM^{-1} for tRNA (Table 1 in III). Interestingly, our study also found that ssDNA inhibits the ATPase activity of $Irc3_{op}$ observed in the presence of other nucleic acid cofactors (Table 2 in III). This is likely due to ssDNA challenging the binding of dsDNA or branched DNA to an overlapping binding site on $Irc3_{op}$.

In our previous articles, we have demonstrated that $Irc3_{sc}$ ATPase activity is stimulated by synthetic dsDNA molecules, branched replication fork-like molecules, and 4-way Holliday junction-like cofactors, while ssDNA and RNA molecules had no detectable activation for $Irc3_{sc}$ (Sedman et al., 2014; Gaidutšik et al., 2016). In those articles, the ATP hydrolysis of $Irc3_{sc}$ was measured by detecting the release of γ-phosphate from the radiolabeled γ^{32}P-ATP which is a much less sensitive method than the currently used NADH-oxidation coupled ATP hydrolysis assay. Moreover, detecting γ-phosphate from the radiolabeled γ^{32}P-ATP is often associated with high radioactive background levels, which could hinder the ATP hydrolysis measurement with weakly stimulating cofactors. Contrary to our previous ATP hydrolysis measurements with $Irc3_{sc}$, $Irc3_{op}$ was stimulated by ssDNA and RNA cofactors and all cofactors containing a dsDNA region (Table 1 in III). All synthetic RNA cofactors used could stimulate the $Irc3_{op}$ ATPase activity but were approximately 5–10-fold less efficient when compared to the corresponding DNA cofactors (Table 1 in III). Furthermore, our results suggest that the most effective cofactor for $Irc3_{op}$ among the tested nucleic acid cofactors is a 50 bp long replication fork-like DNA cofactor. In contrast, Holliday junction-like cofactor was previously found to be the best for Irc3sc (Table 1 in III, Gaidutšik et al., 2016). Additionally, we found that $Irc3_{op}$ is 5–10 times better stimulated by structured native RNA molecules than by synthetic RNA cofactors (Table 1 in III). We suggest that $Irc3_{op}$ has the potential to bind and remodel various structured nucleic acid molecules with a better specificity for branched DNA molecules.

5.4.2. $Irc3_{sc}$ binding to branched DNA cofactors

The apparent preference for branched DNA molecules was already suggested for $Irc3_{sc}$ (Gaidutšik et al., 2016). Here we used DNase I footprinting to understand the structure of $Irc3_{sc}$ complexes with branched DNA cofactors (II). Analysis was started by forming complexes of $Irc3_{sc}$ and replication fork-like model cofactors labeled with radioactive ^{32}P at one of the strands with a 1:1 or 3:1 protein to NA cofactor ratio. Formed $Irc3_{sc}$ complexes with DNA cofactors were subjected to

DNase I digestion for different time periods, followed by the digestion pattern analysis on a 15% (19:1 acrylamide:bis-acrylamide) 7 M urea denaturing gel (Sup. Fig. 3 in II).

The results of the digestion pattern analysis from footprinting of $Irc3_{sc}$ complexes with branched DNA molecules indicated that $Irc3_{sc}$ was capable of protecting the branching point of DNA replication fork-like model structures that contained nascent leading, nascent lagging or neither of the nascent strands (Fig. 5A, B in II). Additionally, the first base pair of both parental duplex strands was protected and up to five nucleotides away from the branching point in the lagging strand template of all used model cofactors (Fig. 5B in II). Interestingly, only a small number of protected nucleotides were detected in the parental duplex upstream of the fork, hinting that Irc3 could be loaded directly onto DNA structures from the branching point and not from the free dsDNA end. Observed stronger protection of the lagging strand raises the hypothesis that $Irc3_{sc}$ has a 3' to 5' polarity.

5.4.3. Measurement of $Irc3_{op}$ nucleic acid binding specificity by fluorescence anisotropy

Our previous analysis of the $Irc3_{op}$ ATPase activity demonstrated a dependence of the enzymatic activity on the type of nucleic acid cofactor used. In contrast to most SF2 helicases, the ATPase of Irc3 is more efficiently stimulated with double-stranded and branched DNA cofactors, k_{cat} 16 s^{-1} and 43 s^{-1}, respectively (Table 1 in III). In the next series of experiments, we used fluorescence anisotropy to measure the complex formation efficiency of $Irc3_{op}$ binding to fluorochrome-labeled synthetic DNA molecules of different lengths (III). The principle of fluorescence anisotropy measurement is based on the polarization of light. When a molecule is excited by polarized light, the emitted fluorescence is also polarized. Therefore, the anisotropy value can describe the degree of polarization of the emitted fluorescence. Here, the sample is excited by polarized light, and the emitted fluorescence is measured using polarizers at both parallel and perpendicular positions. The anisotropy value (A) is then calculated by dividing the difference between the parallel and perpendicular fluorescence intensities by the sum of parallel and two times perpendicular light intensities:

$$A = \frac{I_{\parallel} - I_{\perp}}{I_{\parallel} + 2I_{\perp}}$$

In the equation, (I∥) is the parallel emitted fluorescence signal, and (I⊥) is the perpendicular emitted fluorescence signal. Biomolecules of higher mass have higher light polarization at these experimental conditions due to generally slower molecular movement inside the solution.

The reaction mixes contained 2 nM of ssDNA or dsDNA molecules of 12–50 nt/bp in length titrated with 1–1000 nM of $Irc3_{op}$. The binding data of triplicate

assays were fitted to hyperbolic functions. The complex formation efficiency is characterized by equilibrium dissociation constant K_D, defined as the concentration of $Irc3_{op}$ when 50% of the fluorescein-labeled DNA molecules are in complex with the protein. The K_D was deduced for each type of DNA cofactor (Sup. Fig. 4A, B in III).

Our measurements have shown that ssDNA molecules bound $Irc3_{op}$ with, on average, two times smaller K_D than the double-stranded DNA molecules of the same length, despite being less efficient as cofactors in stimulating the ATPase activity but in line with slightly better specificity measured previously. Moreover, we found that the K_D values of all tested DNA cofactors longer than 21 nt or 21 bp formed a plateau at the measurement curve at approximately 20 nM for ssDNA and 40 nM for dsDNA, hinting that the length of DNA needed for efficient binding by $Irc3_{op}$ is in between 12 and 21 nt/bp (Figure 6A in III).

5.5 Irc3 enzymes are processive translocases

5.5.1. Irc3 enzymes follow the processive model of translocation during ATP hydrolysis

As a part of the next series of experiments, we aimed to distinguish between distributive and processive models of the Irc3 helicases by investigating the impact of the length of a DNA cofactor on the ATP hydrolysis rate of the enzyme (I and III). Here we examined a set of dsDNA cofactors (12–75 bp) prepared by annealing complementary synthetic oligonucleotides. The steady-state rate of ATP hydrolysis was determined using the coupled NADH oxidation assay (see paragraph 5.3.4.). To obtain k_{cat} and K_{DNA} parameters for each DNA cofactor, the measured data points were fitted to either hyperbolic (1) or tight-binding (2) equations.

1. $$v = \frac{[E]k_{cat}[DNA]}{K_{DNA}+[DNA]}$$

2. $$v = [E]k_{cat}\frac{([E]+[DNA]+K_{DNA})-\sqrt{([E]+[DNA]+K_{DNA})^2-4[E][DNA]}}{2[E]}$$

[E] is the enzyme concentration, [DNA] is the DNA cofactor concentration, k_{cat} is the apparent catalytic constant measured for each cofactor type, and K_{DNA} is the cofactor concentration when half of the k_{cat} is reached. The tight-binding equation was used if the measured K_{DNA} was five times or less the used enzyme concentration, enabling us to consider the depletion of the free cofactor pool by forming Irc3-DNA complexes.

We found that the shortest dsDNA cofactor (12 bp) showed no cofactor concentration-dependent stimulatory effect on ATP hydrolysis for $Irc3_{op}$. In contrast,

low and cofactor concentration-dependent ATP hydrolysis was still detectable with $Irc3_{sc}$ (Fig. 4A in III and 4B in I). The double-stranded DNA cofactors that were longer than 12 bp stimulated ATP hydrolysis of both $Irc3_{sc}$ and $Irc3_{op,}$ and the rate of ATP hydrolysis was dependent on the length of the DNA cosubstrate. The k_{cat} increased approximately 7-fold for $Irc3_{sc}$ and 4-fold for $Irc3_{op}$ as the cofactor length increased from 21 to 75 bp (Fig. 4A in III and 4B in I). On the other hand, K_{DNA} decreased 3-fold for $Irc3_{sc}$ and 2-fold for $Irc3_{op}$ as the length of the cosubstrate increased from 21 to 35 base pairs and then remained relatively constant for both enzymes (Fig. 4B in III and 4C in I). This type of behavior of kinetic parameters when k_{cat} but not K_{DNA} is dependent on dsDNA cosubstrate length is not expected for distributive helicases and according to the model (Young et al., 1994) suggests that both $Irc3_{sc}$ and $Irc3_{op}$ are processive translocases with the slowest kinetic step related to the enzyme association with DNA, the first isomerization step before processive translocation or the dissociation at the end of the molecule.

5.5.2. Unwinding of triple-stranded DNA molecules by $Irc3_{sc}$

In this series of experiments, we investigated the translocation of $Irc3_{sc}$ with triple-stranded DNA structure disruption experiments (I). To accomplish this, we constructed triple-stranded DNA structures with a third, shorter ^{32}P-labeled polypyrimidine strand connected with dsDNA duplex via Hoogstein bonds. We created three sets of constructs, one containing a longer segment of dsDNA at one or from both sides of the triple-stranded region and another containing an elongated dsDNA region only on one side, with six nt gaps in either of the dsDNA strands just next to the triple-stranded region (Figure 2A, 3A in I). Additionally, we constructed a control construct where the third strand is approximately the same size as dsDNA, with only short two bp long dsDNA overhangs (Figure 2A in I). Irc3 was incubated with the substrate DNA in the presence of ATP, and the products were analyzed on non-denaturing PAGE, followed by autoradiography (Figure 2, 3 in I).

Our findings revealed that $Irc3_{sc}$ was able to unwind all triple-stranded DNA structures from the first set with similar efficiency, regardless of the position of the dsDNA segment present either before or after the triple-stranded region (Figure 2C, D, E in I). However, $Irc3_{sc}$ could not unwind a triple-stranded structure with short two bp long dsDNA overhangs, indicating that the dsDNA region is necessary for successful enzyme loading (Figure 2B in I). When we introduced constructs from the second group, with six nt long gaps in either strand of the dsDNA region, the ability of $Irc3_{sc}$ to displace the third strand was severely hampered (Figure 3B, C in I). We concluded that $Irc3_{sc}$ requires contact with both DNA strands of the duplex. However, we found that the cofactor containing a gap in the 5' to 3' strand was unwound with better efficiency than the cofactor containing a gap in the 3' to 5' strand, supporting the model of 3' to 5' polarity of $Irc3_{sc}$ (Figure 3B, C in I).

The same experiment was performed with $Irc3_{sc}$-ΔC(29–482) and $Irc3_{sc}$-ΔN(386–689) halves of $Irc3_{sc}$. The purification procedure of truncated $Irc3_{sc}$ forms was similar to the previously discussed for full-length $Irc3_{sc}$ purification (see paragraph 5.2.). We found that Irc3-ΔC(29–482), the N-terminal part of $Irc3_{sc}$ containing the helicase core, had functioning DNA cofactor-stimulated ATP hydrolysis activity. However, the ATPase activity was unchanged between dsDNA and branched DNA cofactors, hinting that Irc3-ΔC(29–482) has lost specificity for branched DNA (Figure 6E in I). Irc3-ΔN(386–689), the C-terminal part of $Irc3_{sc}$, did not hydrolyze ATP but bound branched DNA molecules in the EMSA assay (Figure 6E, H in I). Interestingly, neither of the protein halves was able to displace the third strand from the triplex, suggesting that the isolated N-terminal and C-terminal part of $Irc3_{sc}$ cannot function as a dsDNA translocase (Sup. Fig. 2B, C in I). Our results indicate that the C-terminal domain (CTD) of $Irc3_{sc}$ is responsible for the binding of $Irc3_{sc}$ to branched DNA and is required for dsDNA translocase activity, and the N-terminal domain alone is incapable of processive movement along the DNA lattice, similarly to the RecQ-like subfamily of helicases (Tadokoro et al., 2012; Swan et al., 2014).

5.6. Putative functions of Irc3 proteins in yeast mitochondria

In this study, we aimed to understand better the biochemical properties and possible functions of Irc3 helicase. This SF2 enzyme is conserved in different yeast and fungi species but has no homologs in higher eukaryotes (III). Furthermore, the analysis of the Irc3 sequence indicates that this enzyme has no specific positioning in any currently characterized SF2 helicase subfamilies (see paragraph 5.1.). The deletion of the *IRC3* gene in *S. cerevisiae* leads to a rapid decline in respiratory activity and loss of the functional mitochondrial genome when cells are grown on glucose-containing media (Figure 1C in III and Sedman et al., 2014). In a non-fermentable media selective for mitochondrial respiratory function, the deletion of *IRC3* results in a slow-growth phenotype. This suggests that Irc3 participates in one of the mtDNA repair pathways or has a nonessential role in mtDNA replication or gene expression (see paragraphs 2.3.1. and 2.3.2.).

According to current models of yeast mtDNA replication, classical replication forks with leading and lagging strands are unrequired (see paragraph 2.3.1.). However, mtDNA intermediates that could be associated with recombinational events have been detected in rho^{-} cells with 2D gel electrophoresis in one of our previous studies (Sedman et al., 2014). These intermediates prove that fork formation events can still occur in mitochondria, for example, in the form of recombinational structure migration. Interestingly, the deletion of Irc3 causes a dramatic decrease in these recombinational mtDNA intermediates, and at the same time, the effect could be recovered by double-deletion of mitochondrial RNA polymerase Rpo41 (Sedman et al., 2014). These findings indicate that Irc3

is directly involved in forked DNA metabolism in *S. cerevisiae* mitochondria, and, at the same time, the function of Irc3 is somehow associated with Rpo41.

One of the main focuses of this thesis was the biochemical characterization of Irc3 enzymes. In terms of enzyme kinetics, it has been observed that $Irc3_{sc}$ and its homolog from a thermotolerant yeast *O. polymorpha* $Irc3_{op}$ function as processive monomeric enzymes (see paragraphs 5.3. and 5.5.). Additionally, we have found that the C-terminus of the $Irc3_{sc}$ is essential for translocation activity and is also responsible for the binding of branched DNA molecules (paragraph 5.5.2.). We have demonstrated that $Irc3_{sc}$ disrupts triple-stranded DNA structures by displacing the third DNA molecule from the complex in an ATP-dependent manner while requiring dsDNA adjacent to the triplex and being inhibited by single-stranded gaps. This results in Aβ biochemical classification of the Irc3 protein and supports the previous hypothesis that Irc3 could bind and migrate branched DNA structures, or in other words, stimulate fork regression by a processive mechanism (Ref. I and Gaidutšik et al., 2016).

In another set of biochemical experiments with $Irc3_{op}$, from *O. polymorpha*, we have found that the ATPase activity of $Irc3_{op}$ is the most efficiently stimulated by branched and double-stranded DNA cofactors, and in contrast to $Irc3_{sc}$, ssDNA cofactors also activate ATPase activity (paragraph 5.4.1. and Gaidutšik et al., 2016). Notably, including ssDNA oligonucleotides in ATPase reactions with dsDNA or branched DNA cofactors resulted in competitive inhibition (paragraph 5.4.1.). This phenomenon may have fascinating implications *in vivo*, where free ssDNA could impede certain $Irc3_{op}$ functions, ultimately inhibiting $Irc3_{op}$-dependent branched DNA remodeling. Furthermore, $Irc3_{op}$ ATPase activity was efficiently stimulated by structured RNA purified from *O. polymorpha* mitochondria and weakly stimulated by synthetic RNA cofactors (paragraph 5.4.1.). These findings suggest that $Irc3_{op}$ exhibits dual specificity for both DNA and RNA and may potentially regulate R-loop (dsDNA molecules with ssRNA insertions) formation *in vivo*. This could tie the function of Irc3 with one of the current mtDNA replication models, specifying the importance of mtDNA *ori* regions in replication (Sanchez-Sandoval et al., 2015). According to the proposed model, *ori* regions in the mtDNA of *S. cerevisiae* can be primed by RNA polymerase Rpo41, effectively forming R-loop structures that could be subsequently extended by DNA polymerase Mip1 (see paragraph 2.3.1.).

In addition to Irc3 ties with the yeast mtDNA metabolism, recently, Kaur and Datta showed that $Irc3_{sc}$ co-localizes with the 37S subunit of mitoribosome and is required for mitochondrial translation (Kaur and Datta, 2021). They proposed that $Irc3_{sc}$ may function as an RNA helicase during the elongation stage of translation (Kaur and Datta, 2021). Previously we had no success with the *in vitro* measurement of ATP hydrolysis of $Irc3_{sc}$ with a mitochondrial RNA extract of *S. cerevisiae* (Sedman et al., 2014). It has led us to a not entirely accurate assumption that all Irc3 homologs are DNA-specific enzymes. As a part of this study, we have demonstrated that the ATPase activity of $Irc3_{op}$ is stimulated by bulky structured RNA. These results suggest that Irc3 could be a part of the yeast mitochondrial gene expression organization complex (MIOREX) (see ref. III and

paragraph 5.4.1.). The MIOREX model proposes that mitoribosomes interact with many transiently bound proteins involved in RNA transcription and processing (Kehrein et al., 2015). In a recent study of the *S. cerevisiae* mitochondrial proteome, Irc3 was found to co-localize with RNA post-processing factors Sls1 and Cbp1, RNA helicase Mrh4, and 37S ribosome subunit components Nam9 and Rt35. However, this co-localization occurs in the fraction of protein complexes that have a relatively low molecular weight of approximately 120 kDa, and this suggests that Irc3 could cofractionate with unassembled 37S subunit components or be responsive for mitochondrial subunit biogenesis similarly to Mrh4 (De Silva et al., 2013; Schulte et al., 2023).

In conclusion, the collected data concerning the Irc3 enzymes reveals their potential versatility, encompassing various functions. These functions span from involvement in DNA fork regression within a pathway of mitochondrial DNA repair or replication to its potential contribution to multiple aspects of mitochondrial RNA metabolism in *S. cerevisiae*. The latter may encompass roles in gene expression, structured RNA quality control, translation, and potentially bridging the connection between mitochondrial DNA and RNA metabolisms.

CONCLUSIONS

This study investigates the conservation, characteristics, and potential functional roles of the Irc3 helicase. Despite extensive investigations conducted over decades, knowledge regarding yeast mitochondrial DNA and RNA metabolism is still far from complete. Therefore, we employed various *in vivo* and *in vitro* biochemical tools to elucidate the biological function of the Irc3 helicase with the objective of gaining fresh insights into the processes of yeast nucleic acid metabolism. The main results of this thesis can be summarized as follows:

1. The study identified conserved homologs of the Irc3 helicase in yeasts belonging to the ascomycete and basidiomycete classes within the fungal kingdom, while no homologs were found in other eukaryotes. *In silico* analysis revealed that Irc3 proteins possess a conserved set of helicase motifs, a putative mitochondrial matrix targeting signal, and a C-terminal region with low sequence conservation. Structural predictions using AlphaFold indicated that $Irc3_{sc}$ from *S. cerevisiae* and $Irc3_{op}$ from *O. polymorpha* might exhibit a C-terminal structure resembling the "fist" domain of the Ski2-like subfamily of helicases.
2. *In vivo* complementation assays demonstrated that $IRC3_{op}$ could partially rescue the respiratory deficiency phenotype in the *S. cerevisiae* $irc3_{sc}\Delta$ strain. Furthermore, purified recombinant $Irc3_{op}$ retained approximately 80% of its enzymatic activity at temperatures up to 45 °C, with an optimal ATP hydrolysis temperature of 41 °C, surpassing the previous stability parameters of $Irc3_{sc}$.
3. *In vitro* experiments indicated that recombinant Irc3 proteins exist as monomers in solution and form 1:1 complexes with DNA molecules.
4. The ATPase activity of $Irc3_{op}$ was stimulated by a wide range of synthetic and native cofactors, including replication fork-like DNA molecules, single-stranded DNA, synthetic RNA, and structured native RNA. However, $Irc3_{op}$ exhibited higher specificity for DNA cofactors compared to RNA cofactors.
5. Both $Irc3_{sc}$ and $Irc3_{op}$ displayed processive translocation during ATP hydrolysis, with the rate of ATP hydrolysis depending on the length of the DNA cofactors. Moreover, $Irc3_{sc}$ demonstrated the ability to unwind triple-stranded DNA structures, with a potential 3’ to 5’ polarity and the requirement of contacts with both strands of the DNA duplex.

SUMMARY IN ESTONIAN

Irc3 helikaasi biokeemiliste parameetrite analüüs

Mitokonder on oluline energiatootmises osalev organell, millel on oma väike genoom. Mitokondriaalse genoomi kadumine või kahjustumine põhjustab kõrgemates eukarüootides tavaliselt rakusurma, samal ajal pagaripärm *Saccharomyces cerevisiae* võib elada ilma funktsionaalse mitokondriaalse genoomita, kui seda kasvatada kääritataval süsinikuallikal. See teeb pagaripärmist ideaalse mudeli mitokondriaalse DNA säilitamise uurimisel. Pärmi mitokondriaalse proteoomi koosseisu kuulub ligikaudu 900 valku ja nende hulgast on umbes 25% seotud mitokondriaalse geeniekspressiooni ja DNA säilitamisega. Need valgud mängivad ka olulist rolli seitsme hingamisahelasse kuuluva valgu sünteesil, mis on kodeeritud mitokondriaalses genoomis. Mitokondriaalses geeniekspressioonis osalevate valkude hulgas on *S. cerevisiae* mitokondris vähemalt kuus konserveerunud helikaasi, mis vastutavad mitokondriaalse nukleiinhappe metabolismi ja valkude biosünteesi eest.

Helikaasid on ensüümid, mis kasutavad nukleosiidtrifosfaadi (NTP) sidumise ja hüdrolüüsi energiat DNA või RNA struktuursete ümberkorralduste läbiviimiseks. Helikaasidel on elusrakkudes palju rolle, alates replikatsioonist, rekombinatsioonist ja parandamisest kuni transkriptsiooni, splaissimise, ribosoomi biosünteesi ja translatsioonini. Need valgud mängivad ka olulist rolli mitokondriaalse DNA stabiilsuses ja geenide ekspressioonis. Varasemad uuringud on tuvastanud kolm mitokondriaalset helikaasi (Mhr4, Mss116 ja Suv3), mis on seotud mitokondriaalse RNA metabolismiga, ja kolm (Pif1, Hmi1 ja Irc3) helikaasi mis on seotud DNA säilitamisega. Hiljuti on helikaas Irc3 pälvinud tähelepanu edasiseks uurimiseks, kuna sellel leiti ka potentsiaalne roll mitokondriaalses translatsioonis.

See uuring keskendub peamiselt Saccharomyces cerevisiae Irc3 ($Irc3_{sc}$) valgu ja selle homoloogi $Irc3_{op}$ (*Ogataea polymorpha*, termotolerantne pärm) ulatuslikule uurimisele biokeemiliste meetodite abil. In silico analüüs näitas, et Irc3 helikaasi homolooge leidub nii kottseente kui ka kandseente hulka kuuluvates pärmides, kuid mitte kõrgemates eukarüootides. Nendel homoloogidel on konserveerunud helikaasi motiivide komplekt, oletatav mitokondriaalse maatriksi sihtsignaal ja vähese konserveerumistasemega C-terminaalne piirkond. Struktuuriennustused, kasutades AlphaFoldi, näitasid, et $Irc3_{sc}$ ja $Irc3_{op}$ omavad N-terminuses klassikalisi RecA1 ja RecA2 helikaasi domeene ning C-terminuses arvatavalt struktuuri, mis sarnaneb Ski2-taoliste helikaaside alamperekonna "rusika" domeeniga. Mtr4 valgus vastutab "rusika" domeen, näiteks struktureeritud RNA sidumise eest.

Uuring keskendus $Irc3_{op}$, kui $Irc3_{sc}$ termiliselt stabiilsema homoloogi biokeemilisele iseloomustamisele. $Irc3_{op}$ omab suhteliselt kõrget helikaasi piirkonna järjestuse sarnasust (82%), kuid tal on võrreldes $Irc3_{sc}$-ga lühem C-terminaalne piirkond. *In vivo* komplementatsiooni katsed, kasutades S. cerevisiae $irc3_{sc}\Delta$ tüve, näitasid, et $IRC3_{op}$ suudab osaliselt päästa raku hingamispuudulikkuse fenotüübi

teket. DNA-stimuleeritud ATP hüdrolüüsi katsed erinevatel temperatuuridel näitasid, et $Irc3_{op}$ säilitab ligikaudu 80% oma ensümaatilisest aktiivsusest kuni 45 °C, aktiivsuse maksimumiga 41 °C juures, mis on oluliselt kõrgem kui $Irc3_{sc}$-l. Tsirkulaarse dikroismi spektroskoopia analüüs näitas, et $Irc3_{op}$ sekundaarsed struktuurid sulavad umbes 45 °C juures.

Superperekond 2 helikaaside seas esineb valke mis funktsioneerivad nii monomeeridena kui ka dimeeridena. Meie tulemused näitasid, et Irc3 valgud võivad teoreetiliselt moodustada multimeere, ent mutantsete Irc3 valkude üleekspresseerimise dominant negatiivse fenotüübi analüüs ja hüdrodünaamilised mõõtmised *in vitro* näitasid, et rekombinantsed Irc3 valgud eksisteerivat lahuses monomeeridena. $Irc3_{sc}$-DNA komplekside sedimentatsiooni uuringud kinnitasid, et replikatsioonikahvli laadsete ja Holliday-ristmiku laadsete DNA kofaktoritega moodustuvad põhiliselt stöhhiomeetrilised 1:1 kompleksid.

Järgmisena uurisime Irc3 valkude nukleiinhappe (NA) spetsiifilisust ja translokatsioonimehhanisme. Leidsime, et sünteetilised DNA kofaktorid, sealhulgas replikatsioonikahvli laadne ja üheahelaline DNA (ssDNA), samuti struktureeritud natiivsed RNA molekulid, stimuleerisid $Irc3_{op}$ ATPaasi aktiivsust. Siiski oli $Irc3_{op}$ spetsiifilisem DNA kofaktorite suhtes. Protektsiooni uuringud, kasutades DNaasi I jalajälge meetodit, näitasid, et $Irc3_{sc}$ kaitseb kõige paremini DNA-d endonukleaasi eest replikatsioonikahvli struktuuride hargnemispunkti vahetus läheduses. Fluorestsents-anisotroopia katsed näitasid, et $Irc3_{op}$-l oli suurem afiinsus ssDNA suhtes, kusjuures optimaalseks seondumiseks vajatakse DNA-d pikkusega 12 kuni 21 nukleotiidi või aluspaari. Lisaks näitasid nii $Irc3_{sc}$ kui ka $Irc3_{op}$ ATP hüdrolüüsi käigus protsessiivset translokatsiooni, sest ATP hüdrolüüsi kiirus sõltus DNA kofaktorite pikkusest. $Irc3_{sc}$ näitas võimet lahtikeerata kolmeahelalisi DNA struktuure, mille käigus oli valgul vajalik kontakt DNA dupleksi mõlema ahelaga, samas täheldasime selle protsessi käigus 3' – 5' liikumise polaarsust.

Selle uuringu tulemusena saime me uut toetust eelnevaltes töödes pakutud hüpoteesile, et Irc3 on võimeline siduma ja migreerima hargnenud DNA struktuure või teisisõnu stimuleerima replikatsiooni või reparatsiooni kahvli regressiooni protsessiivse mehhanismi abil. Lisaks viitavad uued andmed sellele, et $Irc3_{op}$-l on spetsiifilisus nii DNA kui ka RNA suhtes ning ta võib potentsiaalselt osaleda RNA metabolismis või siduda pärmi mitokondri DNA ja RNA metabolisme. Näiteks potentsiaalseks valgu rolliks võiks olla R-loop (ssRNA sisestustega dsDNA molekulid) struktuuride moodustumise reguleerimine *in vivo*. See seoks Irc3 funktsiooni ühe praeguse mtDNA replikatsiooni mudeliga, mis väidab mtDNA ori piirkondade tähtsust replikatsioonis. Selle mudeli kohaselt saab *S. cerevisiae* mtDNA ori piirkondi praimeerida RNA polümeraasiga Rpo41, moodustades R-loop struktuure, mida on võimalik hiljem pikendada DNA polümeraasi Mip1 abil. Teiseks potentsiaalseks valgu rolliks võib olla osalemine pärmi mitokondriaalse geeniekspressiooni organisatsiooni kompleksis (MIOREX). Seda rolli toetab asjaolu, et $Irc3_{op}$ ATPaasi aktiivsust stimuleerisid paremini just mahukad struktureeritud RNA molekulid. MIOREX mudeli kohaselt mitoribosoomid interakteeruvad suure hulga ajutiselt seostuvate valkudega, mis tegelevad RNA transkriptsiooni ja töötlemisega. Kuid toetudes hiljutistele proteoomika

töödele kofraktsioneerub Irc3 just kokkupanemata 37S ribosoomi subühiku komponentidega seega võib Irc3 osaleda ribosoomi kokkupanekus ja mitte otse küpse ribosoomi translatsiooni protsessis.

Kokkuvõtteks näitavad kogutud andmed Irc3 ensüümide kohta nende potentsiaalset suurt mitmekülgsust. Irc3 valkude võimalikud funktsioonid ulatuvad osalemisest DNA kahvli regressioonis mitokondriaalse DNA parandamise või replikatsiooni rajas kuni panustamiseni *S. cerevisiae* mitokondriaalse RNA metabolismi aspektidesse. Viimane võib hõlmata rolle geeniekspressioonis, struktureeritud RNA kvaliteedikontrollis ja translatsioonis.

REFERENCES

Abdel-Monem, M., Dürwald, H., Hoffmann-Berling, H., 1976. Enzymic unwinding of DNA. 2. Chain separation by an ATP-dependent DNA unwinding enzyme. Eur. J. Biochem. 65, 441–449. https://doi.org/10.1111/j.1432-1033.1976.tb10359.x

Adelman, C.A., Lolo, R.L., Birkbak, N.J., Murina, O., Matsuzaki, K., Horejsi, Z., Parmar, K., Borel, V., Skehel, J.M., Stamp, G., D'Andrea, A., Sartori, A.A., Swanton, C., Boulton, S.J., 2013. HELQ promotes RAD51 paralogue-dependent repair to avert germ cell loss and tumorigenesis. Nature 502, 381–384. https://doi.org/10.1038/nature12565

Allkanjari, K., Baldock, R.A., 2021. Beyond base excision repair: an evolving picture of mitochondrial DNA repair. Biosci. Rep. 41, BSR20211320. https://doi.org/10.1042/BSR20211320

Alvaro, D., Lisby, M., Rothstein, R., 2007. Genome-wide analysis of Rad52 foci reveals diverse mechanisms impacting recombination. PLoS Genet. 3, e228. https://doi.org/10.1371/journal.pgen.0030228

Amiott, E.A., Jaehning, J.A., 2006. Mitochondrial Transcription Is Regulated via an ATP "Sensing" Mechanism that Couples RNA Abundance to Respiration. Mol. Cell 22, 329–338. https://doi.org/10.1016/j.molcel.2006.03.031

Amunts, A., Brown, A., Bai, X., Llácer, J.L., Hussain, T., Emsley, P., Long, F., Murshudov, G., Scheres, S.H.W., Ramakrishnan, V., 2014. Structure of the Yeast Mitochondrial Large Ribosomal Subunit. Science 343, 1485–1489. https://doi.org/10.1126/science.1249410

Bachrati, C.Z., Hickson, I.D., 2003. RecQ helicases: suppressors of tumorigenesis and premature aging. Biochem. J. 374, 577–606. https://doi.org/10.1042/BJ20030491

Baldacci, G., Bernardi, G., 1982. Replication origins are associated with transcription initiation sequences in the mitochondrial genome of yeast. EMBO J. 1, 987–994. https://doi.org/10.1002/j.1460-2075.1982.tb01282.x

Ballut, L., Marchadier, B., Baguet, A., Tomasetto, C., Séraphin, B., Le Hir, H., 2005. The exon junction core complex is locked onto RNA by inhibition of eIF4AIII ATPase activity. Nat. Struct. Mol. Biol. 12, 861–869. https://doi.org/10.1038/nsmb990

Belon, C.A., Frick, D.N., 2009. Fuel Specificity of the Hepatitis C Virus NS3 Helicase. J. Mol. Biol. 388, 851–864. https://doi.org/10.1016/j.jmb.2009.03.059

Bennett, R.J., Sharp, J.A., Wang, J.C., 1998. Purification and Characterization of the Sgs1 DNA Helicase Activity of Saccharomyces cerevisiae. J. Biol. Chem. 273, 9644–9650. https://doi.org/10.1074/jbc.273.16.9644

Bernstein, D.A., Keck, J.L., 2003. Domain mapping of Escherichia coli RecQ defines the roles of conserved N- and C-terminal regions in the RecQ family. Nucleic Acids Res. 31, 2778–2785. https://doi.org/10.1093/nar/gkg376

Bernstein, J., Patterson, D.N., Wilson, G.M., Toth, E.A., 2008. Characterization of the Essential Activities of Saccharomyces cerevisiae Mtr4p, a 3′→5′ Helicase Partner of the Nuclear Exosome. J. Biol. Chem. 283, 4930–4942. https://doi.org/10.1074/jbc.M706677200

Bifano, A.L., Caprara, M.G., 2008. A DExH/D-box Protein Coordinates the Two Steps of Splicing in a Group I Intron. J. Mol. Biol. 383, 667–682. https://doi.org/10.1016/j.jmb.2008.08.070

Bochman, M.L., Judge, C.P., Zakian, V.A., 2011. The Pif1 family in prokaryotes: what are our helicases doing in your bacteria? Mol. Biol. Cell 22, 1955–1959. https://doi.org/10.1091/mbc.e11-01-0045

Bohnsack, M.T., Martin, R., Granneman, S., Ruprecht, M., Schleiff, E., Tollervey, D., 2009. Prp43 Bound at Different Sites on the Pre-rRNA Performs Distinct Functions in Ribosome Synthesis. Mol. Cell 36, 583–592. https://doi.org/10.1016/j.molcel.2009.09.039

Boiteux, S., Guillet, M., 2004. Abasic sites in DNA: repair and biological consequences in Saccharomyces cerevisiae. DNA Repair 3, 1–12. https://doi.org/10.1016/j.dnarep.2003.10.002

Bourgeois, C.F., Mortreux, F., Auboeuf, D., 2016. The multiple functions of RNA helicases as drivers and regulators of gene expression. Nat. Rev. Mol. Cell Biol. 17, 426–438. https://doi.org/10.1038/nrm.2016.50

Büttner, K., Nehring, S., Hopfner, K.-P., 2007. Structural basis for DNA duplex separation by a superfamily-2 helicase. Nat. Struct. Mol. Biol. 14, 647–652. https://doi.org/10.1038/nsmb1246

Chen, X.J., Butow, R.A., 2005. The organization and inheritance of the mitochondrial genome. Nat. Rev. Genet. 6, 815–825. https://doi.org/10.1038/nrg1708

Chen, X.J., Clark-Walker, G.D., 2018. Unveiling the mystery of mitochondrial DNA replication in yeasts. Mitochondrion 38, 17–22. https://doi.org/10.1016/j.mito.2017.07.009

Chen, X.J., Wang, X., Kaufman, B.A., Butow, R.A., 2005. Aconitase Couples Metabolic Regulation to Mitochondrial DNA Maintenance. Science 307, 714–717. https://doi.org/10.1126/science.1106391

Cheng, X., Dunaway, S., Ivessa, A.S., 2007. The role of Pif1p, a DNA helicase in Saccharomyces cerevisiae, in maintaining mitochondrial DNA. Mitochondrion 7, 211–222. https://doi.org/10.1016/j.mito.2006.11.023

Chi, N.W., Kolodner, R.D., 1994a. Purification and characterization of MSH1, a yeast mitochondrial protein that binds to DNA mismatches. J. Biol. Chem. 269, 29984–29992.

Chi, N.W., Kolodner, R.D., 1994b. The effect of DNA mismatches on the ATPase activity of MSH1, a protein in yeast mitochondria that recognizes DNA mismatches. J. Biol. Chem. 269, 29993–29997.

Clark-Walker, G.D., 1989. In vivo rearrangement of mitochondrial DNA in Saccharomyces cerevisiae. Proc. Natl. Acad. Sci. U. S. A. 86, 8847–8851. https://doi.org/10.1073/pnas.86.22.8847

Clerici, M., Mantiero, D., Guerini, I., Lucchini, G., Longhese, M.P., 2008. The Yku70-Yku80 complex contributes to regulate double-strand break processing and checkpoint activation during the cell cycle. EMBO Rep. 9, 810–818. https://doi.org/10.1038/embor.2008.121

Contamine, V., Picard, M., 2000. Maintenance and Integrity of the Mitochondrial Genome: a Plethora of Nuclear Genes in the Budding Yeast. Microbiol. Mol. Biol. Rev. https://doi.org/10.1128/MMBR.64.2.281-315.2000

Cordin, O., Banroques, J., Tanner, N.K., Linder, P., 2006. The DEAD-box protein family of RNA helicases. Gene 367, 17–37. https://doi.org/10.1016/j.gene.2005.10.019

Costanzo, M.C., Fox, T.D., 1990. Control of Mitochondrial Gene Expression in Saccharomyces Cerevisiae. Annu. Rev. Genet. 24, 91–113. https://doi.org/10.1146/annurev.ge.24.120190.000515

Daugeron, M.-C., Kressler, D., Linder, P., 2001. Dbp9p, a putative ATP-dependent RNA helicase involved in 60S-ribosomal-subunit biogenesis, functionally interacts with Dbp6p. RNA 7, 1317–1334. https://doi.org/10.1017/S1355838201010640

De Bortoli, F., Espinosa, S., Zhao, R., 2021. DEAH-Box RNA Helicases in Pre-mRNA Splicing. Trends Biochem. Sci. 46, 225–238. https://doi.org/10.1016/j.tibs.2020.10.006
De La Cruz, J., Kressler, D., Linder, P., 1999. Unwinding RNA in Saccharomyces cerevisiae: DEAD-box proteins and related families. Trends Biochem. Sci. 24, 192–198. https://doi.org/10.1016/S0968-0004(99)01376-6
De Muyt, A., Jessop, L., Kolar, E., Sourirajan, A., Chen, J., Dayani, Y., Lichten, M., 2012. BLM helicase ortholog Sgs1 is a central regulator of meiotic recombination intermediate metabolism. Mol. Cell 46, 43–53. https://doi.org/10.1016/j.molcel.2012.02.020
De Silva, D., Fontanesi, F., Barrientos, A., 2013. The DEAD box protein Mrh4 functions in the assembly of the mitochondrial large ribosomal subunit. Cell Metab. 18, 712–725. https://doi.org/10.1016/j.cmet.2013.10.007
Del Campo, M., Lambowitz, A.M., 2009. Structure of the Yeast DEAD box protein Mss116p reveals two wedges that crimp RNA. Mol. Cell 35, 598–609. https://doi.org/10.1016/j.molcel.2009.07.032
De Silva, D., Poliquin, S., Zeng, R., Zamudio-Ochoa, A., Marrero, N., Perez-Martinez, X., Fontanesi, F., Barrientos, A., 2017. The DEAD-box helicase Mss116 plays distinct roles in mitochondrial ribogenesis and mRNA-specific translation. Nucleic Acids Res. 45, 6628–6643. https://doi.org/10.1093/nar/gkx426
Druzhyna, N.M., Wilson, G.L., LeDoux, S.P., 2008. Mitochondrial DNA repair in aging and disease. Mech. Ageing Dev. 129, 383–390. https://doi.org/10.1016/j.mad.2008.03.002
Dujon, B., 1981. Mitochondrial genetics and functions [Saccharomyces cerevisiae, yeasts]. Cold Spring Harb. Monogr. Ser. USA.
Duvezin-Caubet, S., Rak, M., Lefebvre-Legendre, L., Tetaud, E., Bonnefoy, N., di Rago, J.-P., 2006. A “petite obligate” mutant of Saccharomyces cerevisiae: functional mtDNA is lethal in cells lacking the delta subunit of mitochondrial F1-ATPase. J. Biol. Chem. 281, 16305–16313. https://doi.org/10.1074/jbc.M513805200
Dziembowski, A., Piwowarski, J., Hoser, R., Minczuk, M., Dmochowska, A., Siep, M., van der Spek, H., Grivell, L., Stepien, P.P., 2003. The yeast mitochondrial degradosome. Its composition, interplay between RNA helicase and RNase activities and the role in mitochondrial RNA metabolism. J. Biol. Chem. 278, 1603–1611. https://doi.org/10.1074/jbc.M208287200
Dzierzbicki, P., Koprowski, P., Fikus, M.U., Malc, E., Ciesla, Z., 2004. Repair of oxidative damage in mitochondrial DNA of Saccharomyces cerevisiae: involvement of the MSH1-dependent pathway. DNA Repair 3, 403–411. https://doi.org/10.1016/j.dnarep.2003.12.005
Ellis, N.A., Groden, J., Ye, T.Z., Straughen, J., Lennon, D.J., Ciocci, S., Proytcheva, M., German, J., 1995. The Bloom’s syndrome gene product is homologous to RecQ helicases. Cell 83, 655–666. https://doi.org/10.1016/0092-8674(95)90105-1
Ephrussi, B., Slonimski, P.P., 1955. Yeast Mitochondria: Subcellular Units involved in the Synthesis of Respiratory Enzymes in Yeast. Nature 176, 1207–1208. https://doi.org/10.1038/1761207b0
Erickson, H.P., 2009. Size and shape of protein molecules at the nanometer level determined by sedimentation, gel filtration, and electron microscopy. Biol. Proced. Online 11, 32–51. https://doi.org/10.1007/s12575-009-9008-x
Fairman-Williams, M.E., Guenther, U.-P., Jankowsky, E., 2010. SF1 and SF2 helicases: family matters. Curr. Opin. Struct. Biol. 20, 313–324. https://doi.org/10.1016/j.sbi.2010.03.011

Fangman, W.L., Henly, J.W., Brewer, B.J., 1990. RP041 – Independent Maintenance of [rho–] Mitochondrial DNA in Saccharomyces cerevisiae Walton L. Fangman. Mol. Cell. Biol. 10, 10–15. https://doi.org/10.1128/mcb.10.1.10-15.1990

Faye, G., Fukuhara, H., Grandchamp, C., Lazowska, J., Michel, F., Casey, J., Getz, G.S., Locker, J., Rabinowitz, M., Bolotin-Fukuhara, M., Coen, D., Deutsch, J., Dujon, B., Netter, P., Slonimski, P.P., 1973. Mitochondrial nucleic acids in the peptite colonie mutants: Deletions and repetitions of genes. Biochimie 55, 779–792. https://doi.org/10.1016/S0300-9084(73)80030-6

Fekete, Z., Ellis, T.P., Schonauer, M.S., Dieckmann, C.L., 2008. Pet127 Governs a 5′ → 3′-Exonuclease Important in Maturation of Apocytochrome b mRNA in Saccharomyces cerevisiae*. J. Biol. Chem. 283, 3767–3772. https://doi.org/10.1074/jbc.M709617200

Fouraux, M.A., Kolkman, M.J.M., Van Der Heijden, A., De Jong, A.S., Van Venrooij, W.J., Pruijn, G.J.M., 2002. The human La (SS-B) autoantigen interacts with DDX15/hPrp43, a putative DEAH-box RNA helicase. RNA 8, 1428–1443. https://doi.org/10.1017/S1355838202021076

Foury, F., 1989. Cloning and Sequencing of the Nuclear Gene MIP1 Encoding the Catalytic Subunit of the Yeast Mitochondrial DNA Polymerase*. J. Biol. Chem. 264, 20552–20560. https://doi.org/10.1016/S0021-9258(19)47098-1

Foury, F., Hu, J., Vanderstraeten, S., 2004. Mitochondrial DNA mutators. Cell. Mol. Life Sci. CMLS 61, 2799–2811. https://doi.org/10.1007/s00018-004-4220-y

Foury, F., Roganti, T., Lecrenier, N., Purnelle, B., 1998. The complete sequence of the mitochondrial genome of *Saccharomyces cerevisiae*. FEBS Lett. 440, 325–331. https://doi.org/10.1016/S0014-5793(98)01467-7

Foury, F., Vanderstraeten, S., 1992. Yeast mitochondrial DNA mutators with deficient proofreading exonucleolytic activity. EMBO J. 11, 2717–2726.

Frick, D.N., 2006. Step-by-Step Progress Toward Understanding the Hepatitis C Virus RNA Helicase. Hepatol. Baltim. Md 43, 1392–1395. https://doi.org/10.1002/hep.21200

Fujikane, R., Shinagawa, H., Ishino, Y., 2006. The archaeal Hjm helicase has recQ-like functions, and may be involved in repair of stalled replication fork. Genes Cells Devoted Mol. Cell. Mech. 11, 99–110. https://doi.org/10.1111/j.1365-2443.2006.00925.x

Gaidutšik, I., Sedman, T., Sillamaa, S., Sedman, J., 2016. Irc3 is a mitochondrial DNA branch migration enzyme. Sci. Rep. 6, 26414. https://doi.org/10.1038/srep26414

Gao, Y., Yang, W., 2020. Different mechanisms for translocation by monomeric and hexameric helicases. Curr. Opin. Struct. Biol. 61, 25–32. https://doi.org/10.1016/j.sbi.2019.10.003

Ghodke, I., Muniyappa, K., 2013. Processing of DNA Double-stranded Breaks and Intermediates of Recombination and Repair by Saccharomyces cerevisiae Mre11 and Its Stimulation by Rad50, Xrs2, and Sae2 Proteins. J. Biol. Chem. 288, 11273–11286. https://doi.org/10.1074/jbc.M112.439315

Golik, P., Szczepanek, T., Bartnik, E., Stepien, P.P., Lazowska, J., 1995. The S. cerevisiae nuclear gene SUV3 encoding a putative RNA helicase is necessary for the stability of mitochondrial transcripts containing multiple introns. Curr. Genet. 28, 217–224. https://doi.org/10.1007/BF00309780

Gorbalenya, A.E., Koonin, E.V., 1993. Helicases: amino acid sequence comparisons and structure-function relationships. Curr. Opin. Struct. Biol. 3, 419–429. https://doi.org/10.1016/S0959-440X(05)80116-2

Greenleaf, A.L., Kelly, J.L., Lehman, I.R., 1986. Yeast RPO41 gene product is required for transcription and maintenance of the mitochondrial genome. Proc. Natl. Acad. Sci. 83, 3391–3394. https://doi.org/10.1073/pnas.83.10.3391

Grivell, L.A., 1989. Nucleo-mitochondrial interactions in yeast mitochondrial biogenesis. Eur. J. Biochem. 182, 477–493. https://doi.org/10.1111/j.1432-1033.1989.tb14854.x

Gupta, S.V., Schmidt, K.H., 2020. Maintenance of Yeast Genome Integrity by RecQ Family DNA Helicases. Genes 11, 205. https://doi.org/10.3390/genes11020205

Guy, C.P., 2005. Archaeal Hel308 helicase targets replication forks in vivo and in vitro and unwinds lagging strands. Nucleic Acids Res. 33, 3678–3690. https://doi.org/10.1093/nar/gki685

Halbach, F., Rode, M., Conti, E., 2012. The crystal structure of S. cerevisiae Ski2, a DExH helicase associated with the cytoplasmic functions of the exosome. RNA 18, 124–134. https://doi.org/10.1261/rna.029553.111

Halls, C., Mohr, S., Del Campo, M., Yang, Q., Jankowsky, E., Lambowitz, A.M., 2007. Involvement of DEAD-box proteins in group I and II intron splicing. Biochemical characterization of Mss116p, ATP-hydrolysis-dependent and -independent mechanisms, and general RNA chaperone activity. J. Mol. Biol. 365, 835–855. https://doi.org/10.1016/j.jmb.2006.09.083

Hamann, F., Enders, M., Ficner, R., 2019. Structural basis for RNA translocation by DEAH-box ATPases. Nucleic Acids Res. 47, 4349–4362. https://doi.org/10.1093/nar/gkz150

He, Y., Andersen, G.R., Nielsen, K.H., 2010. Structural basis for the function of DEAH helicases. EMBO Rep. 11, 180–186. https://doi.org/10.1038/embor.2010.11

He, Y., Staley, J.P., Andersen, G.R., Nielsen, K.H., 2017. Structure of the DEAH/RHA ATPase Prp43p bound to RNA implicates a pair of hairpins and motif Va in translocation along RNA. RNA N. Y. N 23, 1110–1124. https://doi.org/10.1261/rna.060954.117

Hilbert, M., Karow, A.R., Klostermeier, D., 2009. The mechanism of ATP-dependent RNA unwinding by DEAD box proteins. Biol. Chem. 390, 1237–1250. https://doi.org/10.1515/BC.2009.135

Hishida, T., Han, Y.-W., Shibata, T., Kubota, Y., Ishino, Y., Iwasaki, H., Shinagawa, H., 2004. Role of the Escherichia coli RecQ DNA helicase in SOS signaling and genome stabilization at stalled replication forks. Genes Dev. 18, 1886–1897. https://doi.org/10.1101/gad.1223804

Hopfner, K.P., Karcher, A., Craig, L., Woo, T.T., Carney, J.P., Tainer, J.A., 2001. Structural biochemistry and interaction architecture of the DNA double-strand break repair Mre11 nuclease and Rad50-ATPase. Cell 105, 473–485. https://doi.org/10.1016/s0092-8674(01)00335-x

Huang, H.-R., Rowe, C.E., Mohr, S., Jiang, Y., Lambowitz, A.M., Perlman, P.S., 2005. The splicing of yeast mitochondrial group I and group II introns requires a DEAD-box protein with RNA chaperone function. Proc. Natl. Acad. Sci. 102, 163–168. https://doi.org/10.1073/pnas.0407896101

Huber, M.D., Lee, D.C., Maizels, N., 2002. G4 DNA unwinding by BLM and Sgs1p: substrate specificity and substrate-specific inhibition. Nucleic Acids Res. 30, 3954–3961.

Hwang, W., Karplus, M., 2019. Structural basis for power stroke vs. Brownian ratchet mechanisms of motor proteins. Proc. Natl. Acad. Sci. 116, 19777–19785. https://doi.org/10.1073/pnas.1818589116

Imamura, O., Sugawara, M., Furuichi, Y., 1997. Cloning and Characterization of a Putative Human RNA Helicase Gene of the DEAH-Box Protein Family. Biochem. Biophys. Res. Commun. 240, 335–340. https://doi.org/10.1006/bbrc.1997.7585

Jackson, R.N., Klauer, A.A., Hintze, B.J., Robinson, H., van Hoof, A., Johnson, S.J., 2010. The crystal structure of Mtr4 reveals a novel arch domain required for rRNA processing. EMBO J. 29, 2205–2216. https://doi.org/10.1038/emboj.2010.107

Jang, S.H., Jaehning, J.A., 1991. The yeast mitochondrial RNA polymerase specificity factor, MTF1, is similar to bacterial sigma factors. J. Biol. Chem. 266, 22671–22677.

Jarmoskaite, I., Russell, R., 2014. RNA Helicase Proteins as Chaperones and Remodelers. Annu. Rev. Biochem. 83, 697–725. https://doi.org/10.1146/annurev-biochem-060713-035546

Jedrzejczak, R., Wang, J., Dauter, M., Szczesny, R.J., Stepien, P.P., Dauter, Z., 2011. Human Suv3 protein reveals unique features among SF2 helicases. Acta Crystallogr. D Biol. Crystallogr. 67, 988–996. https://doi.org/10.1107/S0907444911040248

Johnson, A.W., Kolodner, R.D., 1995. Synthetic lethality of sep1 (xrn1) ski2 and sep1 (xrn1) ski3 mutants of Saccharomyces cerevisiae is independent of killer virus and suggests a general role for these genes in translation control. Mol. Cell. Biol. 15, 2719–2727. https://doi.org/10.1128/MCB.15.5.2719

Johnson, S.J., Jackson, R.N., 2013. Ski2-like RNA helicase structures: Common themes and complex assemblies. RNA Biol. 10, 33–43. https://doi.org/10.4161/rna.22101

Jumper, J., Evans, R., Pritzel, A., Green, T., Figurnov, M., Ronneberger, O., Tunyasuvunakool, K., Bates, R., Žídek, A., Potapenko, A., Bridgland, A., Meyer, C., Kohl, S.A.A., Ballard, A.J., Cowie, A., Romera-Paredes, B., Nikolov, S., Jain, R., Adler, J., Back, T., Petersen, S., Reiman, D., Clancy, E., Zielinski, M., Steinegger, M., Pacholska, M., Berghammer, T., Bodenstein, S., Silver, D., Vinyals, O., Senior, A.W., Kavukcuoglu, K., Kohli, P., Hassabis, D., 2021. Highly accurate protein structure prediction with AlphaFold. Nature 596, 583–589. https://doi.org/10.1038/s41586-021-03819-2

Kalifa, L., Beutner, G., Phadnis, N., Sheu, S.-S., Sia, E.A., 2009. Evidence for a role of FEN1 in maintaining mitochondrial DNA integrity. DNA Repair 8, 1242–1249. https://doi.org/10.1016/j.dnarep.2009.07.008

Kalifa, L., Quintana, D.F., Schiraldi, L.K., Phadnis, N., Coles, G.L., Sia, R.A., Sia, E.A., 2012. Mitochondrial genome maintenance: roles for nuclear nonhomologous end-joining proteins in Saccharomyces cerevisiae. Genetics 190, 951–964. https://doi.org/10.1534/genetics.111.138214

Kang, D., Hamasaki, N., 2005. Alterations of mitochondrial DNA in common diseases and disease states: aging, neurodegeneration, heart failure, diabetes, and cancer. Curr. Med. Chem. 12, 429–441. https://doi.org/10.2174/0929867053363081

Karow, J.K., Constantinou, A., Li, J.L., West, S.C., Hickson, I.D., 2000. The Bloom's syndrome gene product promotes branch migration of holliday junctions. Proc. Natl. Acad. Sci. U. S. A. 97, 6504–6508. https://doi.org/10.1073/pnas.100448097

Kaur, J., Datta, K., 2021. IRC3 Regulates Mitochondrial Translation in Response to Metabolic Cues in Saccharomyces cerevisiae. Mol. Cell. Biol. 41.

Kehrein, K., Schilling, R., Möller-Hergt, B.V., Wurm, C.A., Jakobs, S., Lamkemeyer, T., Langer, T., Ott, M., 2015. Organization of Mitochondrial Gene Expression in Two Distinct Ribosome-Containing Assemblies. Cell Rep. 10, 843–853. https://doi.org/10.1016/j.celrep.2015.01.012

Kikuma, T., Ohtsu, M., Utsugi, T., Koga, S., Okuhara, K., Eki, T., Fujimori, F., Murakami, Y., 2004. Dbp9p, a Member of the DEAD Box Protein Family, Exhibits DNA Helicase Activity. J. Biol. Chem. 279, 20692–20698. https://doi.org/10.1074/jbc.M400231200

Kim, S.-Y., Hakoshima, T., Kitano, K., 2013. Structure of the RecQ C-terminal Domain of Human Bloom Syndrome Protein. Sci. Rep. 3, 3294. https://doi.org/10.1038/srep03294

Kim, Y.M., Choi, B.-S., 2010. Structure and function of the regulatory HRDC domain from human Bloom syndrome protein. Nucleic Acids Res. 38, 7764–7777. https://doi.org/10.1093/nar/gkq586

Kitano, K., 2014. Structural mechanisms of human RecQ helicases WRN and BLM. Front. Genet. 5. https://doi.org/10.3389/fgene.2014.00366

Kitano, K., Kim, S.-Y., Hakoshima, T., 2010. Structural basis for DNA strand separation by the unconventional winged-helix domain of RecQ helicase WRN. Struct. Lond. Engl. 1993 18, 177–187. https://doi.org/10.1016/j.str.2009.12.011

Kitano, K., Yoshihara, N., Hakoshima, T., 2007. Crystal structure of the HRDC domain of human Werner syndrome protein, WRN. J. Biol. Chem. 282, 2717–2728. https://doi.org/10.1074/jbc.M610142200

Kitao, S., Shimamoto, A., Goto, M., Miller, R.W., Smithson, W.A., Lindor, N.M., Furuichi, Y., 1999. Mutations in RECQL4 cause a subset of cases of Rothmund-Thomson syndrome. Nat. Genet. 22, 82–84. https://doi.org/10.1038/8788

Köster, S., van Pee, K., Yildiz, Ö., 2015. Chapter Eight – Purification, Refolding, and Crystallization of the Outer Membrane Protein OmpG from Escherichia coli, in: Shukla, A.K. (Ed.), Methods in Enzymology, Membrane Proteins – Engineering, Purification and Crystallization. Academic Press, pp. 149–166. https://doi.org/10.1016/bs.mie.2015.01.018

Krause, K., Lopes de Souza, R., Roberts, D.G.W., Dieckmann, C.L., 2004. The Mitochondrial Message-specific mRNA Protectors Cbp1 and Pet309 Are Associated in a High-Molecular Weight Complex. Mol. Biol. Cell 15, 2674–2683. https://doi.org/10.1091/mbc.e04-02-0126

Kucej, M., Butow, R.A., 2007. Evolutionary tinkering with mitochondrial nucleoids. Trends Cell Biol. 17, 586–592. https://doi.org/10.1016/j.tcb.2007.08.007

Kuusk, S., Sedman, T., Jõers, P., Sedman, J., 2005. Hmi1p from Saccharomyces cerevisiae mitochondria is a structure-specific DNA helicase. J. Biol. Chem. 280, 24322–24329. https://doi.org/10.1074/jbc.M500354200

Lahaye, A., Stahl, H., Thines-Sempoux, D., Foury, F., 1991. PIF1: a DNA helicase in yeast mitochondria. EMBO J. 10, 997–1007. https://doi.org/10.1002/j.1460-2075.1991.tb08034.x

Lee, C.M., Sedman, J., Neupert, W., Stuart, R.A., 1999. The DNA helicase, Hmi1p, is transported into mitochondria by a C-terminal cleavable targeting signal. J. Biol. Chem. 274, 20937–20942. https://doi.org/10.1074/jbc.274.30.20937

Leuenberger, P., Ganscha, S., Kahraman, A., Cappelletti, V., Boersema, P.J., von Mering, C., Claassen, M., Picotti, P., 2017. Cell-wide analysis of protein thermal unfolding reveals determinants of thermostability. Science 355, eaai7825. https://doi.org/10.1126/science.aai7825

Levin, M.K., Gurjar, M., Patel, S.S., 2005. A Brownian motor mechanism of translocation and strand separation by hepatitis C virus helicase. Nat. Struct. Mol. Biol. 12, 429–435. https://doi.org/10.1038/nsmb920

Li, Z., Lu, S., Hou, G., Ma, X., Sheng, D., Ni, J., Shen, Y., 2008. Hjm/Hel308A DNA helicase from Sulfolobus tokodaii promotes replication fork regression and interacts with Hjc endonuclease in vitro. J. Bacteriol. 190, 3006–3017. https://doi.org/10.1128/JB.01662-07

Linder, P., Jankowsky, E., 2011. From unwinding to clamping — the DEAD box RNA helicase family. Nat. Rev. Mol. Cell Biol. 12, 505–516. https://doi.org/10.1038/nrm3154

Ling, F., Hori, A., Shibata, T., 2007. DNA Recombination-Initiation Plays a Role in the Extremely Biased Inheritance of Yeast [rho–] Mitochondrial DNA That Contains the Replication Origin ori5. Mol. Cell. Biol. 27, 1133–1145. https://doi.org/10.1128/MCB.00770-06

Ling, F., Makishima, F., Morishima, N., Shibata, T., 1995. A nuclear mutation defective in mitochondrial recombination in yeast. EMBO J. 14, 4090–4101. https://doi.org/10.1002/j.1460-2075.1995.tb00081.x

Ling, F., Shibata, T., 2002. Recombination-dependent mtDNA partitioning: in vivo role of Mhr1p to promote pairing of homologous DNA. EMBO J. 21, 4730–4740. https://doi.org/10.1093/emboj/cdf466

Ling, F., Yoshida, M., Shibata, T., 2009. Heteroduplex joint formation free of net topological change by Mhr1, a mitochondrial recombinase. J. Biol. Chem. 284, 9341–9353. https://doi.org/10.1074/jbc.M900023200

Lohman, T.M., Tomko, E.J., Wu, C.G., 2008. Non-hexameric DNA helicases and translocases: mechanisms and regulation. Nat. Rev. Mol. Cell Biol. 9, 391–401. https://doi.org/10.1038/nrm2394

Lorimer, H.E., Brewer, B.J., Fangman, W.L., 1995. A Test of the Transcription Model for Biased Inheritance of Yeast Mitochondrial DNA. Mol. Cell. Biol. 15, 4803–4809. https://doi.org/10.1128/MCB.15.9.4803

Makovets, S., Blackburn, E.H., 2009. DNA damage signalling prevents deleterious telomere addition at DNA breaks. Nat. Cell Biol. 11, 1383–1386. https://doi.org/10.1038/ncb1985

Malecki, M., Jedrzejczak, R., Puchta, O., Stepien, P.P., Golik, P., 2008. In vivo and in vitro approaches for studying the yeast mitochondrial RNA degradosome complex. Methods Enzymol. 447, 463–488. https://doi.org/10.1016/S0076-6879(08)02222-2

Malecki, M., Jedrzejczak, R., Stepien, P.P., Golik, P., 2007. In vitro Reconstitution and Characterization of the Yeast Mitochondrial Degradosome Complex Unravels Tight Functional Interdependence. J. Mol. Biol. 372, 23–36. https://doi.org/10.1016/j.jmb.2007.06.074

Maleszka, R., Skelly, P. j., Clark-Walker, G. d., 1991. Rolling circle replication of DNA in yeast mitochondria. EMBO J. 10, 3923–3929. https://doi.org/10.1002/j.1460-2075.1991.tb04962.x

Malone, E.G., Thompson, M.D., Byrd, A.K., 2022. Role and Regulation of Pif1 Family Helicases at the Replication Fork. Int. J. Mol. Sci. 23, 3736. https://doi.org/10.3390/ijms23073736

Manthei, K.A., Keck, J.L., 2013. The BLM dissolvasome in DNA replication and repair. Cell. Mol. Life Sci. CMLS 70, 4067–4084. https://doi.org/10.1007/s00018-013-1325-1

Marini, F., Wood, R.D., 2002. A Human DNA Helicase Homologous to the DNA Cross-link Sensitivity Protein Mus308 *. J. Biol. Chem. 277, 8716–8723. https://doi.org/10.1074/jbc.M110271200

Martegani, E., Vanoni, M., Mauri, I., Rudoni, S., Saliola, M., Alberghina, L., 1997. Identification of gene encoding a putative RNA-helicase, homologous to SKI2, in chromosome VII of Saccharomyces cerevisiae. Yeast Chichester Engl. 13, 391–397. https://doi.org/10.1002/(sici)1097-0061(19970330)13:4<391::aid-yea92>3.0.co;2-q

Mason, T.L., Pan, C., Sanchirico, M.E., Sirum-Connolly, K., 1996. Molecular genetics of the peptidyl transferase center and the unusual Var1 protein in yeast mitochondrial ribosomes. Experientia 52, 1148–1157. https://doi.org/10.1007/BF01952114

Mbantenkhu, M., Wang, X., Nardozzi, J.D., Wilkens, S., Hoffman, E., Patel, A., Cosgrove, M.S., Chen, X.J., 2011. Mgm101 is a Rad52-related protein required for mitochondrial DNA recombination. J. Biol. Chem. 286, 42360–42370. https://doi.org/10.1074/jbc.M111.307512

Miyakawa, I., 2017. Organization and dynamics of yeast mitochondrial nucleoids. Proc. Jpn. Acad. Ser. B Phys. Biol. Sci. 93, 339–359. https://doi.org/10.2183/pjab.93.021

Mohaghegh, P., Karow, J.K., Brosh Jr, R.M., Bohr, V.A., Hickson, I.D., 2001. The Bloom's and Werner's syndrome proteins are DNA structure-specific helicases. Nucleic Acids Res. 29, 2843–2849.

Mohr, G., Del Campo, M., Turner, K.G., Gilman, B., Wolf, R.Z., Lambowitz, A.M., 2011. High-throughput genetic identification of functionally important regions of the yeast DEAD-box protein Mss116p. J. Mol. Biol. 413, 952–972. https://doi.org/10.1016/j.jmb.2011.09.015

Mookerjee, S.A., Sia, E.A., 2006. Overlapping contributions of Msh1p and putative recombination proteins Cce1p, Din7p, and Mhr1p in large-scale recombination and genome sorting events in the mitochondrial genome of Saccharomyces cerevisiae. Mutat. Res. Mol. Mech. Mutagen. 595, 91–106. https://doi.org/10.1016/j.mrfmmm.2005.10.006

Morgenstern, M., Stiller, S.B., Lübbert, P., Peikert, C.D., Dannenmaier, S., Drepper, F., Weill, U., Höß, P., Feuerstein, R., Gebert, M., Bohnert, M., van der Laan, M., Schuldiner, M., Schütze, C., Oeljeklaus, S., Pfanner, N., Wiedemann, N., Warscheid, B., 2017. Definition of a High-Confidence Mitochondrial Proteome at Quantitative Scale. Cell Rep. 19, 2836–2852. https://doi.org/10.1016/j.celrep.2017.06.014

Murakami, K., Nakano, K., Shimizu, T., Ohto, U., 2017. The crystal structure of human DEAH-box RNA helicase 15 reveals a domain organization of the mammalian DEAH/RHA family. Acta Crystallogr. Sect. F Struct. Biol. Commun. 73, 347–355. https://doi.org/10.1107/S2053230X17007336

Muzzini, D.M., Plevani, P., Boulton, S.J., Cassata, G., Marini, F., 2008. Caenorhabditis elegans POLQ-1 and HEL-308 function in two distinct DNA interstrand cross-link repair pathways. DNA Repair 7, 941–950. https://doi.org/10.1016/j.dnarep.2008.03.021

Naithani, S., Saracco, S.A., Butler, C.A., Fox, T.D., 2003. Interactions among COX1, COX2, and COX3 mRNA-specific translational activator proteins on the inner surface of the mitochondrial inner membrane of Saccharomyces cerevisiae. Mol. Biol. Cell 14, 324–333. https://doi.org/10.1091/mbc.e02-08-0490

Nakagawa, K., Morishima, N., Shibata, T., 1991. A maturase-like subunit of the sequence-specific endonuclease endo.SceI from yeast mitochondria. J. Biol. Chem. 266, 1977–1984.

Nielsen, K.H., Chamieh, H., Andersen, C.B.F., Fredslund, F., Hamborg, K., Le Hir, H., Andersen, G.R., 2009. Mechanism of ATP turnover inhibition in the EJC. RNA N. Y. N 15, 67–75. https://doi.org/10.1261/rna.1283109

Northall, S.J., Buckley, R., Jones, N., Penedo, J.C., Soultanas, P., Bolt, E.L., 2017. DNA binding and unwinding by Hel308 helicase requires dual functions of a winged helix domain. DNA Repair 57, 125–132. https://doi.org/10.1016/j.dnarep.2017.07.005

Ononye, O.E., Sausen, C.W., Balakrishnan, L., Bochman, M.L., 2020. Lysine acetylation regulates the activity of nuclear Pif1. J. Biol. Chem. 295, 15482–15497. https://doi.org/10.1074/jbc.RA120.015164

O'Rourke, T.W., Doudican, N.A., Mackereth, M.D., Doetsch, P.W., Shadel, G.S., 2002. Mitochondrial Dysfunction Due to Oxidative Mitochondrial DNA Damage Is Reduced through Cooperative Actions of Diverse Proteins. Mol. Cell. Biol. 22, 4086–4093. https://doi.org/10.1128/MCB.22.12.4086-4093.2002

Osinga, K.A., Haan, M.D., Christianson, T., Tabak, H.F., 1982. A nonanucleotide sequence involved in promotion of ribosomal RNA synthesis and RNA priming of DNA replication on yeast mitochondria. Nucleic Acids Res. 10, 7993–8006. https://doi.org/10.1093/nar/10.24.7993

Ozgur, S., Buchwald, G., Falk, S., Chakrabarti, S., Prabu, J.R., Conti, E., 2015. The conformational plasticity of eukaryotic RNA-dependent ATPases. FEBS J. 282, 850–863. https://doi.org/10.1111/febs.13198

Pâques, F., Haber, J.E., 1999. Multiple pathways of recombination induced by double-strand breaks in Saccharomyces cerevisiae. Microbiol. Mol. Biol. Rev. 63, 349–404. https://doi.org/10.1128/mmbr.63.2.349-404.1999

Patel, S.S., Donmez, I., 2006. Mechanisms of Helicases. J. Biol. Chem. 281, 18265–18268. https://doi.org/10.1074/jbc.R600008200

Pena, V., Jovin, S.M., Fabrizio, P., Orlowski, J., Bujnicki, J.M., Lührmann, R., Wahl, M.C., 2009. Common Design Principles in the Spliceosomal RNA Helicase Brr2 and in the Hel308 DNA Helicase. Mol. Cell 35, 454–466. https://doi.org/10.1016/j.molcel.2009.08.006

Percival, K.J., Klein, M.B., Burgers, P.M., 1989. Molecular cloning and primary structure of the uracil-DNA-glycosylase gene from Saccharomyces cerevisiae. J. Biol. Chem. 264, 2593–2598.

Perocchi, F., Jensen, L.J., Gagneur, J., Ahting, U., Mering, C. von, Bork, P., Prokisch, H., Steinmetz, L.M., 2006. Assessing Systems Properties of Yeast Mitochondria through an Interaction Map of the Organelle. PLOS Genet. 2, e170. https://doi.org/10.1371/journal.pgen.0020170

Pike, A.C.W., Shrestha, B., Popuri, V., Burgess-Brown, N., Muzzolini, L., Costantini, S., Vindigni, A., Gileadi, O., 2009. Structure of the human RECQ1 helicase reveals a putative strand-separation pin. Proc. Natl. Acad. Sci. U. S. A. 106, 1039–1044. https://doi.org/10.1073/pnas.0806908106

Piljukov, V., Garber, N., Sedman, T., Sedman, J., 2020. Irc3 is a monomeric DNA branch point-binding helicase in mitochondria of the yeast Saccharomyces cerevisiae. FEBS Lett. 594, 3142–3155. https://doi.org/10.1002/1873-3468.13893

Piljukov, V.-J., Sillamaa, S., Sedman, T., Garber, N., Rätsep, M., Freiberg, A., Sedman, J., 2023. Mitochondrial Irc3 helicase of the thermotolerant yeast Ogataea polymorpha displays dual DNA- and RNA-stimulated ATPase activity. Mitochondrion 69, 130–139. https://doi.org/10.1016/j.mito.2023.02.004

Prasai, K., Robinson, L.C., Scott, R.S., Tatchell, K., Harrison, L., 2017. Evidence for double-strand break mediated mitochondrial DNA replication in Saccharomyces cerevisiae. Nucleic Acids Res. 45, 7760–7773. https://doi.org/10.1093/nar/gkx443

Pyle, A.M., 2008. Translocation and unwinding mechanisms of RNA and DNA helicases. Annu. Rev. Biophys. 37, 317–336. https://doi.org/10.1146/annurev.biophys.37.032807.125908

Ribeyre, C., Lopes, J., Boulé, J.-B., Piazza, A., Guédin, A., Zakian, V.A., Mergny, J.-L., Nicolas, A., 2009. The yeast Pif1 helicase prevents genomic instability caused by G-quadruplex-forming CEB1 sequences in vivo. PLoS Genet. 5, e1000475. https://doi.org/10.1371/journal.pgen.1000475

Richards, J.D., Johnson, K.A., Liu, H., McRobbie, A.-M., McMahon, S., Oke, M., Carter, L., Naismith, J.H., White, M.F., 2008. Structure of the DNA Repair Helicase Hel308 Reveals DNA Binding and Autoinhibitory Domains. J. Biol. Chem. 283, 5118–5126. https://doi.org/10.1074/jbc.M707548200

Rodeheffer, M.S., Shadel, G.S., 2003. Multiple interactions involving the amino-terminal domain of yeast mtRNA polymerase determine the efficiency of mitochondrial protein synthesis. J. Biol. Chem. 278, 18695–18701. https://doi.org/10.1074/jbc.M301399200

Rogowska, A.T., Puchta, O., Czarnecka, A.M., Kaniak, A., Stepien, P.P., Golik, P., 2006. Balance between Transcription and RNA Degradation Is Vital for Saccharomyces cerevisiae Mitochondria: Reduced Transcription Rescues the Phenotype of Deficient RNA Degradation. Mol. Biol. Cell 17, 1184–1193. https://doi.org/10.1091/mbc.e05-08-0796

Sanchez-Sandoval, E., Diaz-Quezada, C., Velazquez, G., Arroyo-Navarro, L.F., Almanza-Martinez, N., Trasviña-Arenas, C.H., Brieba, L.G., 2015. Yeast mitochondrial RNA polymerase primes mitochondrial DNA polymerase at origins of replication and promoter sequences. Mitochondrion 24, 22–31. https://doi.org/10.1016/j.mito.2015.06.004

Sato, H., Miyakawa, I., 2004. A 22kDa protein specific for yeast mitochondrial nucleoids is an unidentified putative ribosomal protein encoded in open reading frame YGL068W. Protoplasma 223, 175–182. https://doi.org/10.1007/s00709-004-0040-z

Schmidt, U., Lehmann, K., Stahl, U., 2002. A novel mitochondrial DEAD box protein (Mrh4) required for maintenance of mtDNA in Saccharomyces cerevisiae. FEMS Yeast Res. 2, 267–276. https://doi.org/10.1016/S1567-1356(02)00109-5

Schulte, U., den Brave, F., Haupt, A., Gupta, A., Song, J., Müller, C.S., Engelke, J., Mishra, S., Mårtensson, C., Ellenrieder, L., Priesnitz, C., Straub, S.P., Doan, K.N., Kulawiak, B., Bildl, W., Rampelt, H., Wiedemann, N., Pfanner, N., Fakler, B., Becker, T., 2023. Mitochondrial complexome reveals quality-control pathways of protein import. Nature 614, 153–159. https://doi.org/10.1038/s41586-022-05641-w

Schulz, V.P., Zakian, V.A., 1994. The saccharomyces PIF1 DNA helicase inhibits telomere elongation and de novo telomere formation. Cell 76, 145–155. https://doi.org/10.1016/0092-8674(94)90179-1

Schürer, K.A., Rudolph, C., Ulrich, H.D., Kramer, W., 2004. Yeast MPH1 gene functions in an error-free DNA damage bypass pathway that requires genes from Homologous recombination, but not from postreplicative repair. Genetics 166, 1673–1686.

Schwer, B., 2008. A conformational rearrangement in the spliceosome sets the stage for Prp22-dependent mRNA release. Mol. Cell 30, 743–754. https://doi.org/10.1016/j.molcel.2008.05.003

Sedman, T., Gaidutšik, I., Villemson, K., Hou, Y., Sedman, J., 2014. Double-stranded DNA-dependent ATPase Irc3p is directly involved in mitochondrial genome maintenance. Nucleic Acids Res. 42, 13214–13227. https://doi.org/10.1093/nar/gku1148

Sedman, T., Garber, N., Gaidutšik, I., Sillamaa, S., Paats, J., Piljukov, V.J., Sedman, J., 2017. Mitochondrial helicase Irc3 translocates along double-stranded DNA. FEBS Lett. 591, 3831–3841. https://doi.org/10.1002/1873-3468.12903

Sedman, T., Jõers, P., Kuusk, S., Sedman, J., 2005. Helicase Hmi1 stimulates the synthesis of concatemeric mitochondrial DNA molecules in yeast Saccharomyces cerevisiae. Curr. Genet. 47, 213–222. https://doi.org/10.1007/s00294-005-0566-4

Sedman, T., Kuusk, S., Kivi, S., Sedman, J., 2000. A DNA helicase required for maintenance of the functional mitochondrial genome in Saccharomyces cerevisiae. Mol. Cell. Biol. 20, 1816–1824. https://doi.org/10.1128/MCB.20.5.1816-1824.2000

Semlow, D.R., Blanco, M.R., Walter, N.G., Staley, J.P., 2016. Spliceosomal DEAH-Box ATPases Remodel Pre-mRNA to Activate Alternative Splice Sites. Cell 164, 985–998. https://doi.org/10.1016/j.cell.2016.01.025

Séraphin, B., Boulet, A., Simon, M., Faye, G., 1987. Construction of a yeast strain devoid of mitochondrial introns and its use to screen nuclear genes involved in mitochondrial splicing. Proc. Natl. Acad. Sci. 84, 6810–6814. https://doi.org/10.1073/pnas.84.19.6810

Séraphin, B., Simon, M., Boulet, A., Faye, G., 1989. Mitochondrial splicing requires a protein from a novel helicase family. Nature 337, 84–87. https://doi.org/10.1038/337084a0

Séraphin, B., Simon, M., Faye, G., 1988. MSS18, a yeast nuclear gene involved in the splicing of intron aI5 beta of the mitochondrial cox1 transcript. EMBO J. 7, 1455–1464. https://doi.org/10.1002/j.1460-2075.1988.tb02963.x

Shibata, T., Ling, F., 2007. DNA recombination protein-dependent mechanism of homoplasmy and its proposed functions. Mitochondrion, Mitochondria and Life 7, 17–23. https://doi.org/10.1016/j.mito.2006.11.024

Shim, E.Y., Chung, W.-H., Nicolette, M.L., Zhang, Y., Davis, M., Zhu, Z., Paull, T.T., Ira, G., Lee, S.E., 2010. Saccharomyces cerevisiae Mre11/Rad50/Xrs2 and Ku proteins regulate association of Exo1 and Dna2 with DNA breaks. EMBO J. 29, 3370–3380. https://doi.org/10.1038/emboj.2010.219

Sickmann, A., Reinders, J., Wagner, Y., Joppich, C., Zahedi, R., Meyer, H.E., Schönfisch, B., Perschil, I., Chacinska, A., Guiard, B., Rehling, P., Pfanner, N., Meisinger, C., 2003. The proteome of Saccharomyces cerevisiae mitochondria. Proc. Natl. Acad. Sci. U. S. A. 100, 13207–13212. https://doi.org/10.1073/pnas.2135385100

Singleton, M.R., Dillingham, M.S., Wigley, D.B., 2007. Structure and mechanism of helicases and nucleic acid translocases. Annu. Rev. Biochem. 76, 23–50. https://doi.org/10.1146/annurev.biochem.76.052305.115300

Smaldino, P.J., Routh, E.D., Kim, J.H., Giri, B., Creacy, S.D., Hantgan, R.R., Akman, S.A., Vaughn, J.P., 2015. Mutational Dissection of Telomeric DNA Binding Requirements of G4 Resolvase 1 Shows that G4-Structure and Certain 3'-Tail Sequences Are Sufficient for Tight and Complete Binding. PloS One 10, e0132668. https://doi.org/10.1371/journal.pone.0132668

Solem, A., Zingler, N., Pyle, A.M., 2006. A DEAD protein that activates intron self-splicing without unwinding RNA. Mol. Cell 24, 611–617. https://doi.org/10.1016/j.molcel.2006.10.032

Steele, D.F., Butler, C.A., Fox, T.D., 1996. Expression of a recoded nuclear gene inserted into yeast mitochondrial DNA is limited by mRNA-specific translational activation. Proc. Natl. Acad. Sci. 93, 5253–5257. https://doi.org/10.1073/pnas.93.11.5253

Stepien, P.P., Margossian, S.P., Landsman, D., Butow, R.A., 1992. The yeast nuclear gene suv3 affecting mitochondrial post-transcriptional processes encodes a putative ATP-dependent RNA helicase. Proc. Natl. Acad. Sci. 89, 6813–6817. https://doi.org/10.1073/ pnas.89.15.6813

Stewart, J.B., Chinnery, P.F., 2021. Extreme heterogeneity of human mitochondrial DNA from organelles to populations. Nat. Rev. Genet. 22, 106–118. https://doi.org/10.1038/s41576-020-00284-x

Sun, H., Karow, J.K., Hickson, I.D., Maizels, N., 1998. The Bloom's syndrome helicase unwinds G4 DNA. J. Biol. Chem. 273, 27587–27592. https://doi.org/10.1074/jbc.273.42.27587

Swan, M.K., Legris, V., Tanner, A., Reaper, P.M., Vial, S., Bordas, R., Pollard, J.R., Charlton, P.A., Golec, J.M.C., Bertrand, J.A., 2014. Structure of human Bloom's syndrome helicase in complex with ADP and duplex DNA. Acta Crystallogr. D Biol. Crystallogr. 70, 1465–1475. https://doi.org/10.1107/S139900471400501X

Szczesny, R.J., Wojcik, M.A., Borowski, L.S., Szewczyk, M.J., Skrok, M.M., Golik, P., Stepien, P.P., 2013. Yeast and human mitochondrial helicases. Biochim. Biophys. Acta BBA – Gene Regul. Mech. 1829, 842–853. https://doi.org/10.1016/j.bbagrm.2013.02.009

Tadokoro, T., Kulikowicz, T., Dawut, L., Croteau, D.L., Bohr, V.A., 2012. DNA binding residues in the RQC domain of Werner protein are critical for its catalytic activities. Aging 4, 417–429. https://doi.org/10.18632/aging.100463

Talwar, T., Vidhyasagar, V., Qing, J., Guo, M., Kariem, A., Lu, Y., Singh, R.S., Lukong, K.E., Wu, Y., 2017. The DEAD-box protein DDX43 (HAGE) is a dual RNA-DNA helicase and has a K-homology domain required for full nucleic acid unwinding activity. J. Biol. Chem. 292, 10429–10443. https://doi.org/10.1074/jbc.M117.774950

Tanaka, N., Schwer, B., 2006. Mutations in PRP43 that uncouple RNA-dependent NTPase Activity and pre-mRNA Splicing Function. Biochemistry 45, 6510–6521. https://doi.org/10.1021/bi052656g

Tanaka, N., Schwer, B., 2005. Characterization of the NTPase, RNA-binding, and RNA helicase activities of the DEAH-box splicing factor Prp22. Biochemistry 44, 9795–9803. https://doi.org/10.1021/bi050407m

Tay, Y.D., Sidebotham, J.M., Wu, L., 2010. Mph1 requires mismatch repair-independent and -dependent functions of MutSα to regulate crossover formation during homologous recombination repair. Nucleic Acids Res. 38, 1889–1901. https://doi.org/10.1093/nar/gkp1199

The UniProt Consortium, 2023. UniProt: the Universal Protein Knowledgebase in 2023. Nucleic Acids Res. 51, D523–D531. https://doi.org/10.1093/nar/gkac1052

Theissen, B., Karow, A.R., Köhler, J., Gubaev, A., Klostermeier, D., 2008. Cooperative binding of ATP and RNA induces a closed conformation in a DEAD box RNA helicase. Proc. Natl. Acad. Sci. 105, 548–553. https://doi.org/10.1073/pnas.0705488105

Trujillo, K.M., Roh, D.H., Chen, L., Komen, S.V., Tomkinson, A., Sung, P., 2003. Yeast Xrs2 Binds DNA and Helps Target Rad50 and Mre11 to DNA Ends *. J. Biol. Chem. 278, 48957–48964. https://doi.org/10.1074/jbc.M309877200

Trujillo, K.M., Sung, P., 2001. DNA structure-specific nuclease activities in the Saccharomyces cerevisiae Rad50*Mre11 complex. J. Biol. Chem. 276, 35458–35464. https://doi.org/10.1074/jbc.M105482200

Tzagoloff, A., Dieckmann, C.L., 1990. PET genes of Saccharomyces cerevisiae. Microbiol. Rev. 54, 211–225. https://doi.org/10.1128/mr.54.3.211-225.1990

Umezu, K., Nakayama, K., Nakayama, H., 1990. Escherichia coli RecQ protein is a DNA helicase. Proc. Natl. Acad. Sci. U. S. A. 87, 5363–5367.
van Brabant, A.J., Ye, T., Sanz, M., German III, J.L., Ellis, N.A., Holloman, W.K., 2000. Binding and melting of D-loops by the Bloom syndrome helicase. Biochemistry 39, 14617–14625. https://doi.org/10.1021/bi0018640
van der Kemp, P.A., Thomas, D., Barbey, R., de Oliveira, R., Boiteux, S., 1996. Cloning and expression in Escherichia coli of the OGG1 gene of Saccharomyces cerevisiae, which codes for a DNA glycosylase that excises 7,8-dihydro-8-oxoguanine and 2,6-diamino-4-hydroxy-5-N-methylformamidopyrimidine. Proc. Natl. Acad. Sci. U. S. A. 93, 5197–5202. https://doi.org/10.1073/pnas.93.11.5197
Velankar, S.S., Soultanas, P., Dillingham, M.S., Subramanya, H.S., Wigley, D.B., 1999. Crystal structures of complexes of PcrA DNA helicase with a DNA substrate indicate an inchworm mechanism. Cell 97, 75–84. https://doi.org/10.1016/s0092-8674(00)80716-3
Vongsamphanh, R., Fortier, P.-K., Ramotar, D., 2001. Pir1p Mediates Translocation of the Yeast Apn1p Endonuclease into the Mitochondria To Maintain Genomic Stability. Mol. Cell. Biol. 21, 1647–1655. https://doi.org/10.1128/MCB.21.5.1647-1655.2001
Walbott, H., Mouffok, S., Capeyrou, R., Lebaron, S., Humbert, O., van Tilbeurgh, H., Henry, Y., Leulliot, N., 2010. Prp43p contains a processive helicase structural architecture with a specific regulatory domain. EMBO J. 29, 2194–2204. https://doi.org/10.1038/emboj.2010.102
Wang, Y., Guthrie, C., 1998. PRP16, a DEAH-box RNA helicase, is recruited to the spliceosome primarily via its nonconserved N-terminal domain. RNA N. Y. N 4, 1216–1229.
Wang, Y., Shadel, G.S., 1999. Stability of the mitochondrial genome requires an amino-terminal domain of yeast mitochondrial RNA polymerase. Proc. Natl. Acad. Sci. 96, 8046–8051. https://doi.org/10.1073/pnas.96.14.8046
Weir, J.R., Bonneau, F., Hentschel, J., Conti, E., 2010. Structural analysis reveals the characteristic features of Mtr4, a DExH helicase involved in nuclear RNA processing and surveillance. Proc. Natl. Acad. Sci. 107, 12139–12144. https://doi.org/10.1073/pnas.1004953107
Wiesenberger, G., Fox, T.D., 1997. Pet127p, a Membrane-Associated Protein Involved in Stability and Processing of Saccharomyces cerevisiae Mitochondrial RNAs. Mol. Cell. Biol. 17, 2816–2824. https://doi.org/10.1128/MCB.17.5.2816
Wong, I., Lohman, T.M., 1992. Allosteric effects of nucleotide cofactors on Escherichia coli Rep helicase-DNA binding. Science 256, 350–355. https://doi.org/10.1126/science.256.5055.350
Woodman, I.L., Brammer, K., Bolt, E.L., 2011. Physical interaction between archaeal DNA repair helicase Hel308 and Replication Protein A (RPA). DNA Repair 10, 306–313. https://doi.org/10.1016/j.dnarep.2010.12.001
Yang, Q., Del Campo, M., Lambowitz, A.M., Jankowsky, E., 2007. DEAD-box proteins unwind duplexes by local strand separation. Mol. Cell 28, 253–263. https://doi.org/10.1016/j.molcel.2007.08.016
You, H.J., Swanson, R.L., Harrington, C., Corbett, A.H., Jinks-Robertson, S., Sentürker, S., Wallace, S.S., Boiteux, S., Dizdaroglu, M., Doetsch, P.W., 1999. Saccharomyces cerevisiae Ntg1p and Ntg2p: broad specificity N-glycosylases for the repair of oxidative DNA damage in the nucleus and mitochondria. Biochemistry 38, 11298–11306. https://doi.org/10.1021/bi991121i

Young, M.C., Kuhl, S.B., von Hippel, P.H., 1994. Kinetic theory of ATP-driven translocases on one-dimensional polymer lattices. J. Mol. Biol. 235, 1436–1446. https://doi.org/10.1006/jmbi.1994.1099

Yu, C.E., Oshima, J., Fu, Y.H., Wijsman, E.M., Hisama, F., Alisch, R., Matthews, S., Nakura, J., Miki, T., Ouais, S., Martin, G.M., Mulligan, J., Schellenberg, G.D., 1996. Positional cloning of the Werner's syndrome gene. Science 272, 258–262. https://doi.org/10.1126/science.272.5259.258

Zassenhaus, H.P., Denniger, G., 1994. Analysis of the role of the NUC1 endo/exonuclease in yeast mitochondrial DNA recombination. Curr. Genet. 25, 142–149. https://doi.org/10.1007/BF00309540

Zhou, J.-Q., Monson, E.K., Teng, S.-C., Schulz, V.P., Zakian, V.A., 2000. Pif1p Helicase, a Catalytic Inhibitor of Telomerase in Yeast. Science 289, 771–774. https://doi.org/10.1126/science.289.5480.771

Zhou, R., Zhang, J., Bochman, M.L., Zakian, V.A., Ha, T., 2014. Periodic DNA patrolling underlies diverse functions of Pif1 on R-loops and G-rich DNA. eLife 3, e02190. https://doi.org/10.7554/eLife.02190

Ziaja, K., Michaelis, G., Lisowsky, T., 1993. Nuclear Control of the Messenger RNA Expression for Mitochondrial ATPase Subunit 9 in a New Yeast Mutant. J. Mol. Biol. 229, 909–916. https://doi.org/10.1006/jmbi.1993.1095

Zuo, X.M., Clark-Walker, G.D., Chen, X.J., 2002. The mitochondrial nucleoid protein, Mgm101p, of Saccharomyces cerevisiae is involved in the maintenance of rho(+) and ori/rep-devoid petite genomes but is not required for hypersuppressive rho(–) mtDNA. Genetics 160, 1389–1400. https://doi.org/10.1093/genetics/160.4.1389

ACKNOWLEDGEMENTS

I would like to express my deepest appreciation to my supervisor, Prof. Juhan Sedman, for giving me the valuable opportunity to pursue my PhD studies in his lab. He has always believed in my abilities and provided patient guidance throughout these years. I am also grateful to Dr. Tiina Sedman for her experimental knowledge, which has helped me with many of my projects.

I am deeply indebted to Prof. Osamu Shimmi for taking the time to review my thesis. I would also like to thank my companions, especially Nataša and Sirelin, who have been with me on this tough journey. They were always ready to discuss my thoughts and ideas, and they also supported me when experiments didn't go as planned, which happened quite often. I am also grateful to Maie for her amazing technical support and constant encouragement throughout these years.

I would like to thank the past and present members of the Department of Biochemistry, including Dr. Riin Kont, Dr. Silja Kuusk, Dr. Jürgen Jalak, and Associate Prof. Priit Väljamäe, for their support.

I would also like to express my gratitude to the members of the Department of Molecular Biology, including Prof. Emeritus Jaanus Remme, Prof. Tiina Tamm, Associate Prof. Aivar Liiv, Dr. Silva Lilleorg, and Dr. Margus Leppik, for generously sharing their knowledge and offering constructive criticism. I also wish to thank past and present PhD students, Dr. Ivan Kisly and Kaspar Reier, for engaging in discussions on various scientific topics.

I also owe a special debt of gratitude to my parents and family, whose unwavering support has made it possible for me to stand where I am today. Finally, I am grateful for the support and encouragement of my friends and girlfriend, which have all been crucial during this challenging journey.

PUBLICATIONS

CURRICULUM VITAE

Name: Vlad-Julian Piljukov
Citizenship: Estonian
Date of birth: 31.03.1993
E-mail: vlad-julian.piljukov@ut.ee

Language skills: Russian (native), Estonian, English

Education

2017–...	Molecular and cell Biology Ph.D. studies
2015–2017	Gene technology master studies
2012–2015	Gene technology bachelor studies
2000–2012	Tartu Annelinna Gymnasium

Fields of research

ETIS RESEARCH FIELD: 1. Biosciences and Environment; 1.1. Biochemistry;
CERCS RESEARCH FIELD: P310 Proteins, enzymology

Professional career

01.10.2022–31.05.2023	University of Tartu, Faculty of Science and Technology, Institute of Molecular and Cell Biology, Junior Research Fellow in Biochemistry (0,50)
01.09.2020–31.08.2022	University of Tartu, Faculty of Science and Technology, Institute of Molecular and Cell Biology, Junior Research Fellow (0,50)

Publications

2023

Piljukov, V.J.; Sillamaa, S.; Sedman, T.; Garber, N.; Rätsep, M.; Freiberg, A.; Sedman, J. (2023). Mitochondrial Irc3 helicase of the thermotolerant yeast Ogataea polymorpha displays dual DNA- and RNA-stimulated ATPase activity. Mitochondrion, 69, 130–139. DOI: 10.1016/j.mito.2023.02.004.

2020

Piljukov, Vlad–Julian; Garber, Natalja; Sedman, Tiina; Sedman, Juhan (2020). Irc3 is a monomeric DNA branch point-binding helicase in mitochondria of the yeast Saccharomyces cerevisiae. FEBS Letters. DOI: 10.1002/1873-3468.13893.

2017

Sedman, Tiina; Garber, Natalja; Gaidutšik, Ilja; Sillamaa, Sirelin; Paats, Joosep; Piljukov, Vlad-J; Sedman, Juhan (2017). Mitochondrial helicase Irc3 translocates along double-stranded DNA. FEBS Letters, 591 (23), 3831–3841. DOI: 10.1002/1873-3468.12903.

ELULOOKIRJELDUS

Nimi: Vlad-Julian Piljukov
Kodakondsus: Eesti
Sünniaeg: 31.03.1993
E-post: vlad-julian.piljukov@ut.ee

Keeleoskus: Vene keel (emakeel), Eesti keel, Inglise keel

Haridustee

2017–...	Molekulaar- ja rakubioloogia doktoriõpe
2015–2017	Geenitehnoloogia magistriõpe
2012–2015	Geenitehnoloogia bakalaureuseõpe
2000–2012	Tartu Annelinna Gümnaasium

Teadustöö põhisuunad
ETIS VALDKOND: 1. Bio- ja keskkonnateadused; 1.1. Biokeemia;
CERCS VALDKOND: P310 Proteiinid, ensümoloogia

Töökohad ja ametid

01.10.2022–31.05.2023	Tartu Ülikool, Loodus- ja täppisteaduste valdkond, molekulaar- ja rakubioloogia instituut, biokeemia nooremteadur (0,50)
01.09.2020–31.08.2022	Tartu Ülikool, Loodus- ja täppisteaduste valdkond, molekulaar- ja rakubioloogia instituut, biomeditsiini ja biotehnoloogia nooremteadur (0,50)

Publikatsioonid

2023

Piljukov, V.J.; Sillamaa, S.; Sedman, T.; Garber, N.; Rätsep, M.; Freiberg, A.; Sedman, J. (2023). Mitochondrial Irc3 helicase of the thermotolerant yeast Ogataea polymorpha displays dual DNA- and RNA-stimulated ATPase activity. Mitochondrion, 69, 130–139. DOI: 10.1016/j.mito.2023.02.004.

2020

Piljukov, Vlad–Julian; Garber, Natalja; Sedman, Tiina; Sedman, Juhan (2020). Irc3 is a monomeric DNA branch point-binding helicase in mitochondria of the yeast Saccharomyces cerevisiae. FEBS Letters. DOI: 10.1002/1873-3468.13893.

2017

Sedman, Tiina; Garber, Natalja; Gaidutšik, Ilja; Sillamaa, Sirelin; Paats, Joosep; Piljukov, Vlad-J; Sedman, Juhan (2017). Mitochondrial helicase Irc3 translocates along double-stranded DNA. FEBS Letters, 591 (23), 3831–3841. DOI: 10.1002/1873-3468.12903.

DISSERTATIONES BIOLOGICAE UNIVERSITATIS TARTUENSIS

1. **Toivo Maimets**. Studies of human oncoprotein p53. Tartu, 1991, 96 p.
2. **Enn K. Seppet**. Thyroid state control over energy metabolism, ion transport and contractile functions in rat heart. Tartu, 1991, 135 p.
3. **Kristjan Zobel**. Epifüütsete makrosamblike väärtus õhu saastuse indikaatoritena Hamar-Dobani boreaalsetes mägimetsades. Tartu, 1992, 131 lk.
4. **Andres Mäe**. Conjugal mobilization of catabolic plasmids by transposable elements in helper plasmids. Tartu, 1992, 91 p.
5. **Maia Kivisaar**. Studies on phenol degradation genes of *Pseudomonas* sp. strain EST 1001. Tartu, 1992, 61 p.
6. **Allan Nurk**. Nucleotide sequences of phenol degradative genes from *Pseudomonas sp.* strain EST 1001 and their transcriptional activation in *Pseudomonas putida.* Tartu, 1992, 72 p.
7. **Ülo Tamm**. The genus *Populus* L. in Estonia: variation of the species biology and introduction. Tartu, 1993, 91 p.
8. **Jaanus Remme**. Studies on the peptidyltransferase centre of the *E.coli* ribosome. Tartu, 1993, 68 p.
9. **Ülo Langel**. Galanin and galanin antagonists. Tartu, 1993, 97 p.
10. **Arvo Käärd**. The development of an automatic online dynamic fluorescense-based pH-dependent fiber optic penicillin flowthrought biosensor for the control of the benzylpenicillin hydrolysis. Tartu, 1993, 117 p.
11. **Lilian Järvekülg**. Antigenic analysis and development of sensitive immunoassay for potato viruses. Tartu, 1993, 147 p.
12. **Jaak Palumets**. Analysis of phytomass partition in Norway spruce. Tartu, 1993, 47 p.
13. **Arne Sellin**. Variation in hydraulic architecture of *Picea abies* (L.) Karst. trees grown under different enviromental conditions. Tartu, 1994, 119 p.
13. **Mati Reeben**. Regulation of light neurofilament gene expression. Tartu, 1994, 108 p.
14. **Urmas Tartes**. Respiration rhytms in insects. Tartu, 1995, 109 p.
15. **Ülo Puurand**. The complete nucleotide sequence and infections *in vitro* transcripts from cloned cDNA of a potato A potyvirus. Tartu, 1995, 96 p.
16. **Peeter Hõrak**. Pathways of selection in avian reproduction: a functional framework and its application in the population study of the great tit (*Parus major*). Tartu, 1995, 118 p.
17. **Erkki Truve**. Studies on specific and broad spectrum virus resistance in transgenic plants. Tartu, 1996, 158 p.
18. **Illar Pata**. Cloning and characterization of human and mouse ribosomal protein S6-encoding genes. Tartu, 1996, 60 p.
19. **Ülo Niinemets**. Importance of structural features of leaves and canopy in determining species shade-tolerance in temperature deciduous woody taxa. Tartu, 1996, 150 p.

20. **Ants Kurg**. Bovine leukemia virus: molecular studies on the packaging region and DNA diagnostics in cattle. Tartu, 1996, 104 p.
21. **Ene Ustav**. E2 as the modulator of the BPV1 DNA replication. Tartu, 1996, 100 p.
22. **Aksel Soosaar**. Role of helix-loop-helix and nuclear hormone receptor transcription factors in neurogenesis. Tartu, 1996, 109 p.
23. **Maido Remm**. Human papillomavirus type 18: replication, transformation and gene expression. Tartu, 1997, 117 p.
24. **Tiiu Kull**. Population dynamics in *Cypripedium calceolus* L. Tartu, 1997, 124 p.
25. **Kalle Olli**. Evolutionary life-strategies of autotrophic planktonic microorganisms in the Baltic Sea. Tartu, 1997, 180 p.
26. **Meelis Pärtel**. Species diversity and community dynamics in calcareous grassland communities in Western Estonia. Tartu, 1997, 124 p.
27. **Malle Leht**. The Genus *Potentilla* L. in Estonia, Latvia and Lithuania: distribution, morphology and taxonomy. Tartu, 1997, 186 p.
28. **Tanel Tenson**. Ribosomes, peptides and antibiotic resistance. Tartu, 1997, 80 p.
29. **Arvo Tuvikene**. Assessment of inland water pollution using biomarker responses in fish *in vivo* and *in vitro*. Tartu, 1997, 160 p.
30. **Urmas Saarma**. Tuning ribosomal elongation cycle by mutagenesis of 23S rRNA. Tartu, 1997, 134 p.
31. **Henn Ojaveer**. Composition and dynamics of fish stocks in the gulf of Riga ecosystem. Tartu, 1997, 138 p.
32. **Lembi Lõugas**. Post-glacial development of vertebrate fauna in Estonian water bodies. Tartu, 1997, 138 p.
33. **Margus Pooga**. Cell penetrating peptide, transportan, and its predecessors, galanin-based chimeric peptides. Tartu, 1998, 110 p.
34. **Andres Saag**. Evolutionary relationships in some cetrarioid genera (Lichenized Ascomycota). Tartu, 1998, 196 p.
35. **Aivar Liiv**. Ribosomal large subunit assembly *in vivo*. Tartu, 1998, 158 p.
36. **Tatjana Oja**. Isoenzyme diversity and phylogenetic affinities among the eurasian annual bromes (*Bromus* L., Poaceae). Tartu, 1998, 92 p.
37. **Mari Moora**. The influence of arbuscular mycorrhizal (AM) symbiosis on the competition and coexistence of calcareous grassland plant species. Tartu, 1998, 78 p.
38. **Olavi Kurina**. Fungus gnats in Estonia (*Diptera: Bolitophilidae, Keroplatidae, Macroceridae, Ditomyiidae, Diadocidiidae, Mycetophilidae*). Tartu, 1998, 200 p.
39. **Andrus Tasa**. Biological leaching of shales: black shale and oil shale. Tartu, 1998, 98 p.
40. **Arnold Kristjuhan**. Studies on transcriptional activator properties of tumor suppressor protein p53. Tartu, 1998, 86 p.
41. **Sulev Ingerpuu**. Characterization of some human myeloid cell surface and nuclear differentiation antigens. Tartu, 1998, 163 p.

42. **Veljo Kisand**. Responses of planktonic bacteria to the abiotic and biotic factors in the shallow lake Võrtsjärv. Tartu, 1998, 118 p.
43. **Kadri Põldmaa**. Studies in the systematics of hypomyces and allied genera (Hypocreales, Ascomycota). Tartu, 1998, 178 p.
44. **Markus Vetemaa**. Reproduction parameters of fish as indicators in environmental monitoring. Tartu, 1998, 117 p.
45. **Heli Talvik**. Prepatent periods and species composition of different *Oesophagostomum* spp. populations in Estonia and Denmark. Tartu, 1998, 104 p.
46. **Katrin Heinsoo**. Cuticular and stomatal antechamber conductance to water vapour diffusion in *Picea abies* (L.) karst. Tartu, 1999, 133 p.
47. **Tarmo Annilo**. Studies on mammalian ribosomal protein S7. Tartu, 1998, 77 p.
48. **Indrek Ots**. Health state indicies of reproducing great tits (*Parus major*): sources of variation and connections with life-history traits. Tartu, 1999, 117 p.
49. **Juan Jose Cantero**. Plant community diversity and habitat relationships in central Argentina grasslands. Tartu, 1999, 161 p.
50. **Rein Kalamees**. Seed bank, seed rain and community regeneration in Estonian calcareous grasslands. Tartu, 1999, 107 p.
51. **Sulev Kõks**. Cholecystokinin (CCK) – induced anxiety in rats: influence of environmental stimuli and involvement of endopioid mechanisms and serotonin. Tartu, 1999, 123 p.
52. **Ebe Sild**. Impact of increasing concentrations of O_3 and CO_2 on wheat, clover and pasture. Tartu, 1999, 123 p.
53. **Ljudmilla Timofejeva**. Electron microscopical analysis of the synaptonemal complex formation in cereals. Tartu, 1999, 99 p.
54. **Andres Valkna**. Interactions of galanin receptor with ligands and G-proteins: studies with synthetic peptides. Tartu, 1999, 103 p.
55. **Taavi Virro**. Life cycles of planktonic rotifers in lake Peipsi. Tartu, 1999, 101 p.
56. **Ana Rebane**. Mammalian ribosomal protein S3a genes and intron-encoded small nucleolar RNAs U73 and U82. Tartu, 1999, 85 p.
57. **Tiina Tamm**. Cocksfoot mottle virus: the genome organisation and translational strategies. Tartu, 2000, 101 p.
58. **Reet Kurg**. Structure-function relationship of the bovine papilloma virus E2 protein. Tartu, 2000, 89 p.
59. **Toomas Kivisild**. The origins of Southern and Western Eurasian populations: an mtDNA study. Tartu, 2000, 121 p.
60. **Niilo Kaldalu**. Studies of the TOL plasmid transcription factor XylS. Tartu, 2000, 88 p.
61. **Dina Lepik**. Modulation of viral DNA replication by tumor suppressor protein p53. Tartu, 2000, 106 p.
62. **Kai Vellak**. Influence of different factors on the diversity of the bryophyte vegetation in forest and wooded meadow communities. Tartu, 2000, 122 p.

63. **Jonne Kotta**. Impact of eutrophication and biological invasionas on the structure and functions of benthic macrofauna. Tartu, 2000, 160 p.
64. **Georg Martin**. Phytobenthic communities of the Gulf of Riga and the inner sea the West-Estonian archipelago. Tartu, 2000, 139 p.
65. **Silvia Sepp**. Morphological and genetical variation of *Alchemilla L.* in Estonia. Tartu, 2000. 124 p.
66. **Jaan Liira**. On the determinants of structure and diversity in herbaceous plant communities. Tartu, 2000, 96 p.
67. **Priit Zingel**. The role of planktonic ciliates in lake ecosystems. Tartu, 2001, 111 p.
68. **Tiit Teder**. Direct and indirect effects in Host-parasitoid interactions: ecological and evolutionary consequences. Tartu, 2001, 122 p.
69. **Hannes Kollist**. Leaf apoplastic ascorbate as ozone scavenger and its transport across the plasma membrane. Tartu, 2001, 80 p.
70. **Reet Marits**. Role of two-component regulator system PehR-PehS and extracellular protease PrtW in virulence of *Erwinia Carotovora* subsp. *Carotovora*. Tartu, 2001, 112 p.
71. **Vallo Tilgar**. Effect of calcium supplementation on reproductive performance of the pied flycatcher *Ficedula hypoleuca* and the great tit *Parus major,* breeding in Nothern temperate forests. Tartu, 2002, 126 p.
72. **Rita Hõrak**. Regulation of transposition of transposon Tn*4652* in *Pseudomonas putida*. Tartu, 2002, 108 p.
73. **Liina Eek-Piirsoo**. The effect of fertilization, mowing and additional illumination on the structure of a species-rich grassland community. Tartu, 2002, 74 p.
74. **Krõõt Aasamaa**. Shoot hydraulic conductance and stomatal conductance of six temperate deciduous tree species. Tartu, 2002, 110 p.
75. **Nele Ingerpuu**. Bryophyte diversity and vascular plants. Tartu, 2002, 112 p.
76. **Neeme Tõnisson**. Mutation detection by primer extension on oligonucleotide microarrays. Tartu, 2002, 124 p.
77. **Margus Pensa**. Variation in needle retention of Scots pine in relation to leaf morphology, nitrogen conservation and tree age. Tartu, 2003, 110 p.
78. **Asko Lõhmus**. Habitat preferences and quality for birds of prey: from principles to applications. Tartu, 2003, 168 p.
79. **Viljar Jaks**. p53 – a switch in cellular circuit. Tartu, 2003, 160 p.
80. **Jaana Männik**. Characterization and genetic studies of four ATP-binding cassette (ABC) transporters. Tartu, 2003, 140 p.
81. **Marek Sammul**. Competition and coexistence of clonal plants in relation to productivity. Tartu, 2003, 159 p
82. **Ivar Ilves**. Virus-cell interactions in the replication cycle of bovine papillomavirus type 1. Tartu, 2003, 89 p.
83. **Andres Männik**. Design and characterization of a novel vector system based on the stable replicator of bovine papillomavirus type 1. Tartu, 2003, 109 p.

84. **Ivika Ostonen**. Fine root structure, dynamics and proportion in net primary production of Norway spruce forest ecosystem in relation to site conditions. Tartu, 2003, 158 p.
85. **Gudrun Veldre**. Somatic status of 12–15-year-old Tartu schoolchildren. Tartu, 2003, 199 p.
86. **Ülo Väli.** The greater spotted eagle *Aquila clanga* and the lesser spotted eagle *A. pomarina*: taxonomy, phylogeography and ecology. Tartu, 2004, 159 p.
87. **Aare Abroi**. The determinants for the native activities of the bovine papillomavirus type 1 E2 protein are separable. Tartu, 2004, 135 p.
88. **Tiina Kahre**. Cystic fibrosis in Estonia. Tartu, 2004, 116 p.
89. **Helen Orav-Kotta**. Habitat choice and feeding activity of benthic suspension feeders and mesograzers in the northern Baltic Sea. Tartu, 2004, 117 p.
90. **Maarja Öpik**. Diversity of arbuscular mycorrhizal fungi in the roots of perennial plants and their effect on plant performance. Tartu, 2004, 175 p.
91. **Kadri Tali**. Species structure of *Neotinea ustulata*. Tartu, 2004, 109 p.
92. **Kristiina Tambets**. Towards the understanding of post-glacial spread of human mitochondrial DNA haplogroups in Europe and beyond: a phylogeographic approach. Tartu, 2004, 163 p.
93. **Arvi Jõers**. Regulation of p53-dependent transcription. Tartu, 2004, 103 p.
94. **Lilian Kadaja**. Studies on modulation of the activity of tumor suppressor protein p53. Tartu, 2004, 103 p.
95. **Jaak Truu**. Oil shale industry wastewater: impact on river microbial community and possibilities for bioremediation. Tartu, 2004, 128 p.
96. **Maire Peters**. Natural horizontal transfer of the *pheBA* operon. Tartu, 2004, 105 p.
97. **Ülo Maiväli**. Studies on the structure-function relationship of the bacterial ribosome. Tartu, 2004, 130 p.
98. **Merit Otsus**. Plant community regeneration and species diversity in dry calcareous grasslands. Tartu, 2004, 103 p.
99. **Mikk Heidemaa**. Systematic studies on sawflies of the genera *Dolerus, Empria,* and *Caliroa* (Hymenoptera: Tenthredinidae). Tartu, 2004, 167 p.
100. **Ilmar Tõnno**. The impact of nitrogen and phosphorus concentration and N/P ratio on cyanobacterial dominance and N_2 fixation in some Estonian lakes. Tartu, 2004, 111 p.
101. **Lauri Saks**. Immune function, parasites, and carotenoid-based ornaments in greenfinches. Tartu, 2004, 144 p.
102. **Siiri Rootsi**. Human Y-chromosomal variation in European populations. Tartu, 2004, 142 p.
103. **Eve Vedler**. Structure of the 2,4-dichloro-phenoxyacetic acid-degradative plasmid pEST4011. Tartu, 2005. 106 p.
104. **Andres Tover**. Regulation of transcription of the phenol degradation *pheBA* operon in *Pseudomonas putida*. Tartu, 2005, 126 p.
105. **Helen Udras**. Hexose kinases and glucose transport in the yeast *Hansenula polymorpha*. Tartu, 2005, 100 p.

106. **Ave Suija**. Lichens and lichenicolous fungi in Estonia: diversity, distribution patterns, taxonomy. Tartu, 2005, 162 p.
107. **Piret Lõhmus**. Forest lichens and their substrata in Estonia. Tartu, 2005, 162 p.
108. **Inga Lips**. Abiotic factors controlling the cyanobacterial bloom occurrence in the Gulf of Finland. Tartu, 2005, 156 p.
109. **Krista Kaasik**. Circadian clock genes in mammalian clockwork, metabolism and behaviour. Tartu, 2005, 121 p.
110. **Juhan Javoiš**. The effects of experience on host acceptance in ovipositing moths. Tartu, 2005, 112 p.
111. **Tiina Sedman**. Characterization of the yeast *Saccharomyces cerevisiae* mitochondrial DNA helicase Hmi1. Tartu, 2005, 103 p.
112. **Ruth Aguraiuja**. Hawaiian endemic fern lineage *Diellia* (Aspleniaceae): distribution, population structure and ecology. Tartu, 2005, 112 p.
113. **Riho Teras**. Regulation of transcription from the fusion promoters generated by transposition of Tn*4652* into the upstream region of *pheBA* operon in *Pseudomonas putida*. Tartu, 2005, 106 p.
114. **Mait Metspalu**. Through the course of prehistory in India: tracing the mtDNA trail. Tartu, 2005, 138 p.
115. **Elin Lõhmussaar**. The comparative patterns of linkage disequilibrium in European populations and its implication for genetic association studies. Tartu, 2006, 124 p.
116. **Priit Kupper**. Hydraulic and environmental limitations to leaf water relations in trees with respect to canopy position. Tartu, 2006, 126 p.
117. **Heili Ilves**. Stress-induced transposition of Tn*4652* in *Pseudomonas Putida*. Tartu, 2006, 120 p.
118. **Silja Kuusk**. Biochemical properties of Hmi1p, a DNA helicase from *Saccharomyces cerevisiae* mitochondria. Tartu, 2006, 126 p.
119. **Kersti Püssa**. Forest edges on medium resolution landsat thematic mapper satellite images. Tartu, 2006, 90 p.
120. **Lea Tummeleht**. Physiological condition and immune function in great tits (*Parus major* l.): Sources of variation and trade-offs in relation to growth. Tartu, 2006, 94 p.
121. **Toomas Esperk**. Larval instar as a key element of insect growth schedules. Tartu, 2006, 186 p.
122. **Harri Valdmann**. Lynx (*Lynx lynx*) and wolf (*Canis lupus*) in the Baltic region: Diets, helminth parasites and genetic variation. Tartu, 2006. 102 p.
123. **Priit Jõers**. Studies of the mitochondrial helicase Hmi1p in *Candida albicans* and *Saccharomyces cerevisia*. Tartu, 2006. 113 p.
124. **Kersti Lilleväli**. Gata3 and Gata2 in inner ear development. Tartu, 2007, 123 p.
125. **Kai Rünk**. Comparative ecology of three fern species: *Dryopteris carthusiana* (Vill.) H.P. Fuchs, *D. expansa* (C. Presl) Fraser-Jenkins & Jermy and *D. dilatata* (Hoffm.) A. Gray (Dryopteridaceae). Tartu, 2007, 143 p.

126. **Aveliina Helm**. Formation and persistence of dry grassland diversity: role of human history and landscape structure. Tartu, 2007, 89 p.
127. **Leho Tedersoo**. Ectomycorrhizal fungi: diversity and community structure in Estonia, Seychelles and Australia. Tartu, 2007, 233 p.
128. **Marko Mägi**. The habitat-related variation of reproductive performance of great tits in a deciduous-coniferous forest mosaic: looking for causes and consequences. Tartu, 2007, 135 p.
129. **Valeria Lulla**. Replication strategies and applications of Semliki Forest virus. Tartu, 2007, 109 p.
130. **Ülle Reier**. Estonian threatened vascular plant species: causes of rarity and conservation. Tartu, 2007, 79 p.
131. **Inga Jüriado**. Diversity of lichen species in Estonia: influence of regional and local factors. Tartu, 2007, 171 p.
132. **Tatjana Krama**. Mobbing behaviour in birds: costs and reciprocity based cooperation. Tartu, 2007, 112 p.
133. **Signe Saumaa**. The role of DNA mismatch repair and oxidative DNA damage defense systems in avoidance of stationary phase mutations in *Pseudomonas putida*. Tartu, 2007, 172 p.
134. **Reedik Mägi**. The linkage disequilibrium and the selection of genetic markers for association studies in european populations. Tartu, 2007, 96 p.
135. **Priit Kilgas**. Blood parameters as indicators of physiological condition and skeletal development in great tits (*Parus major*): natural variation and application in the reproductive ecology of birds. Tartu, 2007, 129 p.
136. **Anu Albert**. The role of water salinity in structuring eastern Baltic coastal fish communities. Tartu, 2007, 95 p.
137. **Kärt Padari**. Protein transduction mechanisms of transportans. Tartu, 2008, 128 p.
138. **Siiri-Lii Sandre**. Selective forces on larval colouration in a moth. Tartu, 2008, 125 p.
139. **Ülle Jõgar**. Conservation and restoration of semi-natural floodplain meadows and their rare plant species. Tartu, 2008, 99 p.
140. **Lauri Laanisto**. Macroecological approach in vegetation science: generality of ecological relationships at the global scale. Tartu, 2008, 133 p.
141. **Reidar Andreson**. Methods and software for predicting PCR failure rate in large genomes. Tartu, 2008, 105 p.
142. **Birgot Paavel**. Bio-optical properties of turbid lakes. Tartu, 2008, 175 p.
143. **Kaire Torn**. Distribution and ecology of charophytes in the Baltic Sea. Tartu, 2008, 98 p.
144. **Vladimir Vimberg**. Peptide mediated macrolide resistance. Tartu, 2008, 190 p.
145. **Daima Örd**. Studies on the stress-inducible pseudokinase TRB3, a novel inhibitor of transcription factor ATF4. Tartu, 2008, 108 p.
146. **Lauri Saag**. Taxonomic and ecologic problems in the genus *Lepraria* (*Stereocaulaceae*, lichenised *Ascomycota*). Tartu, 2008, 175 p.

147. **Ulvi Karu**. Antioxidant protection, carotenoids and coccidians in greenfinches – assessment of the costs of immune activation and mechanisms of parasite resistance in a passerine with carotenoid-based ornaments. Tartu, 2008, 124 p.
148. **Jaanus Remm**. Tree-cavities in forests: density, characteristics and occupancy by animals. Tartu, 2008, 128 p.
149. **Epp Moks**. Tapeworm parasites *Echinococcus multilocularis* and *E. granulosus* in Estonia: phylogenetic relationships and occurrence in wild carnivores and ungulates. Tartu, 2008, 82 p.
150. **Eve Eensalu**. Acclimation of stomatal structure and function in tree canopy: effect of light and CO_2 concentration. Tartu, 2008, 108 p.
151. **Janne Pullat**. Design, functionlization and application of an *in situ* synthesized oligonucleotide microarray. Tartu, 2008, 108 p.
152. **Marta Putrinš**. Responses of *Pseudomonas putida* to phenol-induced metabolic and stress signals. Tartu, 2008, 142 p.
153. **Marina Semtšenko**. Plant root behaviour: responses to neighbours and physical obstructions. Tartu, 2008, 106 p.
154. **Marge Starast**. Influence of cultivation techniques on productivity and fruit quality of some *Vaccinium* and *Rubus* taxa. Tartu, 2008, 154 p.
155. **Age Tats**. Sequence motifs influencing the efficiency of translation. Tartu, 2009, 104 p.
156. **Radi Tegova**. The role of specialized DNA polymerases in mutagenesis in *Pseudomonas putida.* Tartu, 2009, 124 p.
157. **Tsipe Aavik**. Plant species richness, composition and functional trait pattern in agricultural landscapes – the role of land use intensity and landscape structure. Tartu, 2009, 112 p.
158. **Kaja Kiiver**. Semliki forest virus based vectors and cell lines for studying the replication and interactions of alphaviruses and hepaciviruses. Tartu, 2009, 104 p.
159. **Meelis Kadaja**. Papillomavirus Replication Machinery Induces Genomic Instability in its Host Cell. Tartu, 2009, 126 p.
160. **Pille Hallast**. Human and chimpanzee Luteinizing hormone/Chorionic Gonadotropin beta (*LHB/CGB*) gene clusters: diversity and divergence of young duplicated genes. Tartu, 2009, 168 p.
161. **Ain Vellak**. Spatial and temporal aspects of plant species conservation. Tartu, 2009, 86 p.
162. **Triinu Remmel**. Body size evolution in insects with different colouration strategies: the role of predation risk. Tartu, 2009, 168 p.
163. **Jaana Salujõe**. Zooplankton as the indicator of ecological quality and fish predation in lake ecosystems. Tartu, 2009, 129 p.
164. **Ele Vahtmäe**. Mapping benthic habitat with remote sensing in optically complex coastal environments. Tartu, 2009, 109 p.
165. **Liisa Metsamaa**. Model-based assessment to improve the use of remote sensing in recognition and quantitative mapping of cyanobacteria. Tartu, 2009, 114 p.

166. **Pille Säälik**. The role of endocytosis in the protein transduction by cell-penetrating peptides. Tartu, 2009, 155 p.
167. **Lauri Peil**. Ribosome assembly factors in *Escherichia coli.* Tartu, 2009, 147 p.
168. **Lea Hallik**. Generality and specificity in light harvesting, carbon gain capacity and shade tolerance among plant functional groups. Tartu, 2009, 99 p.
169. **Mariliis Tark**. Mutagenic potential of DNA damage repair and tolerance mechanisms under starvation stress. Tartu, 2009, 191 p.
170. **Riinu Rannap**. Impacts of habitat loss and restoration on amphibian populations. Tartu, 2009, 117 p.
171. **Maarja Adojaan**. Molecular variation of HIV-1 and the use of this knowledge in vaccine development. Tartu, 2009, 95 p.
172. **Signe Altmäe**. Genomics and transcriptomics of human induced ovarian folliculogenesis. Tartu, 2010, 179 p.
173. **Triin Suvi**. Mycorrhizal fungi of native and introduced trees in the Seychelles Islands. Tartu, 2010, 107 p.
174. **Velda Lauringson**. Role of suspension feeding in a brackish-water coastal sea. Tartu, 2010, 123 p.
175. **Eero Talts**. Photosynthetic cyclic electron transport – measurement and variably proton-coupled mechanism. Tartu, 2010, 121 p.
176. **Mari Nelis**. Genetic structure of the Estonian population and genetic distance from other populations of European descent. Tartu, 2010, 97 p.
177. **Kaarel Krjutškov**. Arrayed Primer Extension-2 as a multiplex PCR-based method for nucleic acid variation analysis: method and applications. Tartu, 2010, 129 p.
178. **Egle Köster**. Morphological and genetical variation within species complexes: *Anthyllis vulneraria* s. l. and *Alchemilla vulgaris* (coll.). Tartu, 2010, 101 p.
179. **Erki Õunap**. Systematic studies on the subfamily Sterrhinae (Lepidoptera: Geometridae). Tartu, 2010, 111 p.
180. **Merike Jõesaar**. Diversity of key catabolic genes at degradation of phenol and *p*-cresol in pseudomonads. Tartu, 2010, 125 p.
181. **Kristjan Herkül**. Effects of physical disturbance and habitat-modifying species on sediment properties and benthic communities in the northern Baltic Sea. Tartu, 2010, 123 p.
182. **Arto Pulk**. Studies on bacterial ribosomes by chemical modification approaches. Tartu, 2010, 161 p.
183. **Maria Põllupüü**. Ecological relations of cladocerans in a brackish-water ecosystem. Tartu, 2010, 126 p.
184. **Toomas Silla**. Study of the segregation mechanism of the Bovine Papillomavirus Type 1. Tartu, 2010, 188 p.
185. **Gyaneshwer Chaubey**. The demographic history of India: A perspective based on genetic evidence. Tartu, 2010, 184 p.

186. **Katrin Kepp**. Genes involved in cardiovascular traits: detection of genetic variation in Estonian and Czech populations. Tartu, 2010, 164 p.
187. **Virve Sõber**. The role of biotic interactions in plant reproductive performance. Tartu, 2010, 92 p.
188. **Kersti Kangro**. The response of phytoplankton community to the changes in nutrient loading. Tartu, 2010, 144 p.
189. **Joachim M. Gerhold**. Replication and Recombination of mitochondrial DNA in Yeast. Tartu, 2010, 120 p.
190. **Helen Tammert**. Ecological role of physiological and phylogenetic diversity in aquatic bacterial communities. Tartu, 2010, 140 p.
191. **Elle Rajandu**. Factors determining plant and lichen species diversity and composition in Estonian *Calamagrostis* and *Hepatica* site type forests. Tartu, 2010, 123 p.
192. **Paula Ann Kivistik**. ColR-ColS signalling system and transposition of Tn*4652* in the adaptation of *Pseudomonas putida.* Tartu, 2010, 118 p.
193. **Siim Sõber**. Blood pressure genetics: from candidate genes to genome-wide association studies. Tartu, 2011, 120 p.
194. **Kalle Kipper**. Studies on the role of helix 69 of 23S rRNA in the factor-dependent stages of translation initiation, elongation, and termination. Tartu, 2011, 178 p.
195. **Triinu Siibak**. Effect of antibiotics on ribosome assembly is indirect. Tartu, 2011, 134 p.
196. **Tambet Tõnissoo**. Identification and molecular analysis of the role of guanine nucleotide exchange factor RIC-8 in mouse development and neural function. Tartu, 2011, 110 p.
197. **Helin Räägel**. Multiple faces of cell-penetrating peptides – their intracellular trafficking, stability and endosomal escape during protein transduction. Tartu, 2011, 161 p.
198. **Andres Jaanus**. Phytoplankton in Estonian coastal waters – variability, trends and response to environmental pressures. Tartu, 2011, 157 p.
199. **Tiit Nikopensius**. Genetic predisposition to nonsyndromic orofacial clefts. Tartu, 2011, 152 p.
200. **Signe Värv**. Studies on the mechanisms of RNA polymerase II-dependent transcription elongation. Tartu, 2011, 108 p.
201. **Kristjan Välk**. Gene expression profiling and genome-wide association studies of non-small cell lung cancer. Tartu, 2011, 98 p.
202. **Arno Põllumäe**. Spatio-temporal patterns of native and invasive zooplankton species under changing climate and eutrophication conditions. Tartu, 2011, 153 p.
203. **Egle Tammeleht**. Brown bear (*Ursus arctos*) population structure, demographic processes and variations in diet in northern Eurasia. Tartu, 2011, 143 p.
205. **Teele Jairus**. Species composition and host preference among ectomycorrhizal fungi in Australian and African ecosystems. Tartu, 2011, 106 p.

206. **Kessy Abarenkov**. PlutoF – cloud database and computing services supporting biological research. Tartu, 2011, 125 p.
207. **Marina Grigorova**. Fine-scale genetic variation of follicle-stimulating hormone beta-subunit coding gene (*FSHB*) and its association with reproductive health. Tartu, 2011, 184 p.
208. **Anu Tiitsaar**. The effects of predation risk and habitat history on butterfly communities. Tartu, 2011, 97 p.
209. **Elin Sild**. Oxidative defences in immunoecological context: validation and application of assays for nitric oxide production and oxidative burst in a wild passerine. Tartu, 2011, 105 p.
210. **Irja Saar**. The taxonomy and phylogeny of the genera *Cystoderma* and *Cystodermella* (Agaricales, Fungi). Tartu, 2012, 167 p.
211. **Pauli Saag**. Natural variation in plumage bacterial assemblages in two wild breeding passerines. Tartu, 2012, 113 p.
212. **Aleksei Lulla**. Alphaviral nonstructural protease and its polyprotein substrate: arrangements for the perfect marriage. Tartu, 2012, 143 p.
213. **Mari Järve**. Different genetic perspectives on human history in Europe and the Caucasus: the stories told by uniparental and autosomal markers. Tartu, 2012, 119 p.
214. **Ott Scheler**. The application of tmRNA as a marker molecule in bacterial diagnostics using microarray and biosensor technology. Tartu, 2012, 93 p.
215. **Anna Balikova**. Studies on the functions of tumor-associated mucin-like leukosialin (CD43) in human cancer cells. Tartu, 2012, 129 p.
216. **Triinu Kõressaar**. Improvement of PCR primer design for detection of prokaryotic species. Tartu, 2012, 83 p.
217. **Tuul Sepp**. Hematological health state indices of greenfinches: sources of individual variation and responses to immune system manipulation. Tartu, 2012, 117 p.
218. **Rya Ero**. Modifier view of the bacterial ribosome. Tartu, 2012, 146 p.
219. **Mohammad Bahram**. Biogeography of ectomycorrhizal fungi across different spatial scales. Tartu, 2012, 165 p.
220. **Annely Lorents**. Overcoming the plasma membrane barrier: uptake of amphipathic cell-penetrating peptides induces influx of calcium ions and downstream responses. Tartu, 2012, 113 p.
221. **Katrin Männik**. Exploring the genomics of cognitive impairment: whole-genome SNP genotyping experience in Estonian patients and general population. Tartu, 2012, 171 p.
222. **Marko Prous**. Taxonomy and phylogeny of the sawfly genus *Empria* (Hymenoptera, Tenthredinidae). Tartu, 2012, 192 p.
223. **Triinu Visnapuu**. Levansucrases encoded in the genome of *Pseudomonas syringae* pv. tomato DC3000: heterologous expression, biochemical characterization, mutational analysis and spectrum of polymerization products. Tartu, 2012, 160 p.
224. **Nele Tamberg**. Studies on Semliki Forest virus replication and pathogenesis. Tartu, 2012, 109 p.

225. **Tõnu Esko**. Novel applications of SNP array data in the analysis of the genetic structure of Europeans and in genetic association studies. Tartu, 2012, 149 p.
226. **Timo Arula**. Ecology of early life-history stages of herring *Clupea harengus membras* in the northeastern Baltic Sea. Tartu, 2012, 143 p.
227. **Inga Hiiesalu**. Belowground plant diversity and coexistence patterns in grassland ecosystems. Tartu, 2012, 130 p.
228. **Kadri Koorem**. The influence of abiotic and biotic factors on small-scale plant community patterns and regeneration in boreonemoral forest. Tartu, 2012, 114 p.
229. **Liis Andresen**. Regulation of virulence in plant-pathogenic pectobacteria. Tartu, 2012, 122 p.
230. **Kaupo Kohv**. The direct and indirect effects of management on boreal forest structure and field layer vegetation. Tartu, 2012, 124 p.
231. **Mart Jüssi**. Living on an edge: landlocked seals in changing climate. Tartu, 2012, 114 p.
232. **Riina Klais**. Phytoplankton trends in the Baltic Sea. Tartu, 2012, 136 p.
233. **Rauno Veeroja**. Effects of winter weather, population density and timing of reproduction on life-history traits and population dynamics of moose (*Alces alces*) in Estonia. Tartu, 2012, 92 p.
234. **Marju Keis**. Brown bear (*Ursus arctos*) phylogeography in northern Eurasia. Tartu, 2013, 142 p.
235. **Sergei Põlme**. Biogeography and ecology of *alnus*- associated ectomycorrhizal fungi – from regional to global scale. Tartu, 2013, 90 p.
236. **Liis Uusküla**. Placental gene expression in normal and complicated pregnancy. Tartu, 2013, 173 p.
237. **Marko Lõoke**. Studies on DNA replication initiation in *Saccharomyces cerevisiae*. Tartu, 2013, 112 p.
238. **Anne Aan**. Light- and nitrogen-use and biomass allocation along productivity gradients in multilayer plant communities. Tartu, 2013, 127 p.
239. **Heidi Tamm**. Comprehending phylogenetic diversity – case studies in three groups of ascomycetes. Tartu, 2013, 136 p.
240. **Liina Kangur**. High-Pressure Spectroscopy Study of Chromophore-Binding Hydrogen Bonds in Light-Harvesting Complexes of Photosynthetic Bacteria. Tartu, 2013, 150 p.
241. **Margus Leppik**. Substrate specificity of the multisite specific pseudouridine synthase RluD. Tartu, 2013, 111 p.
242. **Lauris Kaplinski**. The application of oligonucleotide hybridization model for PCR and microarray optimization. Tartu, 2013, 103 p.
243. **Merli Pärnoja**. Patterns of macrophyte distribution and productivity in coastal ecosystems: effect of abiotic and biotic forcing. Tartu, 2013, 155 p.
244. **Tõnu Margus**. Distribution and phylogeny of the bacterial translational GTPases and the Mqsr/YgiT regulatory system. Tartu, 2013, 126 p.
245. **Pille Mänd**. Light use capacity and carbon and nitrogen budget of plants: remote assessment and physiological determinants. Tartu, 2013, 128 p.

246. **Mario Plaas**. Animal model of Wolfram Syndrome in mice: behavioural, biochemical and psychopharmacological characterization. Tartu, 2013, 144 p.
247. **Georgi Hudjašov**. Maps of mitochondrial DNA, Y-chromosome and tyrosinase variation in Eurasian and Oceanian populations. Tartu, 2013, 115 p.
248. **Mari Lepik**. Plasticity to light in herbaceous plants and its importance for community structure and diversity. Tartu, 2013, 102 p.
249. **Ede Leppik**. Diversity of lichens in semi-natural habitats of Estonia. Tartu, 2013, 151 p.
250. **Ülle Saks**. Arbuscular mycorrhizal fungal diversity patterns in boreonemoral forest ecosystems. Tartu, 2013, 151 p.
251. **Eneli Oitmaa**. Development of arrayed primer extension microarray assays for molecular diagnostic applications. Tartu, 2013, 147 p.
252. **Jekaterina Jutkina**. The horizontal gene pool for aromatics degradation: bacterial catabolic plasmids of the Baltic Sea aquatic system. Tartu, 2013, 121 p.
253. **Helen Vellau**. Reaction norms for size and age at maturity in insects: rules and exceptions. Tartu, 2014, 132 p.
254. **Randel Kreitsberg**. Using biomarkers in assessment of environmental contamination in fish – new perspectives. Tartu, 2014, 107 p.
255. **Krista Takkis**. Changes in plant species richness and population performance in response to habitat loss and fragmentation.Tartu, 2014, 141 p.
256. **Liina Nagirnaja**. Global and fine-scale genetic determinants of recurrent pregnancy loss. Tartu, 2014, 211 p.
257. **Triin Triisberg**. Factors influencing the re-vegetation of abandoned extracted peatlands in Estonia. Tartu, 2014, 133 p.
258. **Villu Soon**. A phylogenetic revision of the *Chrysis ignita* species group (Hymenoptera: Chrysididae) with emphasis on the northern European fauna. Tartu, 2014, 211 p.
259. **Andrei Nikonov**. RNA-Dependent RNA Polymerase Activity as a Basis for the Detection of Positive-Strand RNA Viruses by Vertebrate Host Cells. Tartu, 2014, 207 p.
260. **Eele Õunapuu-Pikas**. Spatio-temporal variability of leaf hydraulic conductance in woody plants: ecophysiological consequences. Tartu, 2014, 135 p.
261. **Marju Männiste**. Physiological ecology of greenfinches: information content of feathers in relation to immune function and behavior. Tartu, 2014, 121 p.
262. **Katre Kets**. Effects of elevated concentrations of CO_2 and O_3 on leaf photosynthetic parameters in *Populus tremuloides*: diurnal, seasonal and interannual patterns. Tartu, 2014, 115 p.
263. **Külli Lokko**. Seasonal and spatial variability of zoopsammon communities in relation to environmental parameters. Tartu, 2014, 129 p.
264. **Olga Žilina**. Chromosomal microarray analysis as diagnostic tool: Estonian experience. Tartu, 2014, 152 p.

265. **Kertu Lõhmus**. Colonisation ecology of forest-dwelling vascular plants and the conservation value of rural manor parks. Tartu, 2014, 111 p.
266. **Anu Aun**. Mitochondria as integral modulators of cellular signaling. Tartu, 2014, 167 p.
267. **Chandana Basu Mallick**. Genetics of adaptive traits and gender-specific demographic processes in South Asian populations. Tartu, 2014, 160 p.
268. **Riin Tamme**. The relationship between small-scale environmental heterogeneity and plant species diversity. Tartu, 2014, 130 p.
269. **Liina Remm**. Impacts of forest drainage on biodiversity and habitat quality: implications for sustainable management and conservation. Tartu, 2015, 126 p.
270. **Tiina Talve**. Genetic diversity and taxonomy within the genus *Rhinanthus.* Tartu, 2015, 106 p.
271. **Mehis Rohtla**. Otolith sclerochronological studies on migrations, spawning habitat preferences and age of freshwater fishes inhabiting the Baltic Sea. Tartu, 2015, 137 p.
272. **Alexey Reshchikov**. The world fauna of the genus *Lathrolestes* (Hymenoptera, Ichneumonidae). Tartu, 2015, 247 p.
273. **Martin Pook**. Studies on artificial and extracellular matrix protein-rich surfaces as regulators of cell growth and differentiation. Tartu, 2015, 142 p.
274. **Mai Kukumägi**. Factors affecting soil respiration and its components in silver birch and Norway spruce stands. Tartu, 2015, 155 p.
275. **Helen Karu**. Development of ecosystems under human activity in the North-East Estonian industrial region: forests on post-mining sites and bogs. Tartu, 2015, 152 p.
276. **Hedi Peterson**. Exploiting high-throughput data for establishing relationships between genes. Tartu, 2015, 186 p.
277. **Priit Adler**. Analysis and visualisation of large scale microarray data, Tartu, 2015, 126 p.
278. **Aigar Niglas**. Effects of environmental factors on gas exchange in deciduous trees: focus on photosynthetic water-use efficiency. Tartu, 2015, 152 p.
279. **Silja Laht**. Classification and identification of conopeptides using profile hidden Markov models and position-specific scoring matrices. Tartu, 2015, 100 p.
280. **Martin Kesler**. Biological characteristics and restoration of Atlantic salmon *Salmo salar* populations in the Rivers of Northern Estonia. Tartu, 2015, 97 p.
281. **Pratyush Kumar Das**. Biochemical perspective on alphaviral nonstructural protein 2: a tale from multiple domains to enzymatic profiling. Tartu, 2015, 205 p
282. **Priit Palta**. Computational methods for DNA copy number detection. Tartu, 2015, 130 p.
283. **Julia Sidorenko**. Combating DNA damage and maintenance of genome integrity in pseudomonads. Tartu, 2015, 174 p.

284. **Anastasiia Kovtun-Kante**. Charophytes of Estonian inland and coastal waters: distribution and environmental preferences. Tartu, 2015, 97 p.
285. **Ly Lindman**. The ecology of protected butterfly species in Estonia. Tartu, 2015, 171 p.
286. **Jaanis Lodjak**. Association of Insulin-like Growth Factor I and Corticosterone with Nestling Growth and Fledging Success in Wild Passerines. Tartu, 2016, 113 p.
287. **Ann Kraut**. Conservation of Wood-Inhabiting Biodiversity – Semi-Natural Forests as an Opportunity. Tartu, 2016, 141 p.
288. **Tiit Örd**. Functions and regulation of the mammalian pseudokinase TRIB3. Tartu, 2016, 182. p.
289. **Kairi Käiro**. Biological Quality According to Macroinvertebrates in Streams of Estonia (Baltic Ecoregion of Europe): Effects of Human-induced Hydromorphological Changes. Tartu, 2016, 126 p.
290. **Leidi Laurimaa**. *Echinococcus multilocularis* and other zoonotic parasites in Estonian canids. Tartu, 2016, 144 p.
291. **Helerin Margus**. Characterization of cell-penetrating peptide/nucleic acid nanocomplexes and their cell-entry mechanisms. Tartu, 2016, 173 p.
292. **Kadri Runnel**. Fungal targets and tools for forest conservation. Tartu, 2016, 157 p.
293. **Urmo Võsa**. MicroRNAs in disease and health: aberrant regulation in lung cancer and association with genomic variation. Tartu, 2016, 163 p.
294. **Kristina Mäemets-Allas**. Studies on cell growth promoting AKT signaling pathway – a promising anti-cancer drug target. Tartu, 2016, 146 p.
295. **Janeli Viil**. Studies on cellular and molecular mechanisms that drive normal and regenerative processes in the liver and pathological processes in Dupuytren's contracture. Tartu, 2016, 175 p.
296. **Ene Kook**. Genetic diversity and evolution of *Pulmonaria angustifolia* L. and *Myosotis laxa sensu lato* (Boraginaceae). Tartu, 2016, 106 p.
297. **Kadri Peil**. RNA polymerase II-dependent transcription elongation in *Saccharomyces cerevisiae*. Tartu, 2016, 113 p.
298. **Katrin Ruisu**. The role of RIC8A in mouse development and its function in cell-matrix adhesion and actin cytoskeletal organisation. Tartu, 2016, 129 p.
299. **Janely Pae**. Translocation of cell-penetrating peptides across biological membranes and interactions with plasma membrane constituents. Tartu, 2016, 126 p.
300. **Argo Ronk**. Plant diversity patterns across Europe: observed and dark diversity. Tartu, 2016, 153 p.
301. **Kristiina Mark**. Diversification and species delimitation of lichenized fungi in selected groups of the family Parmeliaceae (Ascomycota). Tartu, 2016, 181 p.
302. **Jaak-Albert Metsoja**. Vegetation dynamics in floodplain meadows: influence of mowing and sediment application. Tartu, 2016, 140 p.

303. **Hedvig Tamman**. The GraTA toxin-antitoxin system of *Pseudomonas putida*: regulation and role in stress tolerance. Tartu, 2016, 154 p.
304. **Kadri Pärtel**. Application of ultrastructural and molecular data in the taxonomy of helotialean fungi. Tartu, 2016, 183 p.
305. **Maris Hindrikson**. Grey wolf (*Canis lupus*) populations in Estonia and Europe: genetic diversity, population structure and -processes, and hybridization between wolves and dogs. Tartu, 2016, 121 p.
306. **Polina Degtjarenko**. Impacts of alkaline dust pollution on biodiversity of plants and lichens: from communities to genetic diversity. Tartu, 2016, 126 p.
307. **Liina Pajusalu**. The effect of CO_2 enrichment on net photosynthesis of macrophytes in a brackish water environment. Tartu, 2016, 126 p.
308. **Stoyan Tankov**. Random walks in the stringent response. Tartu, 2016, 94 p.
309. **Liis Leitsalu**. Communicating genomic research results to population-based biobank participants. Tartu, 2016, 158 p.
310. **Richard Meitern**. Redox physiology of wild birds: validation and application of techniques for detecting oxidative stress. Tartu, 2016, 134 p.
311. **Kaie Lokk**. Comparative genome-wide DNA methylation studies of healthy human tissues and non-small cell lung cancer tissue. Tartu, 2016, 127 p.
312. **Mihhail Kurašin**. Processivity of cellulases and chitinases. Tartu, 2017, 132 p.
313. **Carmen Tali**. Scavenger receptors as a target for nucleic acid delivery with peptide vectors. Tartu, 2017, 155 p.
314. **Katarina Oganjan**. Distribution, feeding and habitat of benthic suspension feeders in a shallow coastal sea. Tartu, 2017, 132 p.
315. **Taavi Paal**. Immigration limitation of forest plants into wooded landscape corridors. Tartu, 2017, 145 p.
316. **Kadri Õunap**. The Williams-Beuren syndrome chromosome region protein WBSCR22 is a ribosome biogenesis factor. Tartu, 2017, 135 p.
317. **Riin Tamm**. In-depth analysis of factors affecting variability in thiopurine methyltransferase activity. Tartu, 2017, 170 p.
318. **Keiu Kask**. The role of RIC8A in the development and regulation of mouse nervous system. Tartu, 2017, 184 p.
319. **Tiia Möller**. Mapping and modelling of the spatial distribution of benthic macrovegetation in the NE Baltic Sea with a special focus on the eelgrass *Zostera marina* Linnaeus, 1753. Tartu, 2017, 162 p.
320. **Silva Kasela**. Genetic regulation of gene expression: detection of tissue- and cell type-specific effects. Tartu, 2017, 150 p.
321. **Karmen Süld**. Food habits, parasites and space use of the raccoon dog *Nyctereutes procyonoides*: the role of an alien species as a predator and vector of zoonotic diseases in Estonia. Tartu, 2017, p.
322. **Ragne Oja**. Consequences of supplementary feeding of wild boar – concern for ground-nesting birds and endoparasite infection. Tartu, 2017, 141 p.
323. **Riin Kont**. The acquisition of cellulose chain by a processive cellobiohydrolase. Tartu, 2017, 117 p.

324. **Liis Kasari**. Plant diversity of semi-natural grasslands: drivers, current status and conservation challenges. Tartu, 2017, 141 p.
325. **Sirgi Saar**. Belowground interactions: the roles of plant genetic relatedness, root exudation and soil legacies. Tartu, 2017, 113 p.
326. **Sten Anslan**. Molecular identification of Collembola and their fungal associates. Tartu, 2017, 125 p.
327. **Imre Taal**. Causes of variation in littoral fish communities of the Eastern Baltic Sea: from community structure to individual life histories. Tartu, 2017, 118 p.
328. **Jürgen Jalak**. Dissecting the Mechanism of Enzymatic Degradation of Cellulose Using Low Molecular Weight Model Substrates. Tartu, 2017, 137 p.
329. **Kairi Kiik**. Reproduction and behaviour of the endangered European mink (*Mustela lutreola*) in captivity. Tartu, 2018, 112 p.
330. **Ivan Kuprijanov**. Habitat use and trophic interactions of native and invasive predatory macroinvertebrates in the northern Baltic Sea. Tartu, 2018, 117 p.
331. **Hendrik Meister**. Evolutionary ecology of insect growth: from geographic patterns to biochemical trade-offs. Tartu, 2018, 147 p.
332. **Ilja Gaidutšik**. Irc3 is a mitochondrial branch migration enzyme in *Saccharomyces cerevisiae*. Tartu, 2018, 161 p.
333. **Lena Neuenkamp**. The dynamics of plant and arbuscular mycorrhizal fungal communities in grasslands under changing land use. Tartu, 2018, 241 p.
334. **Laura Kasak**. Genome structural variation modulating the placenta and pregnancy maintenance. Tartu, 2018, 181 p.
335. **Kersti Riibak**. Importance of dispersal limitation in determining dark diversity of plants across spatial scales. Tartu, 2018, 133 p.
336. **Liina Saar**. Dynamics of grassland plant diversity in changing landscapes. Tartu, 2018, 206 p.
337. **Hanna Ainelo**. Fis regulates *Pseudomonas putida* biofilm formation by controlling the expression of *lapA*. Tartu, 2018, 143 p.
338. **Natalia Pervjakova**. Genomic imprinting in complex traits. Tartu, 2018, 176 p.
339. **Andrio Lahesaare**. The role of global regulator Fis in regulating the expression of *lapF* and the hydrophobicity of soil bacterium *Pseudomonas putida*. Tartu, 2018, 124 p.
340. **Märt Roosaare**. *K*-mer based methods for the identification of bacteria and plasmids. Tartu, 2018, 117 p.
341. **Maria Abakumova**. The relationship between competitive behaviour and the frequency and identity of neighbours in temperate grassland plants. Tartu, 2018, 104 p.
342. **Margus Vilbas**. Biotic interactions affecting habitat use of myrmecophilous butterflies in Northern Europe. Tartu, 2018, 142 p.

343. **Liina Kinkar**. Global patterns of genetic diversity and phylogeography of *Echinococcus granulosus* sensu stricto – a tapeworm species of significant public health concern. Tartu, 2018, 147 p.
344. **Teivi Laurimäe**. Taxonomy and genetic diversity of zoonotic tapeworms in the species complex of *Echinococcus granulosus* sensu lato. Tartu, 2018, 143 p.
345. **Tatjana Jatsenko**. Role of translesion DNA polymerases in mutagenesis and DNA damage tolerance in Pseudomonads. Tartu, 2018, 216 p.
346. **Katrin Viigand**. Utilization of α-glucosidic sugars by *Ogataea* (*Hansenula*) *polymorpha.* Tartu, 2018, 148 p.
347. **Andres Ainelo**. Physiological effects of the *Pseudomonas putida* toxin grat. Tartu, 2018, 146 p.
348. **Killu Timm**. Effects of two genes (DRD4 and SERT) on great tit (*Parus major*) behaviour and reproductive traits. Tartu, 2018, 117 p.
349. **Petr Kohout**. Ecology of ericoid mycorrhizal fungi. Tartu, 2018, 184 p.
350. **Gristin Rohula-Okunev**. Effects of endogenous and environmental factors on night-time water flux in deciduous woody tree species. Tartu, 2018, 184 p.
351. **Jane Oja**. Temporal and spatial patterns of orchid mycorrhizal fungi in forest and grassland ecosystems. Tartu, 2018, 102 p.
352. **Janek Urvik**. Multidimensionality of aging in a long-lived seabird. Tartu, 2018, 135 p.
353. **Lisanna Schmidt**. Phenotypic and genetic differentiation in the hybridizing species pair *Carex flava* and *C. viridula* in geographically different regions. Tartu, 2018, 133 p.
354. **Monika Karmin**. Perspectives from human Y chromosome – phylogeny, population dynamics and founder events. Tartu, 2018, 168 p.
355. **Maris Alver**. Value of genomics for atherosclerotic cardiovascular disease risk prediction. Tartu, 2019, 148 p.
356. **Lehti Saag**. The prehistory of Estonia from a genetic perspective: new insights from ancient DNA. Tartu, 2019, 171 p.
357. **Mari-Liis Viljur**. Local and landscape effects on butterfly assemblages in managed forests. Tartu, 2019, 115 p.
358. **Ivan Kisly**. The pleiotropic functions of ribosomal proteins eL19 and eL24 in the budding yeast ribosome. Tartu, 2019, 170 p.
359. **Mikk Puustusmaa**. On the origin of papillomavirus proteins. Tartu, 2019, 152 p.
360. **Anneliis Peterson**. Benthic biodiversity in the north-eastern Baltic Sea: mapping methods, spatial patterns, and relations to environmental gradients. Tartu, 2019, 159 p.
361. **Erwan Pennarun**. Meandering along the mtDNA phylogeny; causerie and digression about what it can tell us about human migrations. Tartu, 2019, 162 p.

362. **Karin Ernits**. Levansucrase Lsc3 and endo-levanase BT1760: characterization and application for the synthesis of novel prebiotics. Tartu, 2019, 217 p.
363. **Sille Holm**. Comparative ecology of geometrid moths: in search of contrasts between a temperate and a tropical forest. Tartu, 2019, 135 p.
364. **Anne-Mai Ilumäe**. Genetic history of the Uralic-speaking peoples as seen through the paternal haplogroup N and autosomal variation of northern Eurasians. Tartu, 2019, 172 p.
365. **Anu Lepik**. Plant competitive behaviour: relationships with functional traits and soil processes. Tartu, 2019, 152 p.
366. **Kunter Tätte**. Towards an integrated view of escape decisions in birds under variable levels of predation risk. Tartu, 2020, 172 p.
367. **Kaarin Parts**. The impact of climate change on fine roots and root-associated microbial communities in birch and spruce forests. Tartu, 2020, 143 p.
368. **Viktorija Kukuškina**. Understanding the mechanisms of endometrial receptivity through integration of 'omics' data layers. Tartu, 2020, 169 p.
369. **Martti Vasar**. Developing a bioinformatics pipeline gDAT to analyse arbuscular mycorrhizal fungal communities using sequence data from different marker regions. Tartu, 2020, 193 p.
370. **Ott Kangur**. Nocturnal water relations and predawn water potential disequilibrium in temperate deciduous tree species. Tartu, 2020, 126 p.
371. **Helen Post**. Overview of the phylogeny and phylogeography of the Y-chromosomal haplogroup N in northern Eurasia and case studies of two linguistically exceptional populations of Europe – Hungarians and Kalmyks. Tartu, 2020, 143 p.
372. **Kristi Krebs**. Exploring the genetics of adverse events in pharmacotherapy using Biobanks and Electronic Health Records. Tartu, 2020, 151 p.
373. **Kärt Ukkivi**. Mutagenic effect of transcription and transcription-coupled repair factors in *Pseudomonas putida.* Tartu, 2020, 154 p.
374. **Elin Soomets**. Focal species in wetland restoration. Tartu, 2020, 137 p.
375. **Kadi Tilk**. Signals and responses of ColRS two-component system in *Pseudomonas putida.* Tartu, 2020, 133 p.
376. **Indrek Teino**. Studies on aryl hydrocarbon receptor in the mouse granulosa cell model. Tartu, 2020, 139 p.
377. **Maarja Vaikre**. The impact of forest drainage on macroinvertebrates and amphibians in small waterbodies and opportunities for cost-effective mitigation. Tartu, 2020, 132 p.
378. **Siim-Kaarel Sepp**. Soil eukaryotic community responses to land use and host identity. Tartu, 2020, 222 p.
379. **Eveli Otsing**. Tree species effects on fungal richness and community structure. Tartu, 2020, 152 p.
380. **Mari Pent**. Bacterial communities associated with fungal fruitbodies. Tartu, 2020, 144 p.

381. **Einar Kärgenberg**. Movement patterns of lithophilous migratory fish in free-flowing and fragmented rivers. Tartu, 2020, 167 p.
382. **Antti Matvere**. The studies on aryl hydrocarbon receptor in murine granulosa cells and human embryonic stem cells. Tartu, 2021, 163 p.
383. **Jhonny Capichoni Massante**. Phylogenetic structure of plant communities along environmental gradients: a macroecological and evolutionary approach. Tartu, 2021, 144 p.
384. **Ajai Kumar Pathak**. Delineating genetic ancestries of people of the Indus Valley, Parsis, Indian Jews and Tharu tribe. Tartu, 2021, 197 p.
385. **Tanel Vahter**. Arbuscular mycorrhizal fungal biodiversity for sustainable agroecosystems. Tartu, 2021, 191 p.
386. **Burak Yelmen**. Characterization of ancient Eurasian influences within modern human genomes. Tartu, 2021, 134 p.
387. **Linda Ongaro**. A genomic portrait of American populations. Tartu, 2021, 182 p.
388. **Kairi Raime**. The identification of plant DNA in metagenomic samples. Tartu, 2021, 108 p.
389. **Heli Einberg**. Non-linear and non-stationary relationships in the pelagic ecosystem of the Gulf of Riga (Baltic Sea). Tartu, 2021, 119 p.
390. **Mickaël Mathieu Pihain**. The evolutionary effect of phylogenetic neighbourhoods of trees on their resistance to herbivores and climatic stress. Tartu, 2022, 145 p.
391. **Annika Joy Meitern**. Impact of potassium ion content of xylem sap and of light conditions on the hydraulic properties of trees. Tartu, 2022, 132 p.
392. **Elise Joonas**. Evaluation of metal contaminant hazard on microalgae with environmentally relevant testing strategies. Tartu, 2022, 118 p.
393. **Kreete Lüll**. Investigating the relationships between human microbiome, host factors and female health. Tartu, 2022, 141 p.
394. **Triin Kaasiku**. A wader perspective to Boreal Baltic coastal grasslands: from habitat availability to breeding site selection and nest survival. Tartu, 2022, 141 p.
395. **Meeli Alber**. Impact of elevated atmospheric humidity on the structure of the water transport pathway in deciduous trees. Tartu, 2022, 170 p.
396. **Ludovica Molinaro**. Ancestry deconvolution of Estonian, European and Worldwide genomic layers: a human population genomics excavation. Tartu, 2022, 138 p.
397. **Tina Saupe**. The genetic history of the Mediterranean before the common era: a focus on the Italian Peninsula. Tartu, 2022, 165 p.
398. **Mari-Ann Lind**. Internal constraints on energy processing and their consequences: an integrative study of behaviour, ornaments and digestive health in greenfinches. Tartu, 2022, 137 p.
399. **Markus Valge**. Testing the predictions of life history theory on anthropometric data. Tartu, 2022, 171 p.
400. **Ants Tull**. Domesticated and wild mammals as reservoirs for zoonotic helminth parasites in Estonia. Tartu, 2022, 152 p.

401. **Saleh Rahimlouye Barabi**. Investigation of diazotrophic bacteria association with plants. Tartu, 2022, 137 p.
402. **Farzad Aslani**. Towards revealing the biogeography of belowground diversity. Tartu, 2022, 124 p.
403. **Nele Taba**. Diet, blood metabolites, and health. Tartu, 2022, 163 p.
404. **Katri Pärna**. Improving the personalized prediction of complex traits and diseases: application to type 2 diabetes. Tartu, 2022, 190 p.
405. **Silva Lilleorg**. Bacterial ribosome heterogeneity on the example of bL31 paralogs in *Escherichia coli*. Tartu, 2022, 189 p.
406. **Oliver Aasmets**. The importance of microbiome in human health. Tartu, 2022, 123 p.
407. **Henel Jürgens**. Exploring post-translational modifications of histones in RNA polymerase II-dependent transcription. Tartu, 2022, 147 p.
408. **Mari Tagel**. Finding novel factors affecting the mutation frequency: a case study of tRNA modification enzymes TruA and RluA. Tartu, 2022, 176 p.
409. **Marili Sell**. The impact of environmental change on ecophysiology of hemiboreal tree species – acclimation mechanisms in belowground. Tartu, 2022, 163 p.
410. **Kaarin Hein**. The hissing behaviour of Great Tit (*Parus major*) females reflects behavioural phenotype and breeding success in a wild population. Tartu, 2022, 96 p.
411. **Maret Gerz**. The distribution and role of mycorrhizal symbiosis in plant communities. Tartu, 2022, 206 p.
412. **Kristiina Nõomaa**. Role of invasive species in brackish benthic community structure and biomass changes. Tartu, 2023, 151 p.
413. **Anton Savchenko**. Taxonomic studies in Dacrymycetes: *Cerinomyces* and allied taxa. Tartu, 2023, 181 p.
414. **Ahto Agan**. Interactions between invasive pathogens and resident mycobiome in the foliage of trees. Tartu, 2023, 155 p.
415. **Diego Pires Ferraz Trindade**. Dark diversity dynamics linked to global change: taxonomic and functional perspective. Tartu, 2023, 134 p.
416. **Madli Jõks**. Biodiversity drivers in oceanic archipelagos and habitat fragments, explored by agent-based simulation models. Tartu, 2023, 116 p.
417. **Ciara Baines**. Adaptation to oncogenic pollution and natural cancer defences in the aquatic environment. Tartu, 2023, 164 p.
418. **Rain Inno**. Placental transcriptome and miRNome in normal and complicated pregnancies. Tartu, 2023, 145 p.
419. **Daniyal Gohar**. Diversity, genomics, and potential functions of fungus-inhabiting bacteria. Tartu, 2023, 138 p.
420. **Sirli Rosendahl**. Fitness effects of chromosomal toxin-antitoxin systems in *Pseudomonas putida*. Tartu, 2023, 154 p.
421. **Mathilde Frédérique E. André**. New Guinea, a hotspot for Human evolution: settlement history and adaptation in northern Sahul. Tartu, 2023, 202 p.